HAL open science

Progress in understanding structure and transport properties of PEDOT-based materials: a critical review

Magatte N. Gueye, Alexandre Carella, Jérôme Faure-Vincent, Renaud Demadrille, Jean-Pierre Simonato

▶ **To cite this version:**

Magatte N. Gueye, Alexandre Carella, Jérôme Faure-Vincent, Renaud Demadrille, Jean-Pierre Simonato. Progress in understanding structure and transport properties of PEDOT-based materials: a critical review. Progress in Materials Science, 2020, 108, pp.100616. 10.1016/j.pmatsci.2019.100616 . hal-03140624

HAL Id: hal-03140624

https://hal.science/hal-03140624v1

Submitted on 21 Dec 2021

HAL is a multi-disciplinary open access archive for the deposit and dissemination of scientific research documents, whether they are published or not. The documents may come from teaching and research institutions in France or abroad, or from public or private research centers.

L'archive ouverte pluridisciplinaire **HAL**, est destinée au dépôt et à la diffusion de documents scientifiques de niveau recherche, publiés ou non, émanant des établissements d'enseignement et de recherche français ou étrangers, des laboratoires publics ou privés.

Distributed under a Creative Commons Attribution - NonCommercial 4.0 International License

Version of Record: https://www.sciencedirect.com/science/article/pii/S0079642519300982
Manuscript_a46adb0a191d99cf775374ea2334eaee

Progress in understanding structure and transport properties of PEDOT-based materials: a critical review

Magatte N. Gueye[1,2,3*], Alexandre Carella[1], Jérôme Faure-Vincent[3], Renaud Demadrille[3], Jean-Pierre Simonato[1*]

1. University Grenoble Alpes, CEA/LITEN/DTNM, MINATEC Campus, F-38054 Grenoble, France

2. Institute for Electronics, Microelectronics and Nanotechnology (IEMN), CNRS, University Lille, 59650 Villeneuve d'Ascq, France

3. University Grenoble Alpes, CEA, CNRS, INAC-SyMMES, F-38054 Grenoble, France

Corresponding Authors:

Magatte Niang Gueye, magatte.gueye@protonmail.com, +33.320 191 817,

Jean-Pierre Simonato, jean-pierre.simonato@cea.fr, +33.438 781 139,

CEA Grenoble, 17 rue des Martyrs, 38054 Grenoble, France.

Abstract

Since the late '80s, a highly stable conductive polymer has been developed, that is poly(3,4-ethylene dioxythiophene), also known as PEDOT. Its increasing conductivity throughout the years combined with its intrinsic stability have aroused great attention both in the academic and industrial fields. The growing importance of PEDOT, can be easily acknowledged through the numerous applications in thermoelectricity, photovoltaics, lighting, sensing, technical coatings, transparent electrodes, bioelectronics, and so forth. Although its high electrical conductivity is strongly established in the literature, the wide range of data shows that disorder, as the limiting factor in charges' transport, hinders the design of materials with optimal

© 2019 published by Elsevier. This manuscript is made available under the CC BY NC user license
https://creativecommons.org/licenses/by-nc/4.0/

performances. The aim of this article is to review and discuss recent progresses dealing with the electrical conductivity and transport properties in PEDOT materials, with special attention on morphological and structural features. Particular emphasis is given to the commercial PEDOT:PSS as well as other PEDOT-based materials stabilized with smaller counter-anions. It appears that the electrical conductivity and the transport mechanisms are closely related to the fabrication process, the crystallinity of the material and the choice of the counter-anions. With the tunable electrical properties, new functionalities appear accessible and add up to the already existing applications that are concisely highlighted.

Keywords

PEDOT, conducting polymers, synthesis, structure, characterization, electronic transport

Introduction

Organic electronics is a field of materials science that deals with the design, synthesis and study of organic materials whose electrical properties are interesting enough to consider them for technical applications. To give that story its fullest insight, we have to go through more than a half century of materials science research and look towards future applications.

The whole story could be said to have begun with the discovery of conducting polymers, or rather the keen interest that arose after the pioneering work of Hideki Shirakawa, Alan Heeger and Alan MacDiarmid.[1,2] They showed that the conductivity of polyacetylene could be tuned over several orders of magnitude. Soon after their discovery, the materials of their studies, namely electrically conductive polymers, were considered as a new generation of materials which exhibit the “electrical and optical properties of metals or semiconductors and which retain the attractive mechanical properties and processing advantages of polymers”.[3]

Conducting polymers stand out for the unique combination of their mechanical, electrical, optoelectronic, thermoelectric, photovoltaic and lighting properties. Among conducting polymers PEDOT has drawn most of

the attention in both academic studies and industrial applications due to its relatively high conductivity and remarkable stability in ambient conditions compared to other polymers, as well as its potential to be transparent in the visible spectrum. The importance of PEDOT is striking when assessing the numerous reviews that have been published over the last two decades, dealing with its synthesis, properties, conductivity enhancement and different viewpoints of applications.[4–20]

The main property of PEDOT that ensures its unique place among conducting polymers is its high and stable electrical conductivity. This latter has been increased up to 6259 S cm^{-1} for thin films and 8797 S cm^{-1} for single crystals.[21–25] These conductivity values are remarkable since they are only one order of magnitude lower than the most conductive metals, namely silver and copper. Such large scale gives an overview of the remarkable advancement performed on the conductivity enhancement, but at the same time, the dispersion of data found in the literature suggests that there is still room for a better understanding of that material. Theories aiming at describing the origin of the enhancement observed in PEDOT:PSS in particular, and all other PEDOT materials in general, are still far from reaching a general consensus. However, the progresses realized these past years unraveled features that allow a deeper understanding of the role of disorder as the main limiting factor in the charge transport in these materials.

Since the optimization of the electrical conductivity is highly sought and that the electrical properties are inherently linked to the transport properties, a deeper understanding of such properties can be highly beneficial for a better design of materials.[26] Due to the importance of PEDOT, lots of reviews are dealing with its synthesis, its integration in devices, and various of its applications.[4,5,14–20,6–13] Several transport mechanisms theories have also been reported but they strongly differ from one PEDOT material to another. Since the understanding of transport properties is highly important for the design of materials with desired structure/properties relationship, in this article, we aim to review transport properties and mechanisms that have been presented and discussed in the literature, taking into account the electrical properties and the associated physical structures of the material.

For that purpose, we present a brief overview of the transport properties in conducting polymers, and we emphasize the breakthrough that PEDOT has represented for conducting polymers. Afterwards, the synthesis of PEDOT materials as well as their general chemical and optical properties are discussed. The progress in electrical properties related to the transport mechanisms reported for PEDOT materials are exposed and eventually, description of selected applications is put forward to further point out the importance of PEDOT materials, be it for current research or future applications.

1. Transport properties in conducting polymers

Conducting polymers are inherently disordered materials. In fact, the material is constituted with polymer chains with various lengths and defects non-uniformly distributed within the chain. Thus there is a combination of various conjugation lengths (the effective distance along which the electrons are delocalized along the chains).

π -π interactions between chains can give rise to weak Van der Waals forces so that polymer chains are more or less well stacked. The overall materials then have crystalline domains whose size can reach tens of nm and amorphous domains, as illustrated in Figure 1.[15,27,28] In such disordered materials, the charge transport is fast along the chains, moderate between the chains and slow between the lamellar planes (Figure 2).[28–31] Also, the chains can be randomly oriented through the x, y or z axes. One can easily understand that transport properties would be optimized in the case of Figure 1a rather than in Figure 1c. It is commonly admitted that high carrier mobility is linked to the degree of order and the relative stacking between the chains. Both high carrier mobility and/or efficient intra- and inter-chain transport are therefore sought in order to optimize the transport properties in conducting polymers.[32]

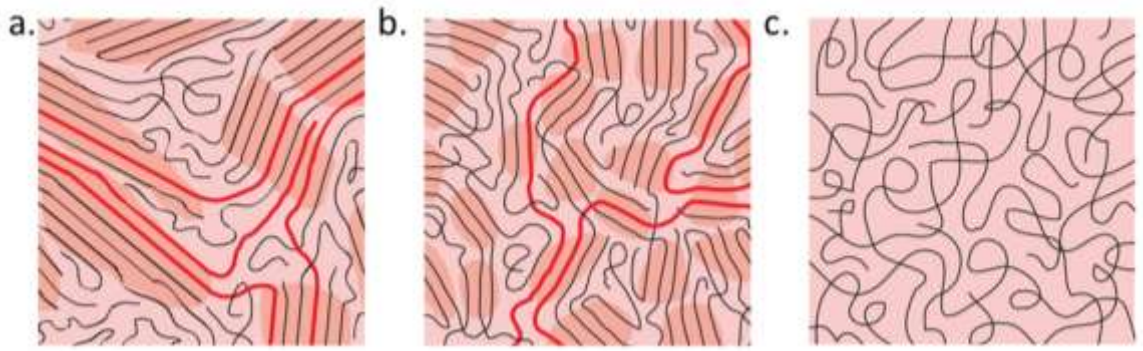

Figure 1. Schematic structure of polymers with different disorder levels. (a) Very ordered, (b) disordered aggregates and (c) completely disordered. Depending on the density of the polymer, long chains (highlighted in red) can connect ordered regions (darker orange ones) without significant loss of the conjugation length. [28]. Copyright 2013, Springer Nature.

As enlightened by Anderson, lack of crystal symmetry and lack of long distance order induce localization of the charges' wavefunctions so that charge transport is only possible through quantum mechanical jumps from a localized site to another.[33] Transport in conducting polymers can therefore be different from that in metals or classical semiconducting materials depending on the extent of disorder.

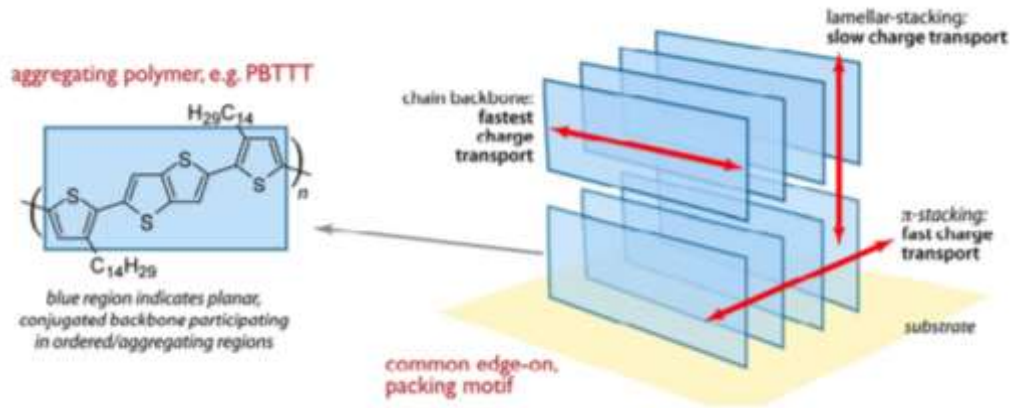

Figure 2. Fast, moderate and slow transport along the chain backbone, the π-π stacking and the lamellar stacking respectively in conducting polymers.[28]. Copyright 2013, Springer Nature.

Transport mechanisms are mainly assessed through the temperature dependence of electrical conductivity from room temperature down to liquid helium temperature, the temperature dependence of the Seebeck coefficient, the magnetic dependence of the electrical conductivity or field effect measurements. The former one has been used predominantly in the literature since it is the most accessible one in order to identify the various transport regimes and that a first general picture can be easily drawn.[34–36]

The electrical conductivity σ of a material is given by Equation 1.

$$\sigma = n|e|\mu \qquad (1)$$

With n the charges carriers' density, e the electronic charge and μ the mobility of the charges.

In metals, the band theory predicts no band gap between the highest occupied energy level and the lowest one. Therefore, electrons can be easily excited to unoccupied states. Without thermal energy at T = 0 K, the highest occupied energy level is called the Fermi level and there is no sharp distinction between occupied and unoccupied states. Above T = 0 K, more and more electrons are excited into higher unoccupied states, which would lead to an increased electrical conductivity. This is however not the case since the increase

number of excited electrons is compensated by their thermal motions. Collisions between electrons and atoms hinders the charge transport so that the mobility μ is decreased, and therefore the mean free path, as well as the electrical conductivity σ (Figure 3d). However the conductivity does not decrease indefinitely and the minimum metallic conductivity compatible with a minimum free path is called the Mott-Ioffe-Regel limit (see Figure 6).

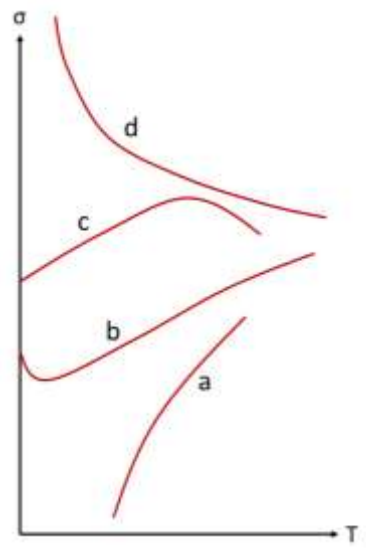

Figure 3. Temperature dependence of conductivity from a semiconductor to a metal: (a) semiconductor, (b) & (c) semiconductor or disordered metal with metallic behavior, (d) metal.

A different mechanism is observed in classical semiconductors such as silicon (Figure 3a). At T = 0 K, the band gap between the valence band and the conduction band does not allow the extraction of charges. Above T = 0 K, more and more valence electrons are excited into the conduction band and n increases. As the density of charge carriers is lower than in the case of metals, collisions do not hinder the transport mechanism and the electrical conductivity increases with temperature.

Contrarily to classical semiconductors in which charges carriers' density n increases with temperature as more and more electrons are excited, in conducting polymers the density is constant (solitons, polarons and bipolarons). Above T = 0 K, the mobility of the charge carriers increases due to thermal motion and so does the electrical conductivity. In highly disordered materials, the Anderson localization predicts the absence of diffusion of the charges all over the material and the localization of their wavefunctions.[27,33] Based on this theory, Mott's variable range hopping (VRH) theory gave a first insight of transport mechanisms in strongly disordered semiconductors. Such model states that the transport of charges is function of the distance between two localized sites and the difference between the associated energies.[27,37] Thus in conducting polymers hopping between two localized states occurs when the thermal vibration of the chain changes the energy of these states. The mobile charge (soliton, polaron or bipolaron) hops from a site to another. This hopping is possible if there is no charge in the terminal site, and if there is a fixed charge nearby (the counter-ion) as there is a strong coupling between the mobile and fixed charges. The conductivity is given by Equation 2:

$$\sigma_{\mathrm{VRH}}(\mathrm{T}) = \sigma_0 \exp\left[-\left(\frac{\mathrm{T}_0}{\mathrm{T}}\right)^{\frac{1}{\mathrm{n}+1}}\right] \qquad (2)$$

With σ_0 characteristic of the overall conductivity, T_0 related to the activation energy (depending both on the physical distance and the energy barrier between two sites) and n the dimension of the conduction. Hence n = 3 corresponds to a 3D hopping between localized sites corresponding to polaron/bipolaron quasiparticles extended over few PEDOT monomer units.[38] When n decreases, some directions are favored, meaning that a certain order or anisotropy has appeared. However, it is noteworthy that n = 1 could also account for two other transport mechanisms, that is a 3D hopping when electrons-electrons Coulomb interactions are taken into account at low temperatures; or a tunneling-like model as described in the following.[39–43] One should therefore be cautious when interpreting n = 1 in Equation 2 and should take into account the morphology or additional measurements such as magnetoresistance before being able

to draw a clear picture between 1D-VRH along parallel 1D chains of conducting polymers, 3D-VRH between localized sites or tunneling between neighboring chains of polaronic clusters.

The hopping model successfully described the behavior of early developed conducting polymers with an important extent of disorder, but is however not totally satisfactory as it cannot explain the relatively high conductivity (> 10 S cm^{-1}) or some metallic behavior in conducting polymers like highly doped polyacetylene, polyaniline or PEDOT.[1,44–48] In 1980, Sheng revisited the hopping model and proposed a model called *fluctuation induced tunneling* inspired from his previous work on *charging-energy-limited tunneling*.[41,42] The latter was developed for granular metals dispersed in a dielectric matrix. Contrarily to Mott's VRH, the charge carriers are thermally activated and an electron is removed from a neutral grain and injected to another neighboring neutral grain *via* tunneling. For semiconductors, Sheng inferred that transport was dominated by charge transfers between large conducting segments rather than hopping between localized states. Thermal vibrations were thought to induce energy fluctuations between two close segments of the polymer which were highly doped so that tunneling of the charges could occur. The *fluctuation induced tunneling* model, given in Equation 3, was able to explain the non-typical semiconducting behavior observed in polyacetylene.

$$\sigma_{\mathrm{Sheng}}(\mathrm{T}) = \sigma_{\mathrm{S}} \exp\left(-\frac{\mathrm{T}_1}{\mathrm{T}+\mathrm{T}_2}\right) \quad (3)$$

Where σ_{S}, T_1 and T_2 are constant parameters, and , T_1 and T_2 the tunneling temperatures depend on the barrier geometry and energy.

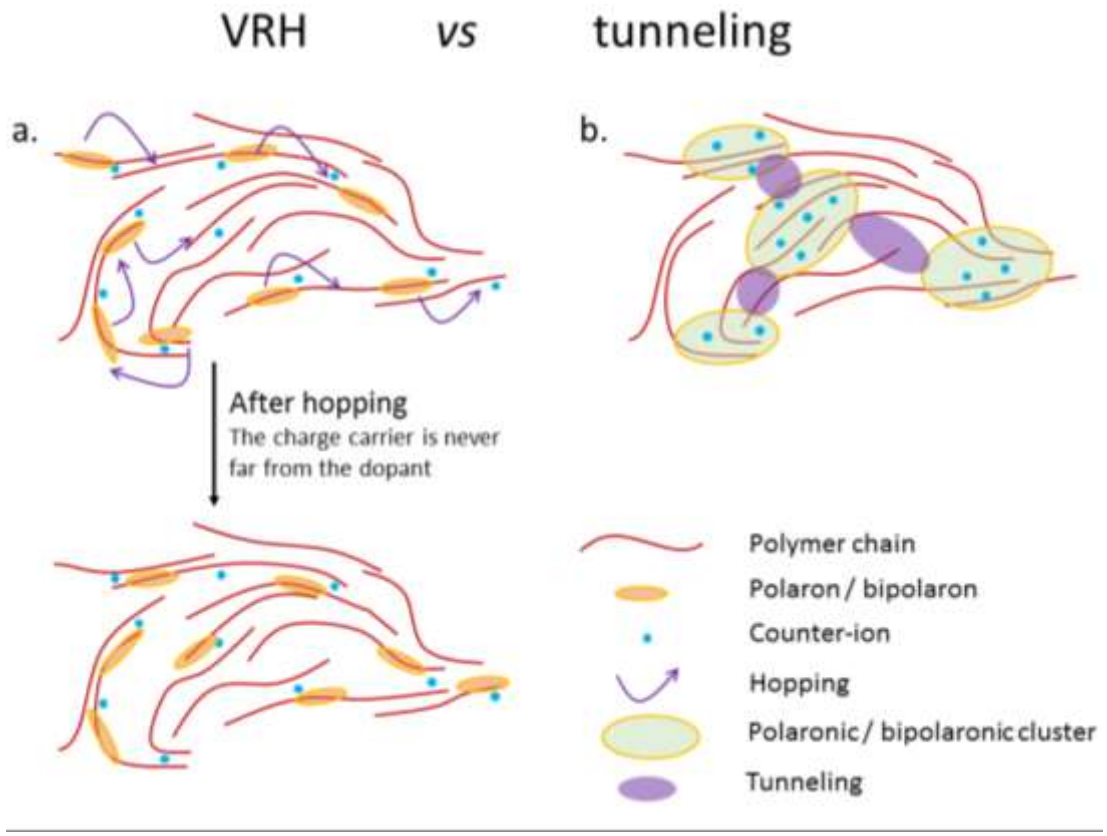

Figure 4. Schematic representation of (a) the variable range hopping model *vs* (b) the tunneling model. Due to the disorder, Anderson localization predicts the localization of the charges carriers' wavefunctions. While charges are strongly delocalized in the first place, inducing VRH, a less pronounced disorder in the second case results in charges that are close enough to induce a local delocalization, the formation of more densely charges zones (polaronic and bipolaronic clusters) and therefore another transport mechanism.

In 1994, Zuppiroli and coworkers, inspired from the fluctuation-induced tunneling model, enlightened the arrangement of charges that could lead to such a model of conduction between large conductive segments.[43] They showed through calculations and temperature dependence conductivity measurements that transport does not occur solely from hopping between single polarons and bipolarons along the chains. Instead, polaronic clusters dispersed in the polymer matrix are created, and similarly to Sheng's model,

hopping can take place between two strongly doped polaronic clusters separated by less doped domains. At T = 0 K, charge carriers stay in the vicinity of the dopants from which they originate. Above zero temperature, hopping depends both on the probability of creating an excited state from an extra electron from one cluster and an extra hole from another, and the probability for the tunneling between clusters (Figure 4). Such model was perfectly described by the fluctuation-induced tunneling in Equation 3. It is noteworthy that "tunneling" here does not refer to the quantum mechanics phenomenon but rather a transfer from a cluster to another as explained in Figure 4.

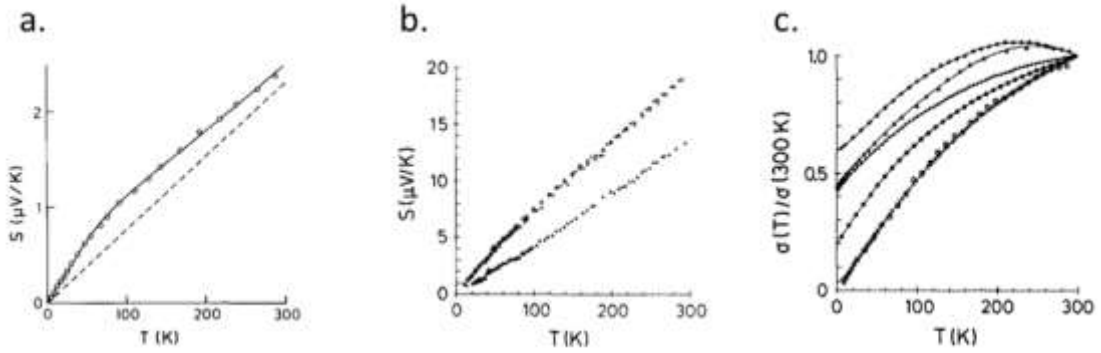

Figure 5. (a) Typical metallic thermopower in Zr-Ni alloy. (b) Approximately linear thermopower in doped polyacetylene. (c) Temperature dependence of conductivity in doped polyacetylene. [49]. Copyright 1991 by Elsevier B.V. (copyright review from Elsevier requested).

With the progress in conducting polymers synthesis and processing, more and more ordered films have been obtained. Some metallic features became so prominent that neither the VRH nor the tunneling theory could describe them. The temperature dependence of conductivity of CSA doped PANI or highly doped polyacetylene had a finite value at zero temperature, and sometimes depicted a negative slope (Figure 3 and Figure 5).[49–51] The dependence on temperature of their conductivity was relatively weak compared to less doped or more disordered materials. Their temperature dependence of thermopower showed a linear

behavior, typical of metals (Figure 5). No energy gap was visible with optical spectroscopy techniques in highly doped polyacetylene. Moreover, it was shown that the counter-ions in the polymer film were spatially removed from the conduction path and that π-π interactions were strong enough to avoid localization of charges.[52] On the other hand, some amorphous alloys and some highly disordered metals were shown to have a much smaller temperature dependence of their conductivity compared to pure metal, and even sometimes depicted a semiconducting behavior.[53] Due to such behavior, they were said to be driven through a metal to semiconductor transition (the so-called Metal-Insulator Transition).[54] Doing the parallel with disordered metals, polyacetylene was described as an anisotropic metal in which the charge density is high enough to create the overlapping of their wavefunctions on long distances and the coupling between the dopant and the charge is weakened. Other polymers such as PANI and PEDOT were also reported to depict such metallic behavior.[3,47,55,56] In such systems, charge transport is similar to that of disordered metals or "quasi1D-metals".[36] Both metallic transports were inspired from disordered or amorphous metals in the metal-insulator transition and then applied for conducting polymers. In the first case, charge carriers wavefunctions overlap so that they can freely diffuse in the polymer matrix but some strong localization effects due to disorder prevent from a crystalline metallic conduction.[36,57] The latter one is mostly reported for anisotropic conducting polymers. In such anisotropic systems the transport properties are exacerbated along the chains direction so that the transport is considered quasi one dimensional. Following are the conductivity laws of disordered metals in Equation 4 and quasi 1D-metals in Equation 5.[52,57]

$$\sigma_{disordered\ metal} = \sigma_0 + mT^{1/2} + BT^{p/2} \qquad (4)$$

Where σ_0 is the "zero temperature" pure metallic conductivity, the second term reflects electrons-electrons interactions and the third term is a correction due to localization effects.

$$\sigma_{\text{quasi 1D-metal}} = \sigma_{\text{m}} \exp\left(\frac{\text{T}_{\text{m}}}{\text{T}}\right) \qquad (5)$$

Where σ_m is a constant parameter and T_m represents the energy of the phonons that can backscatter the charges.[49]

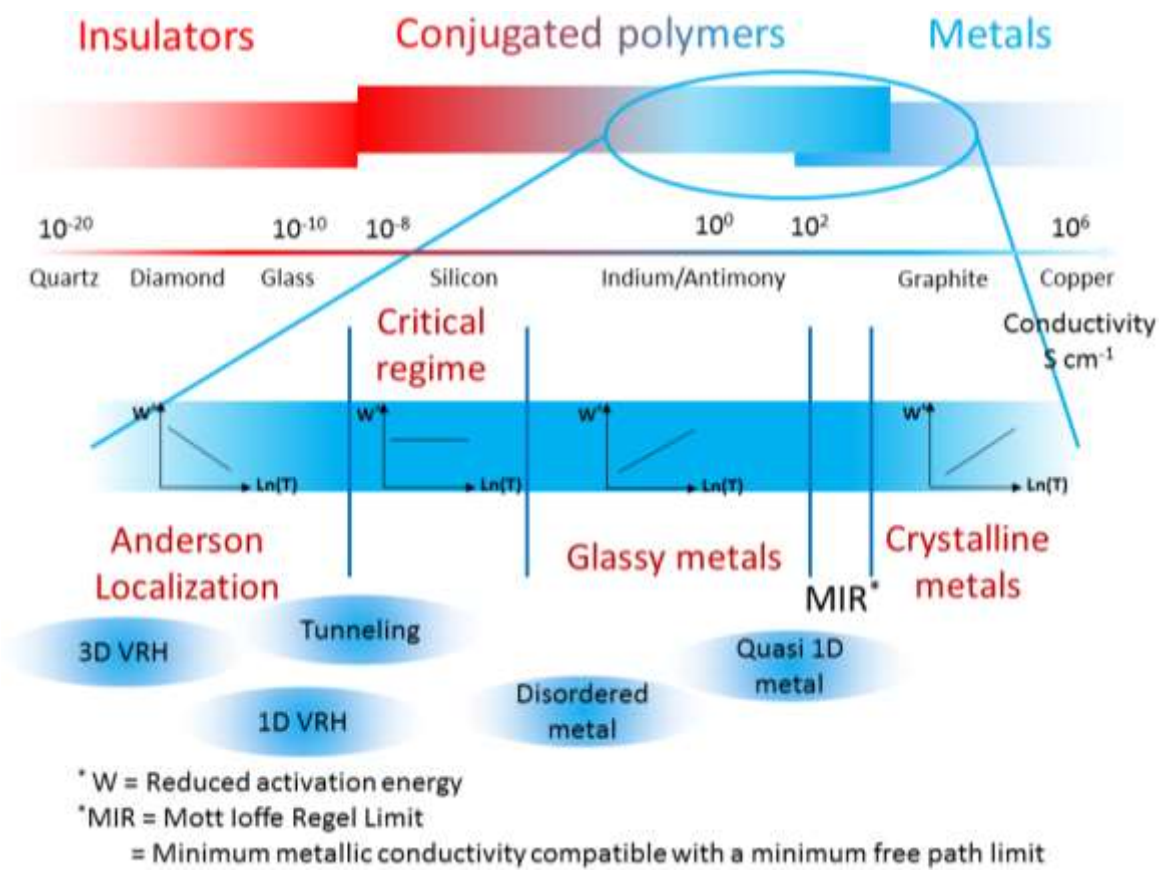

Figure 6. Scheme representing the place of conjugated polymers between metals, semiconductors and insulators. Examples of materials are given as function of their electrical conductivity. The inset corresponds to conducting polymers and schematizes the different transport regimes that can be found around the critical regime of the insulator to metal transition.

Simply put, as summarized in Figure 4 and Figure 6, in disordered conducting polymers, charges are localized and transport is facilitated by hopping from a site to another. In conducting polymers in which some local order can be noticed, polaronic clusters (in crystalline domains or disordered chains) are found and

tunneling can occur between two highly doped segments separated by less doped ones. In heavily doped or very well ordered conducting polymers, coherent transport can occur without the coupling of charge carriers with the counter-ions. Hence, depending on the disorder or the degree of doping, conducting polymers also can lay near the metal-insulator transition (in parallel with early works on disordered metals).[49,50] This metal-insulator transition can be assessed through the reduced activation energy W(T) in Equation 6, which increases (respectively decreases) in the metallic (respectively insulator) regime, as illustrated in Figure 6.[44,58]

$$\mathrm{W(T)} \equiv \frac{E(T)}{kT} = \frac{\mathrm{d[ln(\sigma)]}}{\mathrm{d[ln(T)]}} \qquad (6)$$

Where E(T) is the activation energy characteristic of the transport model and k the Boltzmann constant.

In the critical regime, W(T) is constant and the temperature dependence of conductivity follows a power law as in Equation 7:

$$\sigma(T) \propto T^{-\beta} \qquad (7)$$

With $0.3 < \beta < 1$ in most cases.

Along with the reduced activation energy the resistivity ratio $\rho_r = \frac{\rho(0\ K)}{\rho(300\ K)}$ is a good indicator of the transport regimes and the degree of disorder. A lower ρ_r corresponds to a more ordered film. Indeed, since the drop between the room temperature and the near 0 K resistivity is moderate, the temperature dependence of the resistivity (or the conductivity) is weak meaning that high energy barriers induced by heavy disorder are not encountered.

Progress made in the field of conducting polymers allowed to unravel the importance of the disorder in the transport mechanisms. Conducting polymers appear to stand at the metal-insulator transition and several theories were led in order to shed some light on the different conduction pathways. Even though no consensus could be reached regarding the transport properties, this can be easily explained by the too broad performance of the materials and the different chemistries that build them. Recently, Kang and

Snyder proposed a generalized transport model that takes into account all mechanisms of electronic conduction from metals to hopping insulators.[59] The charge transport is described by Boltzmann transport equations characterized by a transport function σ_E, or in other words probability equations relating the electrical conductivity when mobile carriers have the same energy E to energy states following a Fermi-Dirac distribution. Their model encounters for a percolation of charge carriers from conducting ordered regions through poorly conducting disordered regions and is consistent with the reported structure in conducting polymers.

In the following we will focus on PEDOT, this conducting polymer that aroused, and still does arouse, great attention among academics and industrials.

2. The breakthrough of PEDOT

Polyacetylene is the first conducting polymer reported with conductivities exceeding 10^5 S cm^{-1}, close to that of copper, and transport properties similar to that of a metal.[60] This material is however air-sensitive and not processable, hence not appropriate for industrial applications.[61] Regarding the lack of stability of the π-electron system in the doped state, strategies to solve this issue were developed through the addition of electron donating heteroatoms such as nitrogen (N) or sulfur (S) either in the main chain or as carbon substituent in heterocycles. Researchers then turned their attention to polyaniline, polypyrrole and polythiophene.[62,63] These polymers are in general unstable, infusible and most of them are insoluble, but more stable derivatives have been developed from polythiophenes.[5,64–66] In the search to stable conducting polymers that are relevant for industrial applications, the German Bayer Central Research Department has been highly active. [15,67] When their first attempts to stabilize polyacetylene failed and their works on polypyrrole were aborted, they focused on monoalkoxy and 3,4-dialkoxy substituted thiophenes to increase the stability, and on bicyclic rings structures in order to decrease the steric hindrance.[68]

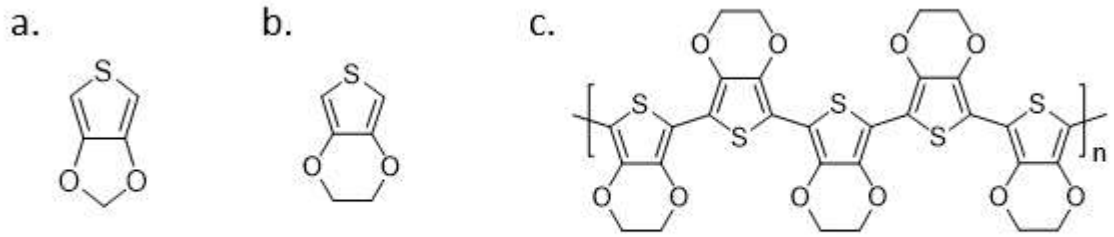

Figure 7. (a) Methylene dioxythiophene (MDOT), (b) 3,4-ethylene dioxythiophene (EDOT) and (c) poly(3,4-ethylene dioxythiophene) (PEDOT).

Their first efforts on the synthesis of 3,4-methylenedioxythiophene (MDOT, see Figure 7) was unsuccessful as they did not manage to isolate a workable amount of the monomer. Subsequently, they focused on 3,4-ethylenedioxythiophene (EDOT), whose success was immediate. After polymerization with an oxidative reagent, i.e. iron(III) chloride, the obtained poly(3,4-ethylenedioxythiophene) (PEDOT) appeared as a breakthrough in conducting polymers, since it was found to be stable in its doped state and depicted conductivities up to 200 S cm^{-1}. [63,68,69] The synthesized PEDOT straightforwardly found applications in capacitors.[21] After the first oxidative polymerization of PEDOT reported by researchers from Bayer AG in 1988, they also investigated the first electro-polymerized PEDOT the same year.[22]

The electrical conductivity of PEDOT and its air and water stability were interesting. However, chemically synthesized PEDOT is black, insoluble and infusible while electrochemically synthesized PEDOT can only be formed on conductive substrates. An alternative processable solution was strongly desirable. Bayer's scientists found it shortly after during a collaboration with chemists from Agfa, who were looking for new antistatic coatings for their photographic films. As a matter of fact, the available material they used as antistatic coating, namely the sodium salt of polystyrene sulfonate, (PSSNa), suffered from humidity

dependence of its conductivity. By oxidizing EDOT with persulfates and polymerizing in the presence of PSS in water, they obtained an aqueous dispersion of PEDOT stabilized with PSS^- as counter-anion, which showed high stability.[4,70] Subsequently, PEDOT:PSS, and PEDOT in general, became highly valuable for both industrials and academics.

3. Synthesis of PEDOT

The development of PEDOT took advantage of all the expertise already accumulated from the earlier development on conducting polymers.[44,46,71] The techniques that will be described in the following part were already used for other polymers. The report we propose herein is limited to the scope of PEDOT for the sake of conciseness.

PEDOT can be synthesized through three main polymerization reactions:

- Transition metal-mediated coupling of dihalogeno derivatives of EDOT
- Electrochemical polymerization of EDOT-based monomers
- Oxidative chemical polymerization of EDOT-based monomers

These synthesis routes will be briefly introduced. The interested reader can refer to more specialized articles, reviews or books.[5,15,72]

3-1. Transition mediated coupling of dihalogeno derivatives of EDOT

In the synthetic routes that will be presented hereinafter, PEDOT is mainly present in its more stable oxidized p-doped form and is hard to de-dope due to the stabilizing effect of the electron donating dialkoxy groups. Regarding the interest to study the neutral PEDOT, Yamamoto *et al*. carried out polycondensation of 2,5-dichloro-3,4-ethylenedioxythiophene, following a reaction with a Ni(0) reagent, the scheme is presented

in Figure 8.[73] The dark purple product was however not soluble and therefore not amenable for molecular weight calculations, similarly to other doped PEDOT.

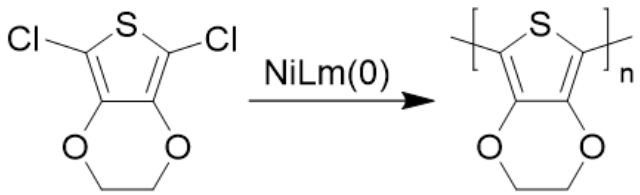

Figure 8. Nickel based polycondensation for neutral PEDOT synthesis. [73]

3-2. Electrochemical polymerization of EDOT-based monomers

PEDOT can be electrochemically polymerized in a three-electrode cell containing an electrolyte solution, the monomer (EDOT or EDOT derivatives) and the oxidant which can be added in the form of salts. PEDOT is formed on the anode's surface, commonly used ones being indium tin oxide (ITO), carbon paper or Au.[74,75] The reaction is fast and both supported and free-standing films can be obtained. The obtained product is transparent-blue to dark blue depending on the thickness, with conductivities up to 2074 S cm^{-1}.[76–78]

3-3. Oxidative chemical polymerization of EDOT-based monomers

Only routes using the EDOT monomer are presented hereinafter, Roncali *et al*. having already reviewed various synthesis methods for EDOT-based systems.[72]

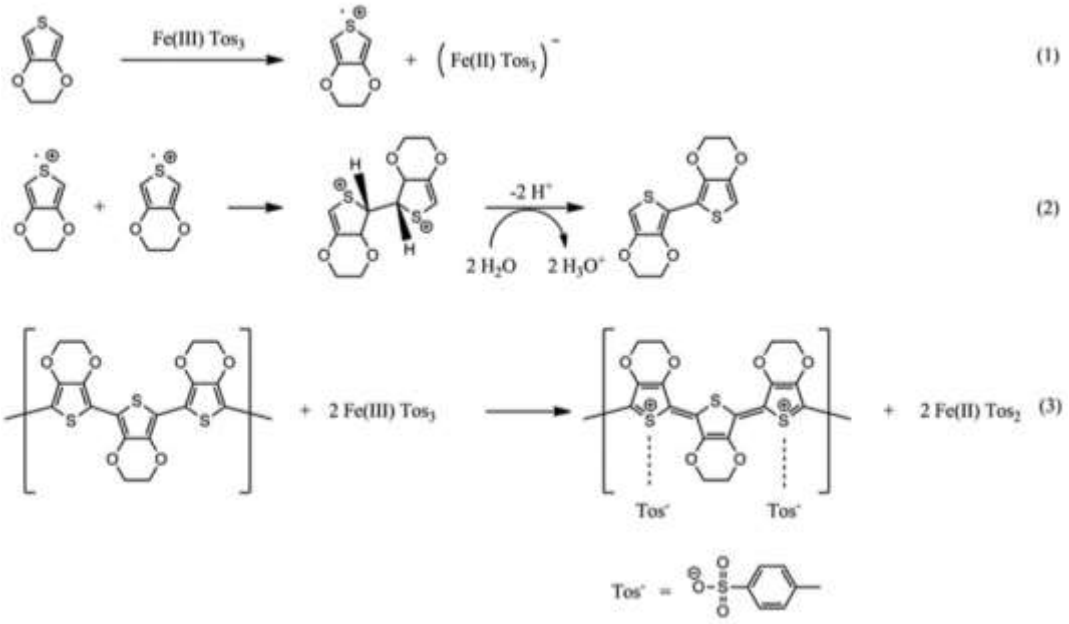

Figure 9. Proposed mechanism for the synthesis of PEDOT:Tos as reproduced from Mueller and coworkers' work.[79] Copyright 2012, Elsevier Ltd. (copyright review from Elsevier requested).

PEDOT can be polymerized from the monomer EDOT, which is commercially available. Iron (III) complexes proved to be efficient oxidants, the standard redox potential of the cation being high (0.77 V).[80] They also provide the counter-anion to stabilize the oxidized PEDOT.[81] Iron complexes that can be found in the literature are mainly:

- Iron(III) chloride ($FeCl_3$)
- Iron(III) *para*-toluenesulfonate or tosylate ($Fe(Tos)_3$) with Tos = ($CH_3C_6H_4SO_3^-$)
- Iron(III) camphor sulfonate ($Fe(C_7H_7OSO_3)_3$
- Iron(III) methanesulfonate or mesylate ($Fe(CH_3SO_3)_3$)
- Iron(III) trifluoromethanesulfonate or triflate ($Fe(OTf)_3$) with OTf = ($CF_3SO_3^-$)

The most commonly used in the literature is $Fe(Tos)_3$, which is even commercialized in a solution ready to use for the synthesis of PEDOT (Baytron C from HC Stark). The polymerization mechanism, although not fully understood, can be described as in Figure 9.[79,81]

- (1) Fe(III) oxidizes EDOT and is reduced to Fe(II)
- (2) Two oxidized EDOT combine into a 2-EDOT dimer which is further deprotonated by surrounding water molecules
- (3) Steps (1) and (2) are repeated in order to form polymer chains. Remaining Fe(III) ions dope the formed PEDOT and Tos^- ions are inserted as counter-anions in order to stabilized the doped PEDOT.

Several oxidative chemical polymerization methods can be found in the literature. The most common one, introduced with the first synthesis of PEDOT by Bayer AG in 1988, consists in introducing oxidizing agents in a mixture of the monomer and a solvent. A dark and insoluble product is precipitated. It is insoluble and infusible, and therefore cannot be processed easily. Conductivities of few tens S cm^{-1} were first reported.[68]

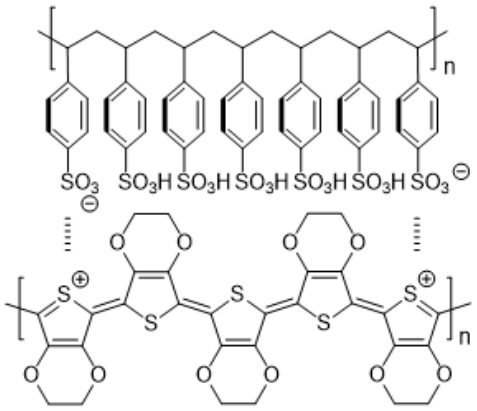

Figure 10. Chemical structure of PEDOT:PSS.

In 1990 a second processable method was introduced by Bayer AG. EDOT is polymerized in an aqueous polyelectrolyte solution (typically PSS) in the presence of $Na_2S_2O_8$ as the oxidizing agent. PEDOT is then stabilized by the counter-anion PSS^- and the blue dispersion resulting from that reaction, namely PEDOT:PSS whose structure can be found in Figure 10, is processable so that thin (~100 nm) to thick (> 1 µm) films can be obtained. The mechanically robust, transparent (depending on the thickness) and insoluble film has a high intrinsic conductivity up to 10 S cm^{-1} which, through decades of research, was improved up to 4839 S cm^{-1}.[82] Moreover, it is commercialized so that it was integrated in many devices and several relevant applications were able to emerge.[83]

In 1994 a third polymerization method suitable for surface films formation was reported by de Leeuw and coworkers since the commercially available PEDOT:PSS did not reach conductivities exceeding 10 S cm^{-1} at that time.[84] A solution containing *n*-butanol as a solvent, $Fe(Tos)_3$ as an oxidant, EDOT as the monomer and imidazole as a base inhibitor was spin-coated on a glass or plastic substrate. Polymerization occurred when the deposited film was heated up to 110 °C. The black, insoluble and infusible film obtained after rinsing with water and n-butanol exhibited conductivities up to 550 S cm^{-1}.[85] This method did however not

yield reproducible and homogeneous films at first. Later Hohnholz *et al*. also reported PEDOT grown directly on glass substrates from two solutions of the monomer EDOT and the oxidant iron(III) chloride.[86] These "*in-situ*" deposition techniques did not grow as much interest as the other ones.

In 2004 Winther-Jensen *et al*. reported a new oxidative polymerization route with conductivities exceeding 1000 S cm^{-1}.[87] That vapor phase polymerization (VPP) consisted of exposing a surface covered with a mixture of $Fe(Tos)_3$ as the oxidant, pyridine as a base to moderate the strength of the oxidant and EDOT vapors (Figure 11).[80,88,89]

Winther-Jensen and coworkers noticed that EDOT could participate in an acid initiated polymerization, whereby a partially conjugated polymer is formed, which leads to short conjugation lengths. The addition of a base is therefore of interest to prevent unwanted acidic side reactions. As a consequence, better results were obtained by adding pyridine in the VPP chamber.

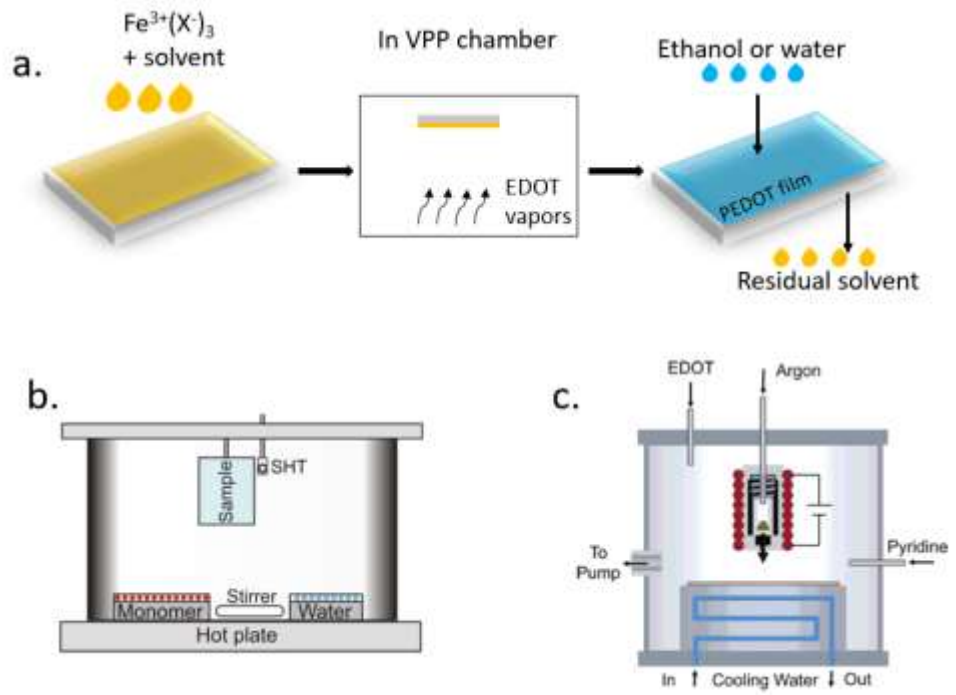

Figure 11. (a) Vapor phase polymerization principle (VPP). (b) VPP chamber, as reproduced from Murphy and coworkers' work.[90] (c) Another quite similar principle (chemical vapor deposition, CVD) principle as reproduced from Gleason and coworker's work.[88] It is slightly different from VPP. In here, no solvents are used and the oxidant is heated in the crucible that faces the substrate on which EDOT is adsorbed. Copyright 2010, Elsevier Ltd. (copyright review from Elsevier requested) Copyright 2006, American Chemical Society.

They further developed de Leeuw's solution-cast polymerization method in 2005.[91] Actually, de Leeuw and coworkers primarily added imidazole as a base to control the speed of polymerization as stated hereinbefore. However, the polymerization does not start before the removal of imidazole which requires high temperature heating (~ 110 °C). Moreover, imidazole, as most other N-H containing chemicals, coordinates to Fe(III), resulting in an undesired formation of crystals.[91] By using pyridine instead of imidazole as a basic inhibitor to control the acidity of the oxidative solution, good film forming properties were demonstrated and conductivities exceeding 1000 S cm^{-1} were routinely achieved.

These two new routes, surpassing by far all the previous routes reported so far in terms of conductivity (> 1000 S cm^{-1}), have been dominating the synthesis of PEDOT in the academic field ever since.

In 2006 Gleason and coworkers reported oxidative chemical vapor deposition (o-CVD), a solventless technique that does not require any pre-treatment nor wetting of the substrate surface.[88] The monomer EDOT and the oxidant $FeCl_3$ were both introduced in a vacuum chamber and PEDOT was grown on glass slides, silicon wafers, poly(ethylene terephthalate) or paper. The conductivity of PEDOT stabilized with chloride counter-anions reached 105 S cm^{-1} and conductivities were raised after acidic treatment up to 1620 S cm^{-1} when HBr is employed.[92]

Recently, liquid phase depositional polymerization (LPDP) was reported in order to emancipate from some drawbacks inherent to VPP and o-CVD.[93,94] Since these techniques are sensitive to moisture, since the dimension of the chamber limits the sample's size and since acidic side reactions take place without addition of organic bases, LPDP allows to overcome those drawbacks by implementing the polymerization directly into liquid phase. A substrate coated with the oxidant is suspended in EDOT solution to synthesize PEDOT coating *in situ*. Conductivities up to 362 S cm^{-1} are reached.[95]

In the following section of the review, when oxidative chemical polymerization is encountered, vapor phase polymerization will be referred to as VPP, oxidative chemical vapor deposition as o-CVD, polymerization on a substrate from a deposited oxidative solution as solution-cast polymerization and all other polymerization routes as chemical oxidation. It is important to understand that all three methods can be referred to as "*in-situ* oxidative chemical polymerization" in the literature and that the distinction we suggest here is only for the sake of clarity. Moreover, while numerous PEDOT-based composites materials are reported in the literature, we only focus here on PEDOT stabilized with counter-anions and non-hybridized with other materials. Readers can refer to other reviews for more information on those composite materials.[11]

4. Chemical properties of PEDOT materials

PEDOT chains are short, only up to few tens of monomer units.[96,97] Scanning tunneling microscopy (STM) of electro-polymerized PEDOT, high angle annular dark-field (HAADF) scanning tunneling microscopy of o-CVD PEDOT and transmission electron microscopy (TEM) of solution-cast polymerized PEDOT showed short PEDOT chains with around 10 to 20 monomer units.[98,99] Neutral PEDOT is in an aromatic state and undergoes a distortion from aromatic to quinoid form during doping, as schematized in Figure 12.[15,100]

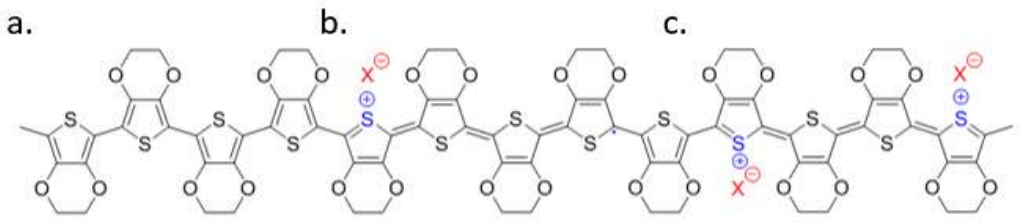

Figure 12. PEDOT in different states: (a) neutral, (b) polaron, (c) bipolaron.

The polymerization results in a polymer whose doping level is approximately 33 % (1 dopant for 3 monomer units).[100] PEDOT being insoluble in any common solvent, “standard” solution characterization techniques (such as NMR spectroscopy) cannot be used, and features such as their molecular weight remain often unraveled. Electronic and vibrational spectroscopies are however possible on thin or thick films and pieces of information such as their energy gap, their elemental composition, their doping level or their chemical state can be assessed.

5. Optical properties and doping level in PEDOT materials

In saturated polymers (all carbon atoms are sp^3 hybridized), the atomic orbitals merge into molecular ones and quantum physics predicts the arrangement of the energy levels into σ bonding and σ* antibonding

states. Energy bands are created and the gap between the filled valance band (σ bonding) and the empty conduction band (σ* antibonding) is too high, typically higher than 6 eV, which renders the polymer insulating.[101]

In conjugated polymers, quantum physics also predicts the formation of π bonding and π* antibonding states after the creation of a molecular orbital from the p atomic orbitals. These states are respectively the highest occupied molecular orbital (HOMO) and the lowest unoccupied molecular orbital (LUMO). The longer the chain becomes, the more states are created within these states and the energy gap between the HOMO and the LUMO decreases (Figure 13). When the chain becomes long enough (supposedly infinite) the molecular orbitals are so close that discretization ceases and energy bands are created, a completely filled valence band (VB) whose highest energy is the HOMO and a completely empty conduction band (CB) whose lowest energy is the LUMO. The energy gap between the HOMO and the LUMO is comprised between 1 and 4 eV, hence rendering conjugated polymers semi-conductors (Figure 13).[102]

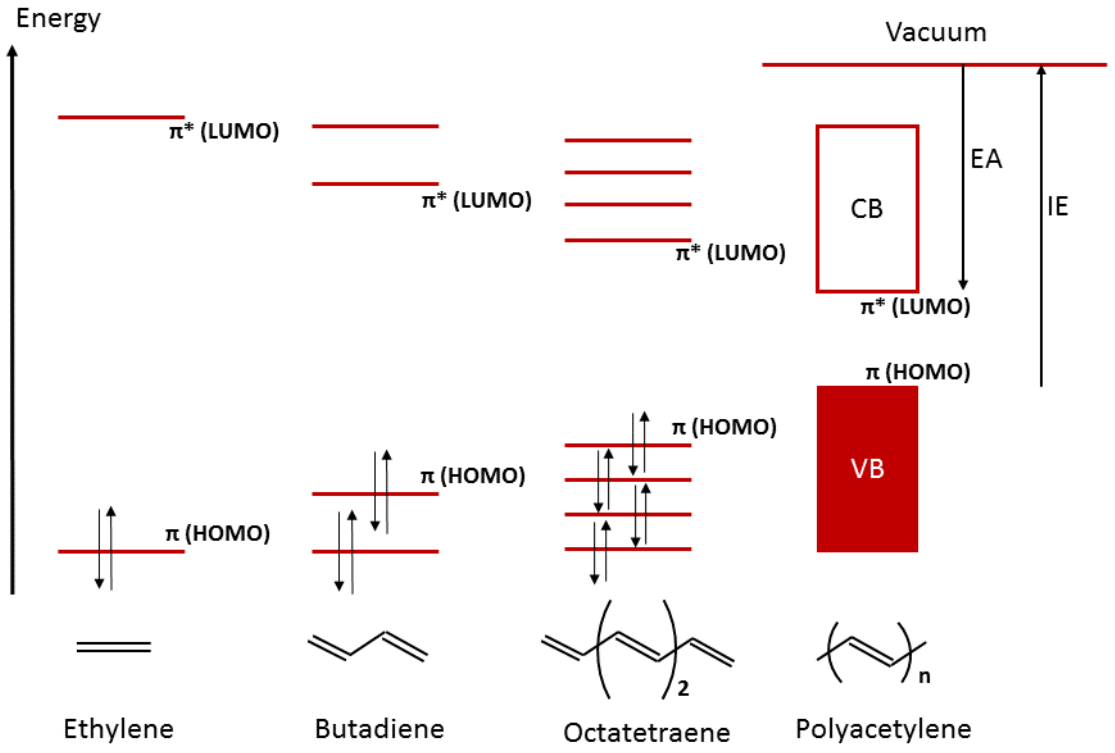

Figure 13. Band structure building in conjugated polymers. Reproduced after[101].

The optical features of PEDOT at various oxidation levels are schematized in Figure 14A and can be measured using ultraviolet-visible-near infrared (UV-Vis-NIR) spectroscopy. Figure 14B gives the evolution of the optical signatures from a neutral chain to a fully doped film. Neutral PEDOT is dark purple/blue and has an optical absorption gap around 1.5 eV.[74,103] When oxidized, new energy states are introduced in the band gap in the NIR region outside the visible range, and PEDOT becomes transparent in the visible range.

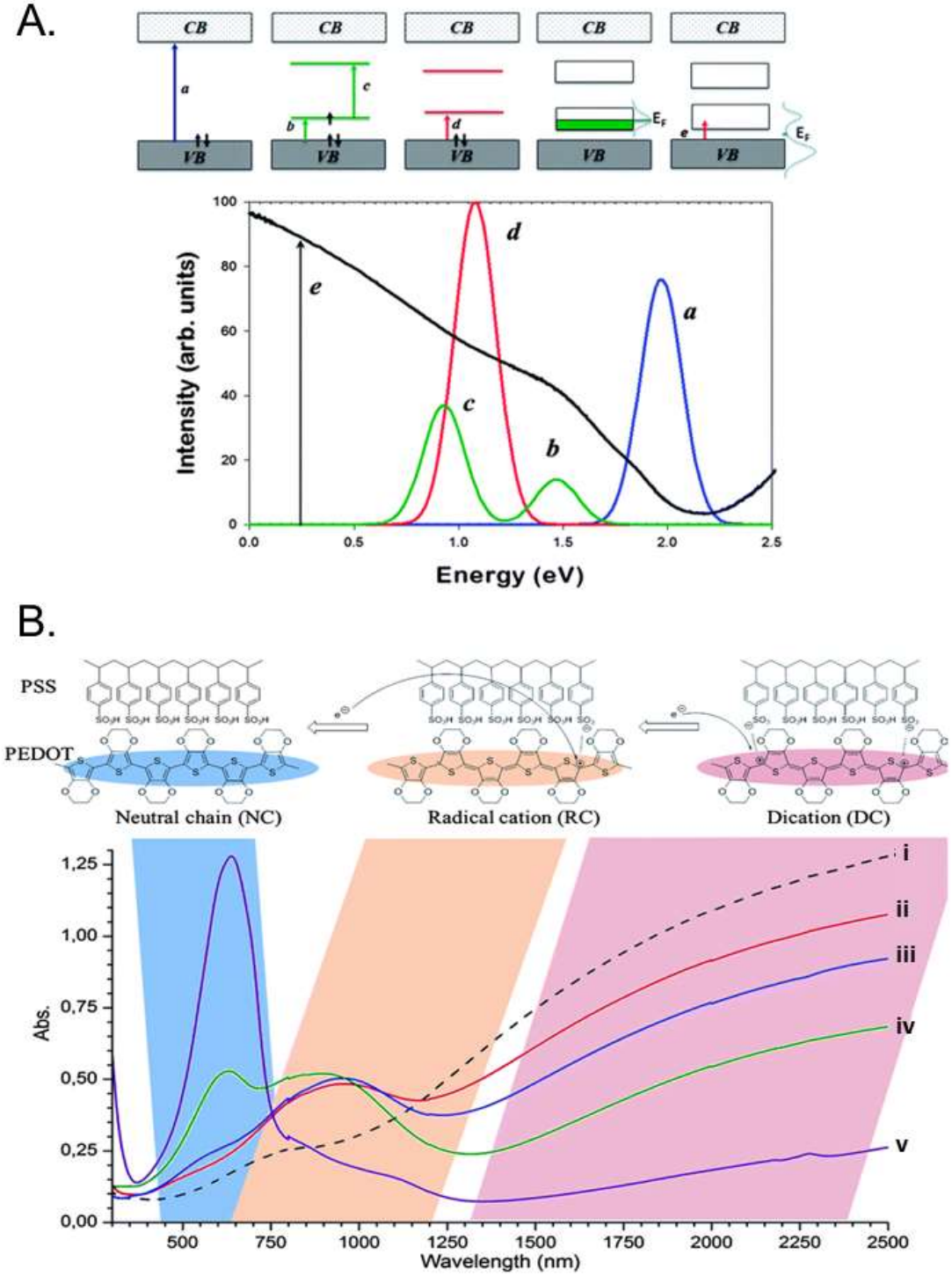

Figure 14. Evolution of the electronic characteristic of PEDOT at different doping levels.

(A) Upper image: from left to right: a neutral chain ('**a**' no charges are present in the chain and the corresponding transition in UV-Vis-NIR in the lower image is a band in the visible range), a chain with a polaron ('**b** & **c**' in UV-Vis-NIR, the energy transitions that are detected correspond to the transition from the VB to the polaronic band and the transition from the occupied state to the non-occupied state of the polaronic band. Those transitions appear at the end of the visible range), a chain with a bipolaron ('**e**' the transition in the bipolaronic band occurs in the NIR region), an intrachain or interchain polaron network inducing a polaronic band and an intrachain or interchain bipolaron network inducing a bipolaronic band ('**e**' in these last two cases, all transitions that can occur and which are due to the neutral chains, the polarons and the bipolarons are represented, hence giving such so know UV-Vis-NIR spectrum of PEDOT).[104]

(B) PEDOT chains with different doping states (upper image) and their corresponding UV-Vis-NIR spectra (lower image), from the most oxidized (i) to the less oxidized state (v).[105]

Copyright 2012, Royal Society of Chemistry (copyright review from Elsevier requested).
Copyright 2014, Royal Society of Chemistry (copyright review from Elsevier requested).

The optical properties of PEDOT find interesting applications in electrochromic devices and transparent electrodes. In the former case, the good electrochromic properties are controlled electrochemically by varying the doping level.[74,103,106] In the latter one the thickness of the film plays an important role. The thinner the film, the more transparent it becomes.[107] Recently Brooke *et al*. reported highly conductive and transparent PEDOT:OTf and PEDOT:Sulf comparable to ITO.[108] Their results are in good agreement with previously reported studies.[107]

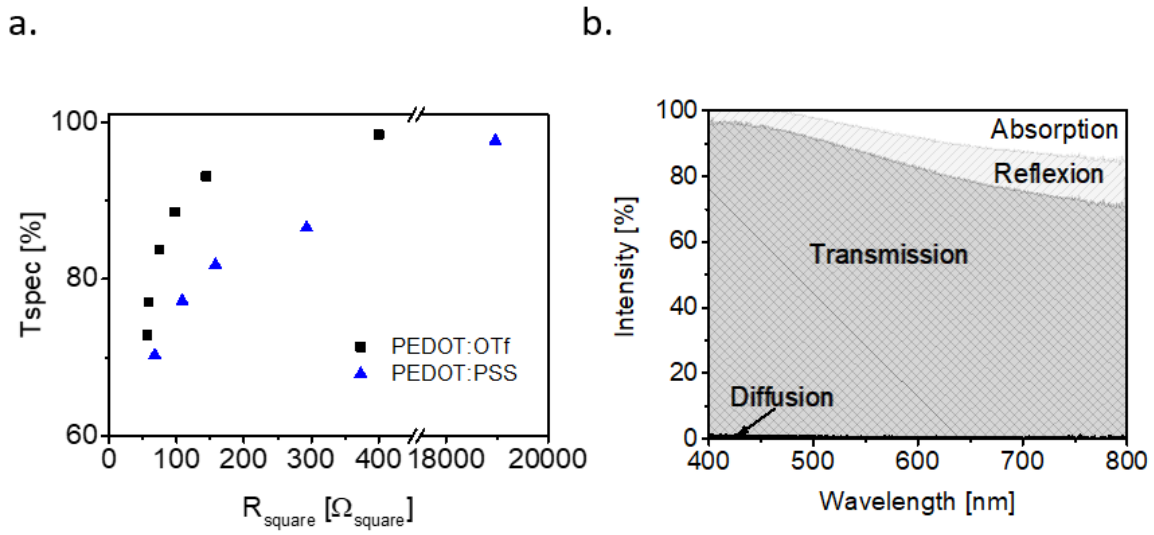

Figure 15. (a) Dependence of the specular transmittance at 550 nm as function of the sheet resistance of PEDOT:PSS and PEDOT:OTf. (b) Optical properties of PEDOT:Sulf in the visible range.[107]

In parallel to UV-Vis-NIR spectroscopy that gives information on the doping state, the doping level can be assessed through X-Ray photoelectron spectrometry (XPS) for PEDOT stabilized with small counter-anions.[96,97]

As can be seen in Figure 16, the sulfur S2p contribution originates from the thiophene rings and the counter-anion as they have different chemical environments. Therefore, using XPS surface elemental analysis technique, one can have access to the ratio PEDOT to counter-anion. In the case of PEDOT:PSS, PSS consists of a few hundreds of monomers whereas PEDOT only consists of some units to some tens.[96,97] Using XPS studies, combined with AFM imaging, Jönsson and coworkers suggested a grain-like structure for the PEDOT:PSS films, with a non-homogeneous distribution of PEDOT and PSS in the grains and an excess of PSSH around the grains. They inferred that those grains are probably defined by PSS random coils with PEDOT chains through coulombic interactions, and that the areas between the grains are probably filled with excess neutral PSSH.[97] Thus the PEDOT to PSS ratio only gives information on the quantity of PSS in

the films.[77] In the case of PEDOT stabilized with small counter-anions such as tosylate, the non-polymeric nature of the counter-anion prevents it from being in excess. Therefore, the ratio PEDOT to counter-anion is considered to give direct access to the doping level of PEDOT, which was calculated to be between 25 and 35 %.[5,77,109]

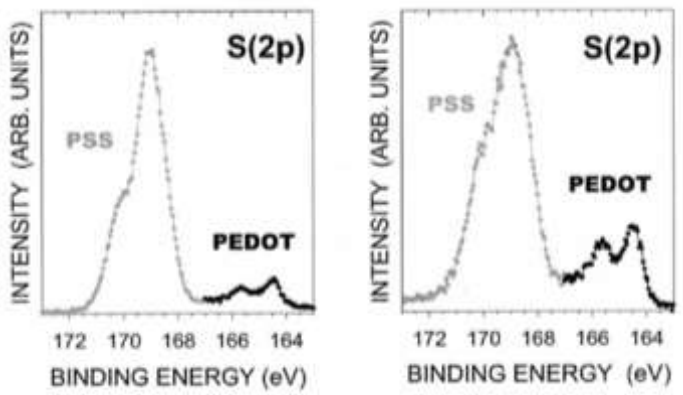

Figure 16. Typical sulfur doublet response of PEDOT:PSS polymer blends probed using XPS. The shift of S2p doublet between thiophene and PSS is clearly represented. The two figures represent PEDOT:PSS with more (left) or less (right) excess PSS.[13] Copyright 2001, Elsevier Science B.V. (copyright review from Elsevier requested).

6. Transport properties in PEDOT films

For all the applications that emerged after the synthesis of PEDOT:PSS, highly stable, processable and conductive PEDOT films have been the focus of intense research. In that respect, two main routes were studied, enhancement of the electrical conductivity of the commercially available PEDOT:PSS, and development of PEDOT based materials stabilized with smaller counter-anions such as chloride, tosylate, triflate, or sulfate.

6-1. PEDOT:PSS

6-1-1. Electrical conductivity through years

At first, commercialized PEDOT:PSS exhibited conductivities from 0.1 to 10 S cm^{-1}. Conducting polymers such as polyacetylene or polyaniline were routinely treated with organic solvents in order to increase their conductivities. MacDiarmid and coworkers introduced the concept of “secondary doping”, that should not be confused with “primary doping” which takes place during the oxidative polymerization of EDOT.[71] They stated that “secondary doping is very similar in many respects to primary doping. Phenomenologically, treatment of a polymer, already doped by a primary dopant, with an apparently 'inert' substance (secondary dopant) may increase the conductivity of the polymer by several orders of magnitude with concomitant changes in electronic spectra and, frequently, degree of crystallinity. *It differs from primary doping in that the changes, depending on the primary-secondary dopant combination employed, may frequently persist, possibly to a reduced extent, upon removal of the secondary dopant*”. Based on these works, Kim *et al*. added different solvents in an aqueous dispersion of PEDOT:PSS purchased from Bayer AG and increased the conductivity from 0.8 to 80 S cm^{-1} by adding dimethyl sulfoxide (DMSO).[110] They did not observe change in the doping level or in the polymer chain conformation as evidenced by electron paramagnetic resonance (EPR), XPS and X-Ray diffraction (XRD). Temperature dependence of conductivity measurements showed that PEDOT:PSS approaches the critical regime of the metal-insulator transition (activation energy W not temperature dependent, see Figure 6) when an organic solvent is added. The increase in conductivity was assumed to be due to a screening effect induced by the polar solvent which decreases the coulombic interactions between the charges on PEDOT and its PSS counter-anion. Jönsson and coworkers also investigated the chemical and morphological changes induced by the addition of solvents, at the origin of the increased conductivity. [13,96,97] Their XPS studies revealed an increase in the PEDOT-to-PSS ratio after mixing with solvents, which they attributed to some segregation of PSS excess from the surface of the grains and removal from the surface of the films. This was later observed by Crispin *et al*. as can be seen in the

atomic force microscopy (AFM) images in Figure 17.[111] This phenomenon induces a better connection between PEDOT:PSS grains and hence more efficient pathways for charge transport.

From that point onwards, various organic solvents were experimented such as dimethyl sulfoxide (DMSO), N,N-dimethylformamide (DMF), 1-methyl-2-pyrrolidone (NMP), glycerol, sorbitol, methanol, ethanol, isopropanol, ethylene glycol (EG), and so forth. Ouyang *et al*. showed that the treatment with EG induces a change from coil to linear or expanded coil structure.[112] Moreover, the conductivity enhancement strongly depends on the chemical structure of the solvent. Compounds with two or more polar groups are expected to be more efficient since the interaction between the dipoles of the solvents and the dipoles or charges of the polymer chains are thought to be at the origin of the conformational changes.

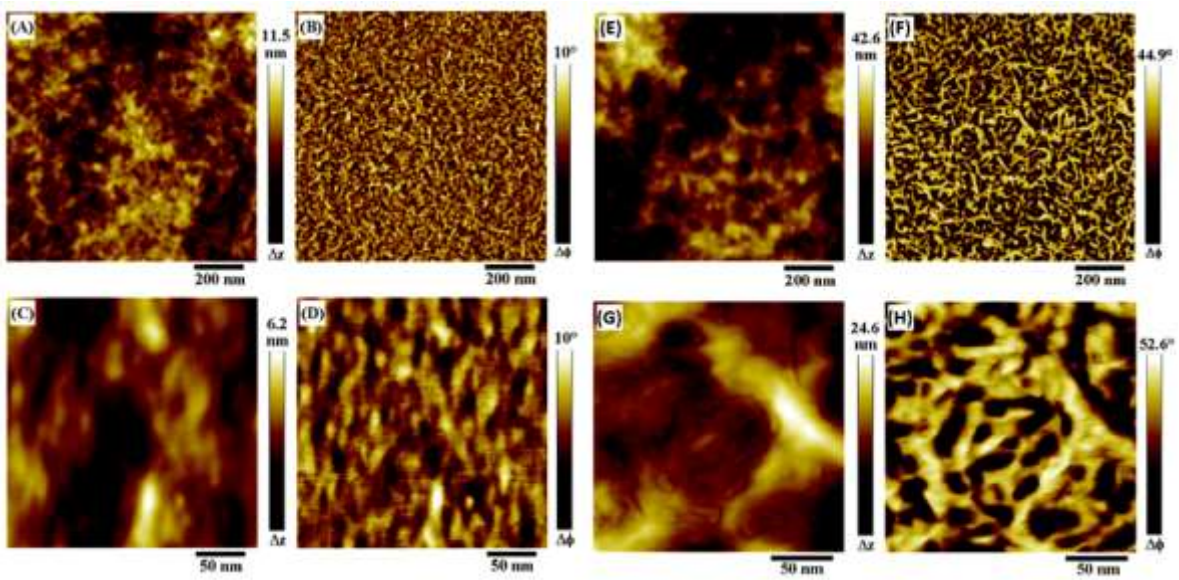

Figure 17. AFM topography images (A, C) and phase images (B, D) of PEDOT: PSS without solvent addition. In the phase images, darker areas correspond to softer zones. The sharp contrast suggests two phases, one PEDOT-rich (the brighter zones) and one PSS-rich (the darker zones). Therefore, PEDOT:PSS particles are surrounded by excess PSS.[111]

AFM topography images (E, G) and phase images (F, H) of PEDOT: PSS after DEG addition. PSS rich regions are swollen after the solvent addition so that PEDOT-rich regions are more interconnected.[111] Copyright 2006, American Chemical Society.

Crispin and coworker's completed their previous works (from Jönsson *et al.*) and showed that all three proposed mechanisms were not contradictory.[111] They suggested that the PEDOT:PSS blends correspond to a dispersion of PEDOT:PSS particles in the water-PSSH solution. Without additional solvent, a film is deposited with PEDOT:PSS particles surrounded by excess PSS (Figure 17). When adding diethylene glycol (DEG) to PEDOT:PSS emulsion, the high boiling point of DEG, compared to that of water, induces a much more slower evaporation of the solvent which swells the PSS-rich regions (Figure 17) and induces screening effects between the polymer and its dopant. This leads macroscopically to a better connection between

PEDOT rich grains and at the microscopic level to the change from coil to linear conformation that Ouyang suggested.

Using AFM and transport measurements, Nardes *et al*. confirmed that the increase in conductivity happens under thermal annealing due to the presence of high boiling solvent and that the aggregation of PEDOT rich grains is accompanied with their broadening.[113,114]

By optimizing the solvent and thermal post-treatments after the addition of EG in the PEDOT:PSS dispersion, Müller-Meskamp and co-workers reported a conductivity of 1418 S cm^{-1}, explained by the removal of PSS excess, together with the reordering and conformational changes reported previously, and supported by the decrease of thickness and a constant transmittance.[115] From that point onward, post-treatment was always combined with the addition of organic solvents and conductivities up to 1647 S cm^{-1} were reported, and even of up to 4600 S cm^{-1} after further shearing .[116,117] Even though the efficiency of the addition of, or post-treatment with, organic solvents is commonly admitted (Figure 18), the real mechanisms behind such enhancement are still subjected to debate and intensive studies are going on.[114,118,119]

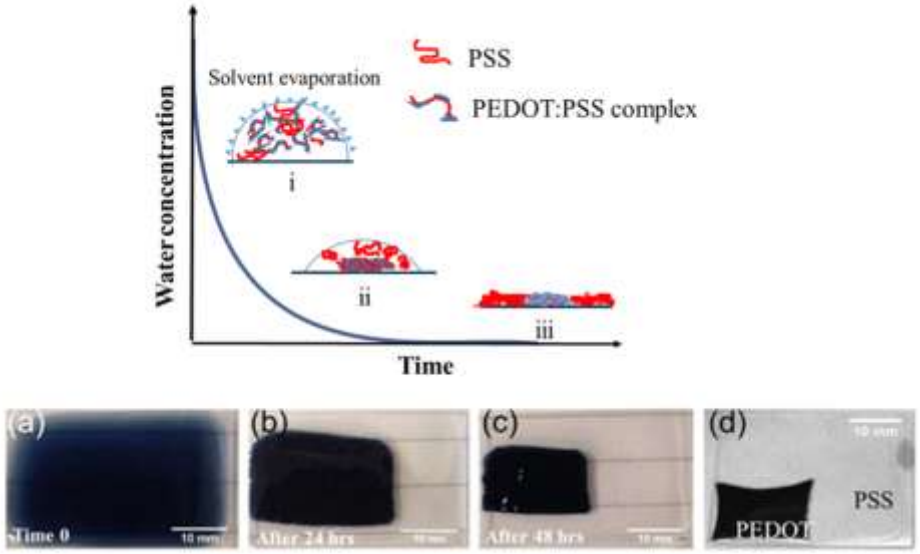

Figure 18. Upper scheme: illustration of the phase separation when a high boiling point solvent is added in the PEDOT dispersion. That illustration is accompanied with an optical proof of such phase segregation (lower figure).[120] Copyright 2015, American Chemical Society.

Apart from polar and high boiling point solvents (pre- and post-treatments), ionic liquids, anionic surfactants and salts were also added with some success in the aqueous PEDOT:PSS dispersion before deposition.[121–127] Ionic liquids such as 1-ethyl-3-methylimidazolium tetracyanoborate (EMIM TCB) help to increase the electrical conductivity up to 2084 S cm^{-1}.[121,122] The mechanisms responsible for the conductivity increase are similar to the ones proposed in the case of high boiling point organic solvents, namely “secondary doping” and the phase separation between PEDOT-rich and PSS-rich domains. [127]

In the case of anionic surfactants and salts, the proposed mechanisms behind the conductivity enhancement are different as schematized in Figure 19. As a matter of fact, PEDOT positive charges are stabilized by PSS negative charges *via* coulombic interactions. The excess PSS anions are solvated with water, hence explaining the good dispersion. The PSS adopts a coil conformation that the PEDOT follows. However, the repeating PEDOT unit being shorter than the PSS one, distortion occurs and charges are localized so that the

conduction pathways are not optimized. That could partly explain the VRH transport model relevant in PEDOT:PSS, compared to treated ones or PEDOT with small counter-anions (explanations are provided hereinafter). After addition of anionic surfactants (Figure 19A), the negatively charged surfactants stabilize the PEDOT positive charges which free themselves from the PSS ones, so that the distortion disappears. The optimization of the conduction pathways results in an increase of conductivity from 0.16 to 80 S cm^{-1}. When adding salts (Figure 19B), they induce charge screening and conformation changes in PEDOT:PSS. The cation of the salt binds some PSS which is further washed of the film while the anion replaces some of the PSS as counter-anion of PEDOT charges. The conductivity increases from 0.2 to 140 S cm^{-1}. Even though some ions still remain in the film, it was shown that ionic conduction is not responsible for the conductivity enhancement.

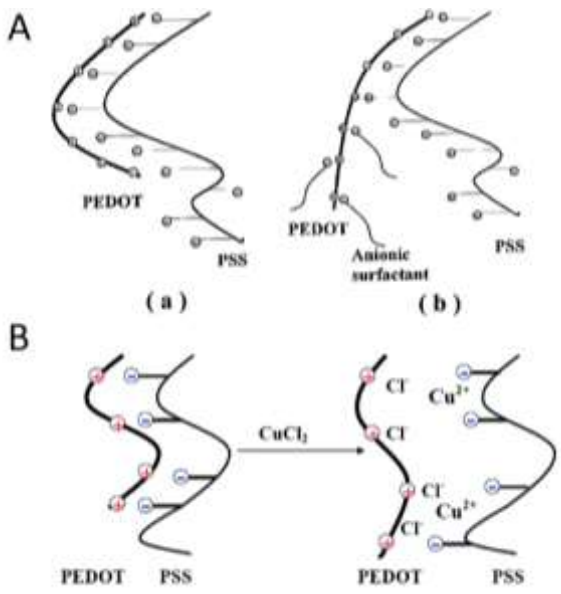

Figure 19. (A) Schematic structure of a PEDOT segment and a PSS segment in water (a) without and (b) with the addition of anionic surfactant.[123] (B) Schematic structures of PEDOT:PSS before and after $CuCl_2$ treatment.[124] Copyrights 2008 and 2009, American Chemical Society.

Pre- and post-treatments with organic solvents or salts in order to increase the conductivity of PEDOT:PSS have been extensively proposed in the literature. Thanks to the increasing reported values of conductivity, new applications have emerged. Especially, PEDOT has appeared as a promising thermoelectric material owing to its good flexibility, processability, low cost, thermal stability and thermoelectric properties that add to the electrical ones.[128] Moreover, with conductivities exceeding 1000 S cm^{-1}, PEDOT:PSS has approached ITO performances and has been thought as a relevant alternative to advantageously replace ITO in several applications.[6,8,100,115] Figure 21b summarizes the main state of the art of PEDOT:PSS conductivities obtained from the so-called "secondary doping".

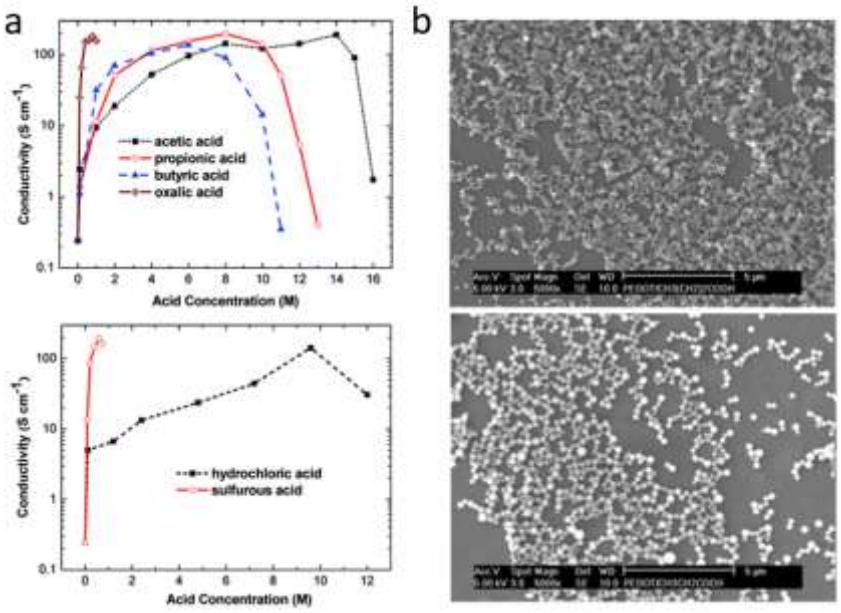

Figure 20. (a) Conductivity enhancement after post-treatment with various acids. (b) SEM images of PEDOT:PSS films treated with 8 M propionic acid (upper) and 6 M butyric acid (lower). The particles are PSSH particles which segregate after acid treatment and can easily be washed off.[129] Copyright 2010, American Chemical Society.

Besides that “secondary doping”, Ouyang proposed in 2010 a new post-treatment using organic and inorganic acids such as acetic acid, propionic acid, butyric acid, oxalic acid, sulfurous acid and hydrochloric acid on PEDOT:PSS samples.[129] The conductivity increased from 0.2 to more than 200 S cm^{-1} as shown in Figure 20a, and that improvement was attributed to acid-assisted PSSH loss from the PSS as explained in Figure 20b, and to conformational changes of the PEDOT chains.[96]

Thanks to acid treatments, the conductivity has drastically increased through the years up to 4839 S cm^{-1}.[82,130–135]. Compared to secondary doping, the mechanisms behind the conductivity improvement were less controverted and mostly attributed to the washing-off of the PSS excess accompanied with some conformational modifications. Xia et al. explained that upon acid treatment, some PSS^- ions get neutralized by the protons of the acids (H_2SO_4 in their study). Given the fact that the pKa of H_2SO_4 (-6.4) is higher than that of PSSH (-2.8), PSS^- are protonated during acid treatment and some of the original counter-anions are replaced by hydrogenosulfate.[130] Such assumptions were also more recently acknowledged by Kumar *et al*.[135] However this was not observed by other groups, who showed that no ions derived from the acids were present at the end.[132,133] In any case, phase separation occurs due to the non-coulombic interaction with neutral PSSH chains and the remaining PEDOT chains are elongated for enhanced transport performances (Figure 23).

One can wonder where the practicability lies when using harsh sulfuric acid treatments, which are not compatible with plastic substrates. Actually, a transfer printing process has been developed so that the treated PEDOT film can be transferred from glass to a plastic substrate. That technique requires yet fine control of the adhesion and the yield of large and uniform films can be rather low.[133] Other weaker acids, such as phosphoric acid, lead to conductivities as high as 1460 S cm^{-1}. This value is not as high as in sulfuric acid treatment, but it was shown that the sheet resistance was similar. The lower conductivity is accounted to a higher thickness due to less PSS removal after phosphoric acid treatment.[134]

Figure 21 outlines the main advances in terms of acid-treated PEDOT:PSS.

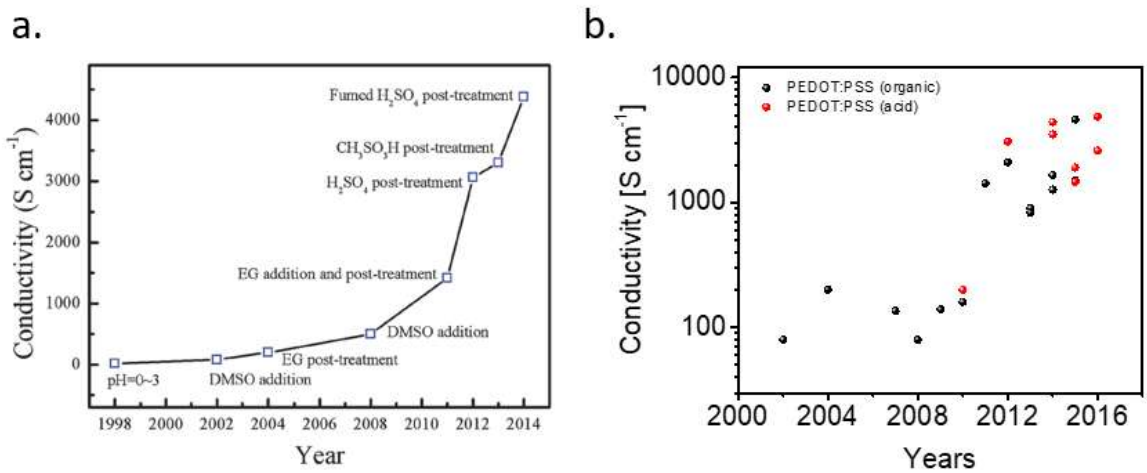

Figure 21. (a) Timeline of conductivity values for PEDOT:PSS.[19] Copyright 2015, John Wiley and Sons. (b) Conductivity enhancement of PEDOT:PSS through years. References are given in Table 1.

6-1-2. Structure

The research on conductivity improvement of PEDOT-based materials was systematically carried out with special care to investigate the morphology and the structure of the deposited films. By synthesizing more ordered structures, the mobility, and hence the electrical conductivity, is expected to increase.[32] The morphology and structure of the films were then very often scrutinized in order to understand the conductivity enhancement and the inherent transport mechanisms.

For PEDOT:PSS, a core-shell structure was inferred as early as 1999.[96] It consists of a highly hydrophobic PEDOT-rich core surrounded by highly hydrophilic PSS-rich shell. A PEDOT:PSS core of around 10~100 nm was demonstrated through years using various techniques (XPS, AFM, STM-based spectroscopy, TEM), with the actual size being highly dependent on the filtering processes during manufacturing .[13,96,109,136,137]

Diffraction measurements of the PEDOT:PSS dispersion confirmed the presence of aggregates composed of PSS micelles whereby a PEDOT core stands.[138–140]

SAXS and GIWAXS were both used to study the effect of secondary doping, organic solvent post-treatment and sulfuric acid treatment. It is found that addition of organic solvents in the PEDOT:PSS dispersion increases the crystallinity by interconnecting the PEDOT nanocrystals due to the swelling of the PSS domains. This increases the carrier mobility.[138,141] At the same time, the post-treatment reduces the PSS content of the films which increases the carrier density.[82,142] In both cases, a stronger inter-chain was observed as well as an evolution from face-on to edge-on configuration (Figure 22).[143] AFM measurements before and after anionic surfactant treatment suggested that the morphology is changed and the main hypothesis was the disappearance of some PSS chains that surround the PEDOT:PSS globules.[123] In the case of inorganic salts post treatment, AFM measurements showed the appearance of big domains. The authors then suggested that the surface morphological change after salt treatment on PEDOT:PSS is similar to that after high boiling point solvent.[124]

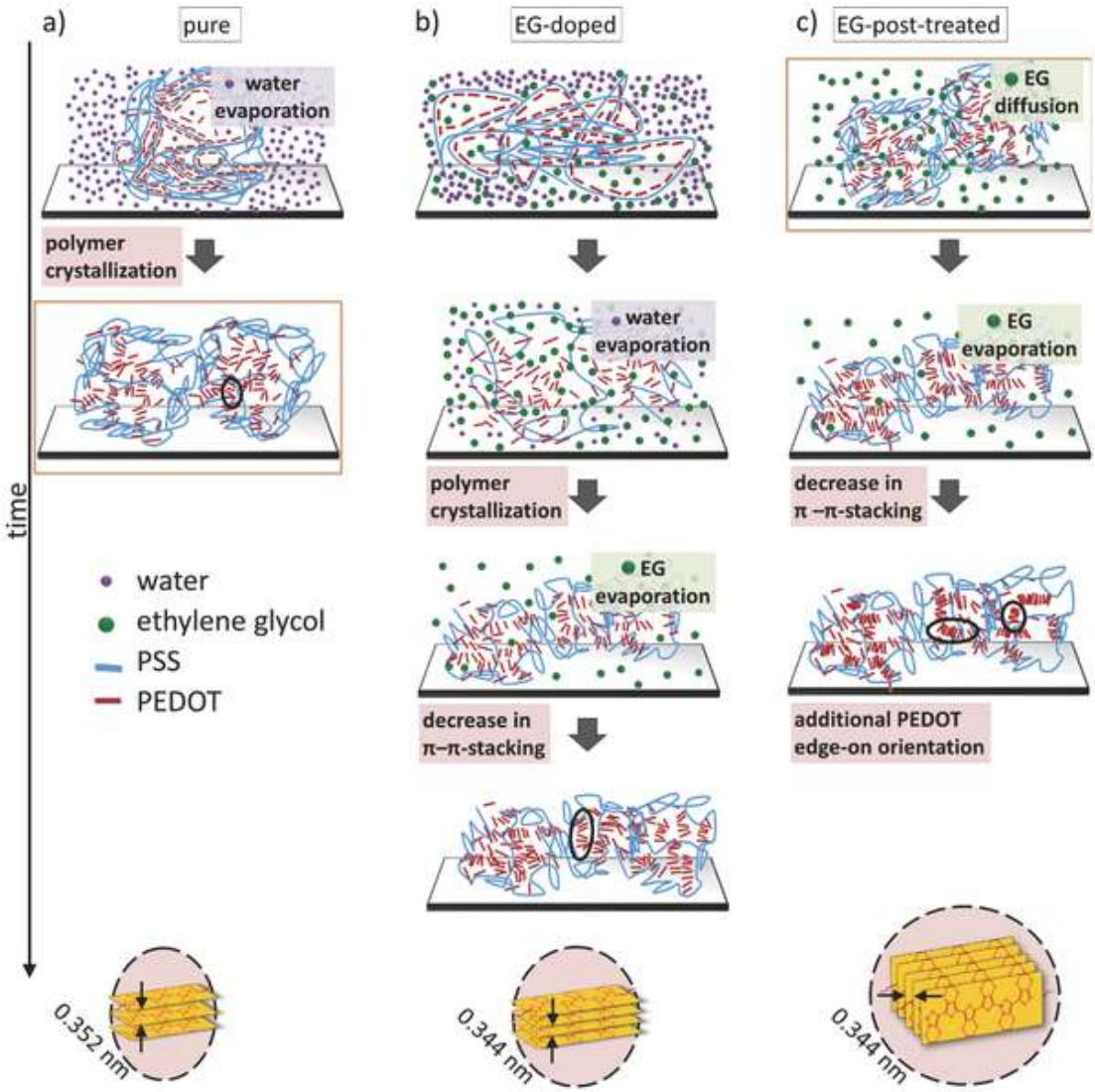

Figure 22. Schematic model of the kinetic processes during film formation of (a) pure, (b) EG-doped, and (c) EG-post-treated PEDOT:PSS.[143] Copyright 2015, John Wiley and Sons.

On the other hand, after sulfuric acid treatment, a morphological change from a grain-like to a fibrous structure has been demonstrated as illustrated in Figure 23.[132,133,135]

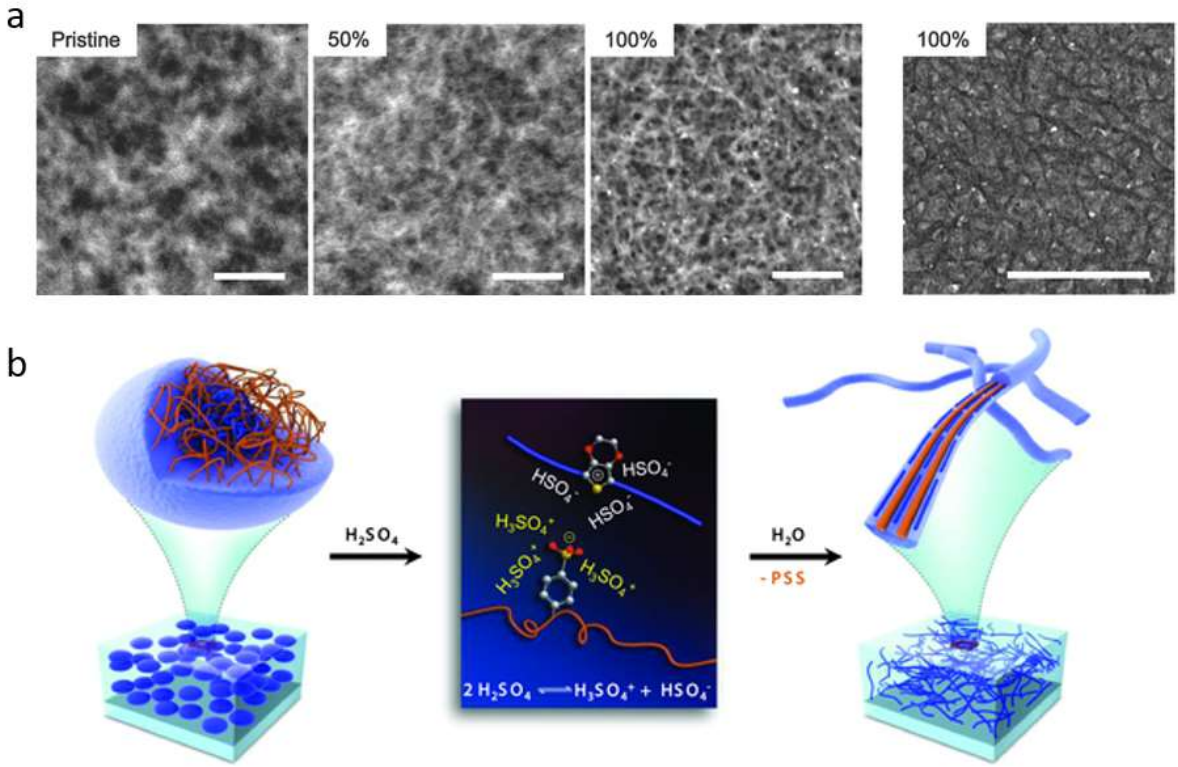

Figure 23. (a) HAAD-STEM images of PEDOT:PSS treated with different sulfuric acid concentrations. (b) A mechanism is proposed for the structural rearrangement of PEDOT:PSS after acid treatment. Sulfuric acid undergoes auto-pyrolysis leading to HSO_4^- and $H_3SO_4^+$, helping segregation of the negatively charged PSS and the positively charged PEDOT. Thanks to strong π-π interactions between PEDOT chains, the amorphous PEDOT:PSS grains (left) are reformed into crystalline PEDOT:PSS nanofibrils (right).[132] Copyright 2013, John Wiley and Sons.

6-1-3. Transport

Changes on the mobility, carriers' density, conformation and structure after organic solvent or acid treatments highly impact the transport mechanisms in PEDOT:PSS films. The transport properties are mostly assessed through the temperature variation of the electrical conductivity from room temperature down to

Helium boiling point temperature, and even lower, as explained previously. The conduction mechanisms proposed for PEDOT systems benefited from earlier works on conducting polymers and disordered metallic systems.[49,144] The first comprehensive study on the transport mechanisms in PEDOT:PSS was given by Aleshin *et al*.[145] From their temperature dependence of conductivity down to 6 K, they inferred a strong dependence to the temperature with characteristic resistivity ratios $\rho_r > 10^5$, sign of a highly disordered system with a strong temperature dependence of its conductivity. Moreover, the conductivity variations followed Equation 2 with n = 1. Knowing that there is no strong agreement on the relevant model to be used to describe such behavior, they eliminated the 3D VRH theory with predominant electrons-electrons interactions since such dependence should not be the case in the whole temperature range, which they observed. The non-dependence of the pre-exponential factor to the temperature swept away the quasi-1D VRH model. On the other hand, since microscopy techniques such as SEM revealed heterogeneous structure, the model of tunneling between polaronic clusters imbedded in an insulating matrix seemed more appropriate.

Upon "secondary doping" or post-treatment with an organic solvent, a systematic improvement of the transport properties has been observed. Kim *et al*. showed that pristine PEDOT:PSS follows the same temperature dependence of their conductivity as Aleshin *et al*. and attributed it to a 1D-VRH model.[110] Upon addition of organic solvent, treated films approached the critical regime of the metal/insulator transition as evidenced by the zero-slope of the reduced activation energy and also by the power law characteristic of the temperature dependence of conductivity of materials near the critical regime. Ouyang *et al*., Ashizawa *et al*. and more recently Xiong *et al*. also reported a 1D-VRH and a decrease of the energy barrier between PEDOT chains (decrease of T_0 in Equation 2) which was interpreted as a longer localization length of the charges consistent with better coupling of PEDOT chains.[112,146,147] Nardes *et al*. linked the morphology they observed after sorbitol addition with the transport mechanism. After the addition of sorbitol PEDOT-rich, particles observed using scanning tunneling microscopy (STM) arrange along lines,

hence inducing a transition from 3D VRH to quasi-1D VRH.[114] In all cases, lower resistivity ratios after the different treatments show that disorder is highly attenuated in those films.

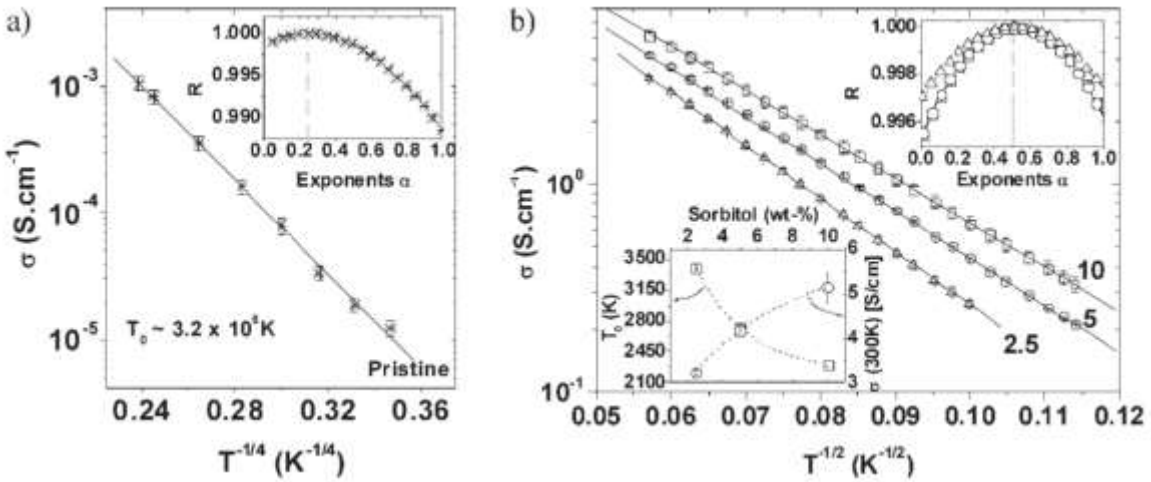

Figure 24. Temperature dependence of the conductivity for (a) pristine PEDOT:PSS sample and (b) PEDOT:PSS samples treated with (Δ) 2.5 wt%, (○) 5 wt% and (□) 10 wt% of sorbitol concentration added to the aqueous dispersion used for spin-coating of the films. Straight lines are fits to Equation (2) to the data in the main panel plotted versus α=1/n+1. The vertical dashed line represents α = ¼ in (a) and ½ in (b). Lower left inset of (b): evolution of T_0 and σ at 300 K as a function of sorbitol concentration, the dashed lines serve to guide the eye.[114] Copyright 2008, John Wiley and Sons.

The transport properties of PEDOT:PSS after acid treatment were less studied. Xia *et al*. reported a 1D VRH transport mechanism but resistivity measurements were carried out only down to 110 K which is not sufficient to draw a clear conclusion.[129] More recently Kumar *et al*. suggested that after acid treatment, the conductivity is enhanced thanks to the elongation of PEDOT chains and the reduction in density of PSS regions.[135] Therefore, they modeled the electronic conduction as a heterogeneous model with higher conductivity PEDOT-rich regions connected in series with lower conductivity PSS-rich regions. In the first regions transport was said to be through quasi-1D metallic conduction (Equation 5) while a temperature

assisted tunneling takes place through the other ones (Equation 3). Even though their model fitted their experimental data, it should be noted that temperature dependence conductivity measurements were only carried out from 300 K to 500 K and all samples depicted a negative slope that the authors attributed to a metallic behavior.

6-1-4. Conclusion

Mechanisms behind conductivity enhancement in PEDOT:PSS after addition of specific organic solvents in PEDOT:PSS dispersion or after post-treatment is still subjected to debate.[19] Recently computational studies including density functional theory calculations and molecular dynamics simulations investigated the mechanisms behind the addition of DMSO in PEDOT:PSS.[148] It appears that DMSO dissolves the PSS shell so that PEDOT in the core can be released and self-aggregates, which leads to phase separation of PEDOT and PSS, as experimentally observed.

Post-treatment with organic solvents washes off the excess PSS while post-treatment with acids also favors the washing-off of excess PSS and sometimes the introduction of some counter-anions from the conjugate bases of the acids. Whatever the treatment is, the structure is improved and PEDOT-rich domains are better interconnected.

In as-deposited films, PEDOT chains organize in a more or less ordered structure. In disordered PEDOT films such as untreated PEDOT:PSS the high disorder induces the localization of the charges as known as Anderson localization. In such systems, hopping between localized states was proposed as the main electronic conduction mechanism following Equation 2.[19,129] In PEDOT:PSS however, VRH was always reported with n = 1 and most of the time attributed to quasi-1D VRH. It should be noted that the temperature dependence of conductivity measurements was rarely achieved down to very low temperatures, and that at least three conduction models are reported to fit Equation 2 (3D VRH with strong electrons-electrons interaction, quasi 1D VRH and tunneling between neighboring chains of polaronic clusters).[112,129] Nonetheless after organic solvent or acid treatment, the systematic decrease of T_0 and

the systematic decrease of the slope of W are all indicative of a reduced disordered and enhanced charge transport mechanisms.

6-2. PEDOT with small counter-anions other than Tosylate, Triflate and Sulfate

6-2-1. Electrical conductivity and structure

First PEDOT materials were synthesized directly in solution by adding the monomer and the oxidant (mostly $FeCl_3$) in a solution (mostly acetonitrile or benzonitrile) or through electrochemical polymerization as reported previously.[21,68,69] In the first case, electrical conductivities barely reached 30 S cm^{-1} while they went up to 200 S cm^{-1} for electrochemically polymerized PEDOT materials. The synthesis and commercialization of PEDOT:PSS soon evinced chemical oxidation, and even though electrochemical polymerization requires conductive substrate, the polymerization is fast, the technique scalable and the synthesized materials more conductive than PEDOT:PSS at that time.

In late 1990's Aleshin and coworkers published a series of articles with PEDOT films prepared by anodic oxidation of EDOT. The electrochemical cell contained the monomer EDOT, the electrolyte propylene carbonate and various salts which were tetrabutylammonium hexafluorophosphate, tetrafluoroborate or trifluoromethanesulfonate. The obtained PEDOT:PF_6, PEDOT:BF_4 and PEDOT:OTf had conductivities around 200 – 300 S cm^{-1}.[75,145,149,149–152]

Culebras *et al*. also reported PEDOT materials synthesized via electrochemical deposition with several counter-anions. The authors expected the change of the counter-anion to modify the conducting properties of PEDOT. They hence achieved PEDOT:ClO_4 at 753 S cm^{-1}, PEDOT:PF_6 at 1000 S cm^{-1} and PEDOT:BTFMSI (bis(trifluoromethylsulfonyl)imide) at 2074 S cm^{-1}.[78] The increase of the conductivity was tentatively correlated with the size of the counter-anion. Bigger ones were supposed to modify the conformation from coil to linear and hence to improve electronic transport properties as shown in Figure 25.

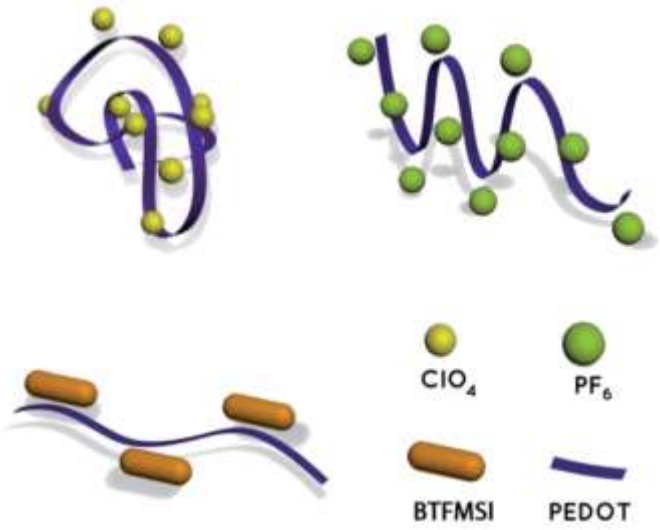

Figure 25. PEDOT conformation in the presence of different counter-anions.[78] Copyright 2014, Royal Society of Chemistry (copyright review from Elsevier requested).

The works on VPP opened routes to highly conductive PEDOT materials stabilized with small counter-anions.[153] For instance, Kim *et al*. reported VPP PEDOT with either $FeCl_3$ or $Fe(Tos)_3$ as oxidant and conductivities reaching 2000 and 4500 S cm^{-1} respectively.[89] More recently Wang *et al*. reported o-CVD PEDOT polymerized with $FeCl_3$ as oxidant and further treated with HBr water solution. By optimizing the deposition time and temperature they manage to control the crystallization and morphology and reach electrical conductivities up to 6259 S cm^{-1}, the highest value reported up to now.[25] Such enhancement was attributed to an increase mobility while the charge carrier density remained roughly constant as evidenced by Seebeck coefficient and work function measurements. A higher mobility was obtained because face-on arrangement was preferred to edge-on one at higher deposition temperatures and that energy barrier of the inter-crystallite carrier transport was much lower in the face-on films.

One can also cite the remarkable work of Cho *et al*. who synthesized single crystals PEDOT nanowires with conductivities ranging from 7619 to 8797 S cm^{-1}.[24] Such single crystals were grown from EDOT monomers

that were self-assembled and crystallized during VPP within nanoscale channels of a mold having $FeCl_3$ catalysts. Fe was efficiently removed by methanol washing but the Cl^- counter-anions remained in the PEDOT crystals so as to serve as a major dopant.

The morphology and the structure of PEDOT films, and subsequently the electrical conductivity, depend on the deposition technique to a large extent. While electrochemical polymerization leads to an amorphous structure and a granular aspect, VPP and o-CVD enables more ordered structures and even single crystals as discussed above.[25,89,151,154,155] The very ordered structure in the case of VPP is attributed to the bottom-up process and can be controlled through base additives. In the case of o-CVD the structure can be greatly enhanced by grafting PEDOT to the substrate.[156] Ugur *et al*. showed that grafted PEDOT:Br polymerized in a face-on structure, while both face-on and edge-on structure were observed in ungrafted PEDOT:Br (Figure 26).[99] As shown later on by Wang *et al.*, the face-on orientation leads to higher mobility and hence in their case, to higher electrical conductivity.[25] This assertion was also comforted by theoretical calculations of Gonzales et al. who reported that good crystallinity and high edge on content were not sufficient for a high mobility in PEDOT films.[157] It is noteworthy that in the case of PEDOT:PSS preferred edge-on orientation was shown to favor a better electrical conduction.[143]

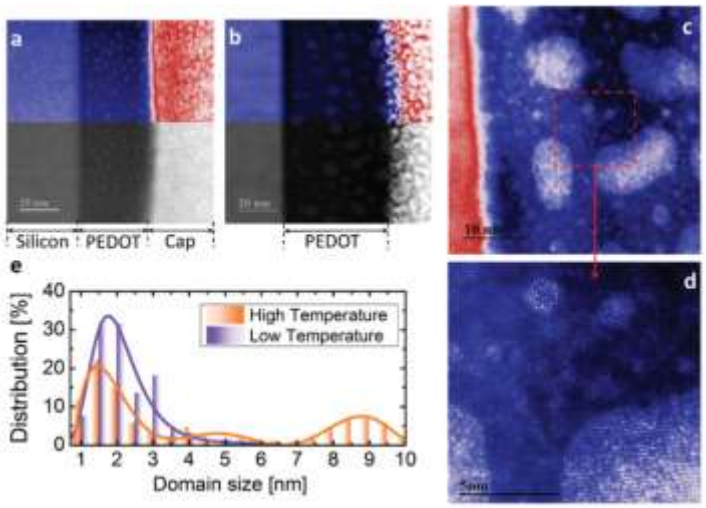

Figure 26. The HAADF STEM image of cross sections of the interfaces of grafted PEDOT films grown at (a) 100 °C and (b) 200 °C. The top halves of both images are color-enhanced to clearly elucidate the crystalline domains surrounded by an amorphous matrix. High-resolution images for the film synthesized at 200 °C are shown in (c) and enlarged in (d), providing a direct evidence on the well-organized large crystallites. (e) Histogram of statistical domain size distribution obtained from images (a) and (b), showing the broader distribution and larger crystallite size for the film grown at high temperature (200 °C).[99] Copyright 2015, John Wiley and Sons.

7-2-3. Transport

Aleshin and coworkers gave a first insight of charge transport properties in general and metallic conduction in particular in PEDOT films synthesized through electrochemical polymerization and stabilized with small counter-anions, together with their work on PEDOT:PSS.[75,145,149] The electrical conductivity of electrochemically polymerized PEDOT:PF_6, PEDOT:BF_4 and PEDOT:OTf was studied from room temperature down to 1.4 K, along with their magneto-conductivity. For all samples very weak temperature dependence of their resistivity is reported with a resistivity ratio ρ_r = 1.5-2.8. The conductivity decreases from 300 K down to 10 K and a positive temperature coefficient of resistivity is observed below 10 K for the most

metallic samples ($\rho_r < 2.1$). The conductivity response typically followed that of disordered metals in Equation 4 and supplementary magneto-conductance measurements further enlightened that strong electron – electron interactions took place at low temperature hence enhancing the metallic behavior while weak localization effects occurred at higher T hence limiting the metallic signature.[75,149,149,150]

Gleason and co-workers also investigated the transport mechanisms in PEDOT:Br through temperature dependence of conductivity from room temperature down to 10 K.[99] PEDOT:Br was synthesized through o-CVD of PEDOT and $FeCl_3$ and rinsing of the deposited film with HBr. Contrarily to Aleshin and co-workers' findings, no strong metallic response was observed, but similarly to them, the temperature dependence of the resistivity was very weak and extrapolated 0 K values of the resistivity were non-null. Due to the structure observed with HAADF-STEM presented in Figure 26, the authors described the transport mechanisms as a "coarse grained" VRH model. As a matter of fact, the authors reported a broad distribution of crystalline domains size which swell with increasing polymerization temperature. They suggested that due to the structure, hopping takes place between crystallites hence following a 3D Mott VRH Model (Equation 2 with n = 3). As the crystalline domains broaden, their wavefunctions overlap and inter-crystallites Coulomb interactions become predominant so that transport is controlled by 3D Efros-Shklovskii VRH (Equation 2 with n = 1). "Coarse grained" VRH model is therefore a hopping mechanism taking into account both the electrons-electrons interactions between crystallites as well as the lack of those interactions when the crystallites get too far apart and not broad enough. In their later work where they reported the record conductivity 6259 S cm^{-1}, a clear metallic behavior is however observed.[25] The reduced activation energy showed a positive slope in the whole range of temperature. Theoretical charge carriers' density deduced from the Drude model and the experimental one measured by Hall effect both gave the charge carriers' density in the range of metallic polymers. Moreover, they fabricated PEDOT-Si Schottky diode arrays for radio frequency identification, hence validating the observed metallic nature of the PEDOT films. To better understand the transport properties, they used the model developed by Kang and Snyder reported

hereinbefore. Such model validated the increase of the charge carriers' mobility in the face-on orientation as they experimentally observed.

6-2-3. Conclusions

PEDOT stabilized with small counter-anions other than tosylate, triflate and sulfate have been far less studied than PEDOT:PSS mostly because the performances are similar to those of PEDOT:PSS and that this latter one is more easily processable. Recently however, Gleason and coworkers developed o-CVD with $FeCl_3$ and by finely engineering the crystallinity and configuration of PEDOT thin films post treated with HBr they reported a record high electrical conductivity of 6259 S ccm^{-1} and a remarkably high carrier mobility.

The structure of PEDOT thin films highly depends on the processing method (VPP, o-CVD or electrochemical polymerization) and the nature and size of the counter-anions. In most reports a metallic behavior was observed and the temperature dependence of the conductivity was less pronounced than in the case of PEDOT:PSS.

6-3. PEDOT:Tos

6-3-1. Electrical conductivity

In 2004, Winther-Jensen's works on VPP demonstrated conductivities exceeding 1000 S cm^{-1}, hence arousing great interest among researchers.[87,88,158] PEDOT:PSS is processable, but conductivities were barely reaching 200 S cm^{-1} at that time.[112] PSS, the stabilizer counter-anion which allows dispersion in water, is insulating and in excess, thus hindering the conduction mechanisms. PEDOT stabilized with smaller counter-anions were deposited either using oxidative chemical polymerization or electro-polymerization. While the former one led to non-uniform barely processable material, the later one required conductive substrate for the deposition.[5] The new method proposed by Winther-Jensen *et al*. allowed not only to have highly conductive films, but also to deposit on any substrate, insulator or not.

Apart from the acidic side reactions which hampered PEDOT chains' growth and which were readily taken care of by adding a base (typically pyridine), the water uptake aroused as another issue for good film forming properties. As a matter of fact, the two more common oxidants for VPP are $FeCl_3$ and $Fe(Tos)_3$. These salts show a good water affinity, thus leading to the formation of hydrate crystallites which are detrimental to the conduction properties (see Figure 27). But at the same time, the presence of water within the VPP chamber was shown to be crucial since it was helping deprotonating the EDOT-dimer, therefore allowing polymerization to occur (see Figure 9).[159,160] Murphy and coworkers introduced a smart solution to that issue. Water being mandatory, and at the same time detrimental to the polymerization process, they added a surfactant in order to inhibit the crystallization of the oxidant hydrate. The surfactants used in their work were glycol based, typically the amphiphilic copolymers poly(ethylene glycol)-*ran*-poly(propylene glycol) (PEG-*ran*-PPG) and poly(ethylene glycol) – poly(propylene glycol) – poly(ethylene glycol) (PEG-PPG-PEG) , consisting of hydrophobic PPG blocks and hydrophilic PEG blocks.[159,160] These surfactants, besides suppressing the crystallization of the oxidant (Figure 27), also moderate the polymerization rate as proved by quartz crystal microbalance measurements (QCM), so that a base is no longer necessary.[90,160] They further demonstrated that the glycol-based surfactant complexes the oxidant in order to control the reaction rate.[79,161] Conductivities up to 3400 S cm^{-1} were achieved, a performance associated to the increased molecular ordering within the PEDOT film, and to the semi-metallic behavior of such materials.[89,162–165]

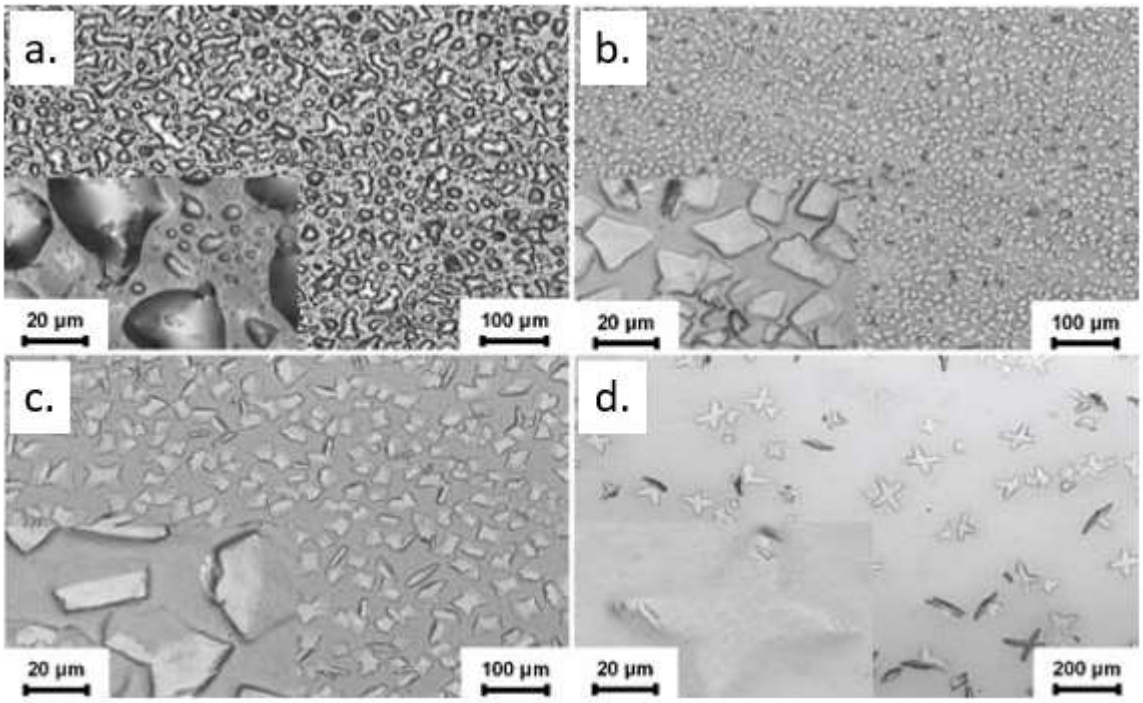

Figure 27. Crystallization of the oxidant. PEDOT:Tos film post-polymerization (VPP) and prior to ethanol wash. (a) No PEG-ran—PPG, (b) 5wt. % PEG-ran-PPG, (c) 10 wt. % PEG-ran-PPG, (d) 15 wt. % PEG-ran-PPG. Image reproduced from Murphy and coworkers' article.[159] Copyright 2008, John Wiley and Sons.

Following the example of PEDOT:PSS, VPP PEDOT:Tos was also treated with sulfuric acid. A strong increase in conductivity was noticed, from 944 to 1750 S cm^{-1}. Such treatment was shown to increase the doping level as evidenced by shifts in Raman spectroscopy, to wash some of the remaining PEG-PPG-PEG in the film after deposition, and to replace some tosylate counter-anions as inferred from the shifts of energy measured by XPS.[166]

Figure 28 depicts the state of the art conductivity using VPP, and other comparable techniques such as vacuum-VPP and o-CVD methods.

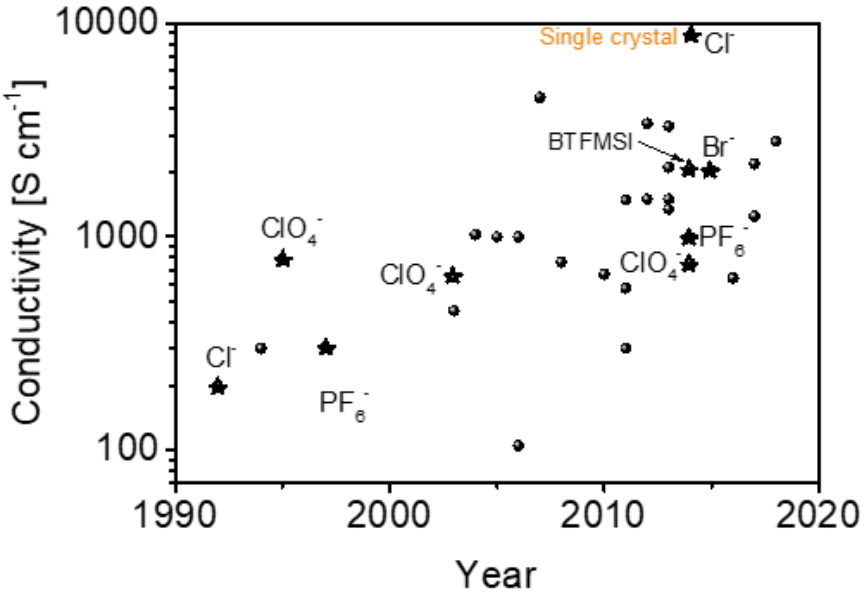

Figure 28. Conductivity enhancement through years. PEDOT:Tos materials are represented with spheres, PEDOT stabilized with other counter-anions with stars. The corresponding counter-anions are displayed accordingly. References are given in Table 1.

No long after Winther-Jensen pioneering works on VPP, the same group also reported solution-cast polymerization of PEDOT:Tos with conductivities exceeding 1000 S cm^{-1} using the same reactants, but deposited by spin-coating.[91] Even though such method was previously reported, the conductivities did not exceed 550 S cm^{-1}. The over 1000 S cm^{-1} conducting PEDOT:Tos deposited by spin-coating yet did not generate as much interest as the VPP method despite its inherent advantages: deposition on both conducting or insulating substrates, films as homogeneous, conducting and transparent as in VPP, solution processable and highly ordered, no vacuum needed.[84,91,167] Only few reports dealing with conductivity enhancement using solution-cast polymerization were published.[47,168]

6-3-2. Structure

Inganäs and coworkers carried out the first comprehensive study of the structural characteristics of PEDOT in general, and of PEDOT:Tos in particular.[167] They studied solution-cast polymerized PEDOT:Tos using grazing incidence wide angle X-Ray scattering (GIWAXS) with synchrotron radiation. The spin-coated material was smooth, homogeneous, and the oxidation level was calculated to be 25 % using XPS. Their results also showed that the material was highly anisotropic and in a paracrystalline state, with dopant anions forming distinct planes that alternate with stacks of the polymer chains as in Figure 29. The lattice parameters in the orthorhombic structure as depicted in Figure 29 were calculated to be a = 14.0 Å, b = 6.8 Å and c = 7.8 Å. A metallic behavior was found in the plane and a dielectric behavior out of the plane of the films.[167] Such structure for PEDOT was further proved though years and remained the same for all PEDOT films, whatever the counter-anions.[24,47,138,139] The lattice parameters as well as the crystalline degree (relative order) however change from a PEDOT material to another, from a deposition technique to another, and even sometimes from a sample to another.

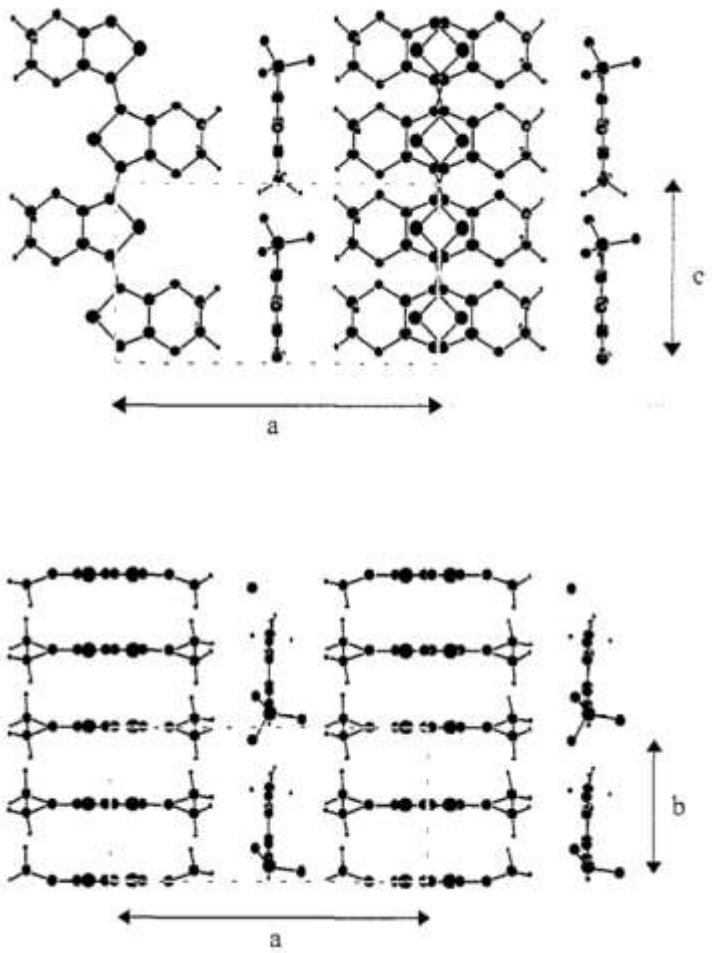

Figure 29. Structure model of PEDOT:Tos. The substrate is normal to the a-axis.[167] Copyright 1999, Elsevier B.V. (copyright review from Elsevier requested).

Comparisons between VPP PEDOT, chemically oxidized PEDOT, electro-polymerized PEDOT and PEDOT:PSS (non-acid treated) prove that VPP PEDOT exhibits the highest conductivity and optical transmission, attributed to increased molecular ordering and smoother morphology as confirmed by XRD, SEM and AFM.[169] A highly crystalline structure similar to that of VPP PEDOT can be obtained in the case of PEDOT:PSS only after post-treatment with sulfuric acid.[132,133]

The importance of engineering a fine structure on the conductivity of PEDOT was evidenced by Cho *et al*.[24] Given the fact that disorder in PEDOT films highly affects chains alignment which hinders the inter-

chain transport, they grew PEDOT single nanocrystals in nano-sized molds. The high conductivity obtained, namely 8797 S cm^{-1} with a doping level as small as 10 %, was associated to the entirely crystalline nature of the synthesized PEDOT, whose lattice parameters (a = 11.01 Å, b = 4.64 Å and c = 7.91 Å) inferred a tighter packed structure than those reported for films of PEDOT:PSS (a = 14 Å, b = 7 Å) or PEDOT:Tos (a = 14.0 Å, b = 6.8 Å and c = 7.8 Å.) (the lattice parameters a, b and c are defined as in Figure 29).

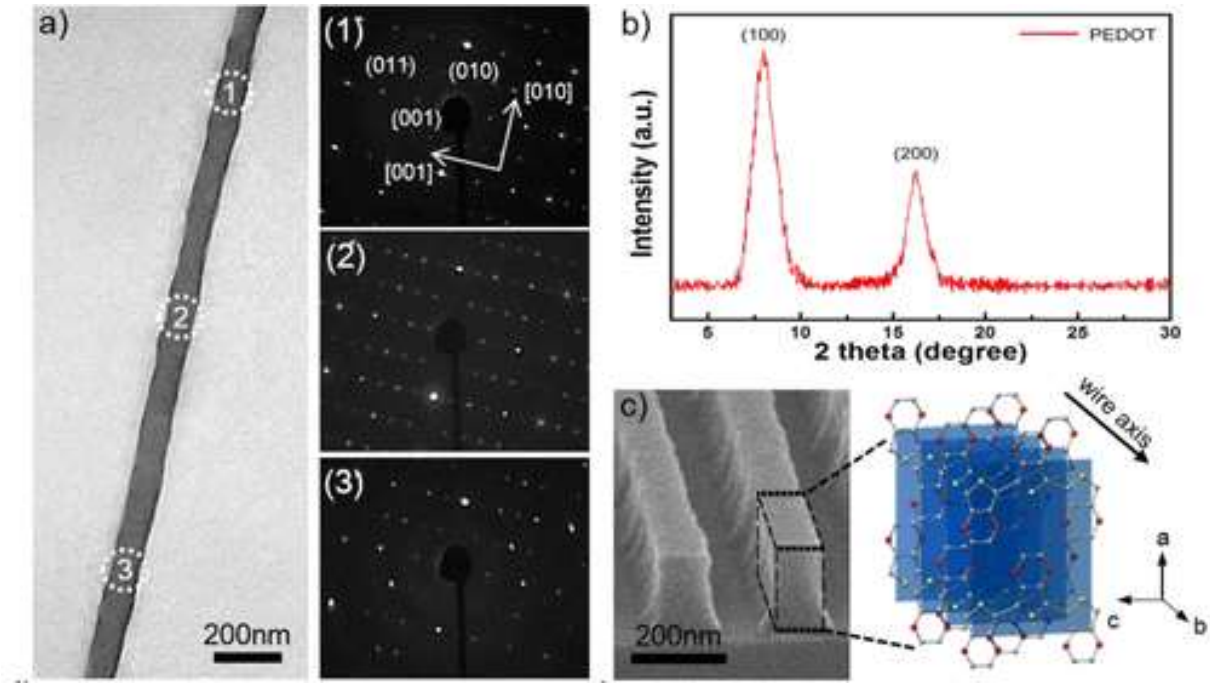

Figure 30. Single crystal PEDOT nanowires as synthesized by Cho *et al*.[24] (a) TEM images of a PEDOT nanowire and the corresponding SAED patterns taken at three different areas. (b) XRD pattern of a PEDOT nanowire. (c) Illustration of the crystal structure of the single-crystal PEDOT nanowire along the nanowire direction. Copyright 2014, American Chemical Society.

6-3-3. Transport

Compared to PEDOT:PSS, charge transport in PEDOT:Tos was less studied. However PEDOT:Tos together with organic solvent, ionic liquid or acid treated PEDOT:PSS nowadays routinely exhibit conductivities above

1500 S cm^{-1} so that they are readily described to depict a metallic behavior.[122,130,161–163] Bubnova and coworkers showed that PEDOT:Tos displayed a metallic behavior from 77 K to 370 K with an increasing electrical conductivity when the temperature decreases.[163] Simultaneously DEG-treated PEDOT:PSS showed a transition from semiconducting to metallic behavior with only a slight dependence on the temperature and non-treated PEDOT:PSS exhibited a typical semiconducting behavior although the temperature dependence was weak (Figure 31).

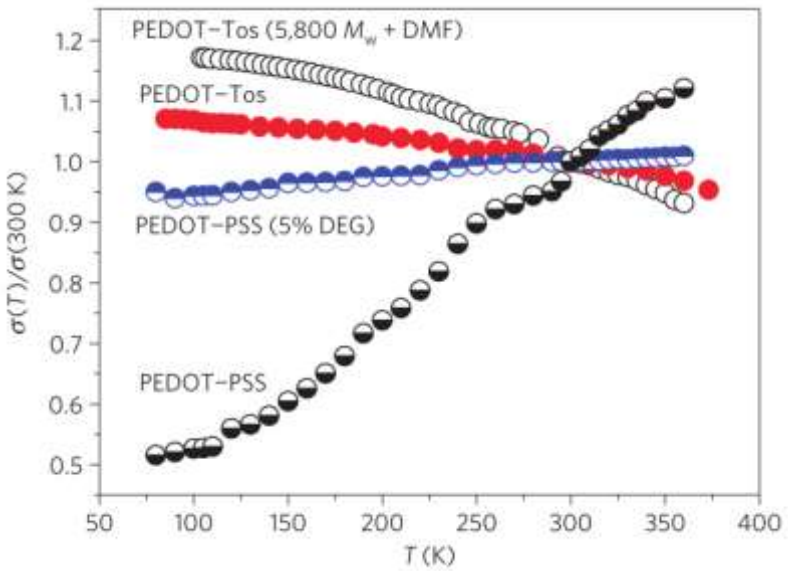

Figure 31. Temperature dependence of the electrical conductivity (normalized to 300K) for various PEDOT:Tos and PEDOT:PSS samples.[163] Copyright 2013, Springer Nature.

Such large variations in the transport properties in various PEDOT samples have been explained in terms of the nature of the majority charge carriers and the content of disordered.[163] In highly disordered materials, charges are distributed and do not form a continuous band. From an energetics point of view, the Fermi energy lies in the middle of the polaronic band if charges are polarons or between the valence band and the bipolaronic band in the case of bipolarons. A fermi glass is therefore obtained as illustrated by Bubnova *et al*. (Figure 32). That is a material in which charges are localized at the Fermi level and whose

wave functions do not possess any long range interaction. In such systems, the transport is described to take place mostly by hopping, following Mott VRH model in Equation 2 (Figure 4).[163]

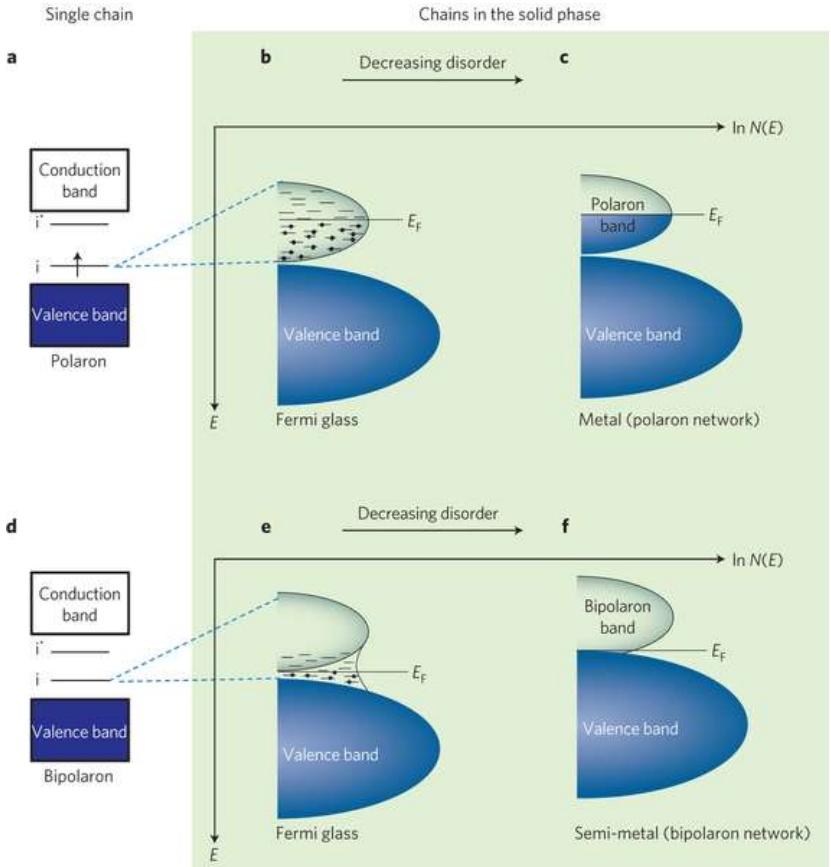

Figure 32. Representation of the electronic structure in PEDOT materials and in conducting polymers in general. a–c, If the majority charge carriers are polarons: (a) a polymer chain with one polaron, (b) the logarithm of the density of states (DOS) lnN(E) disordered material (c) as well as for a more ordered (metallic) system. In the latter case, the Fermi level lies in a delocalized polaron band while it was surrounded with localized states in the former case. d–f, If the majority charge carriers are bipolarons: (d) a polymer chain with one bipolaron, (e) lnN(E) for an disordered bipolaronic polymer solid, (f) as well as for a more ordered (semi-metallic) solid. The Fermi level lies between the valence band and the empty bipolaron band in the latter case.[163] Copyright 2013, Springer Nature.

With increasing order, polymer chains are better stacked and the charges are more delocalized. In polymers where polarons are the majority charges' carriers, wavefunctions overlap over several chains, a polaronic band is created, in the middle of which the Fermi level lies. The polymer hence depicts a metallic behavior as depicted in Figure 32 and observed in other conducting polymers such as the polyaniline.[36,46,49]

PEDOT is known to hold bipolarons charge carriers rather than polarons ones as evidenced by EPR.[163] In highly disordered PEDOT films (such as non-treated PEDOT:PSS), bipolarons are localized as in the case of polarons and the materials is a Fermi glass. In that respect, several studies reported VRH transport properties in PEDOT:PSS films.[113,114,170] In highly ordered PEDOT films (such as PEDOT:Tos or PEDOT:OTf reported by Murphy's, Crispin's, Hadziioannou or Simonato's groups), inter-chains transport is favored as well, but the bipolaronic band and the valence one slightly overlap, and the Fermi level lies within the interface.[47,162,163,171] Such system is described as a semi-metal, a material in which metallic and hopping transport compete and where the leading mechanism is directed by the degree of order and the ratio between polarons and bipolarons.[142,163] With an intermediary degree of order (intermediary meaning a state in which the chains' alignment is good enough to allow some delocalization of the charges, but not good enough for the Fermi level to lie within a full band), a transition from 3 D VRH to a more anisotropic 1 D VRH or quasi-metallic transport can be encountered. That is the case for solvent-treated PEDOT:PSS in which such transitions were previously reported.[110,113,114] Such explanation was validated by Munoz *et al*. through computational calculations.[172] The modeling of the density of states in PEDOT based on its morphology and electronic structure allowed them to observe this insulator to semi-metallic transition.

6-3-4. Conclusion

PEDOT:Tos, mostly deposited by vapor phase polymerization and sometimes by solution-cast polymerization is far more ordered and conductive than PEDOT:PSS. This is mainly due to the absence of insulating PSSH and the presence of smaller non-hindering tosylate counter-anions.

Transport properties in these materials were less studied than in the case of PEDOT:PSS. Main studies showed semi-metallic or metallic features in PEDOT:Tos which is subsequently described as a semi-metal, a material in which metallic and hopping transport compete and where the leading mechanism is governed by the degree of disorder. Parallel to these experimental observations of the highly ordered structure and metallic features in PEDOT:Tos, Zozoulenko and colleagues reported comprehensive work on the structure, morphology and transport properties in these materials using computational calculations and simulations.[38,157,172–174] Their results were discussed in light of literature data and highlighted the influence of the oxidation level, the solvent and water content, the type of counter-anion and the nature of the substrate on the chain length, the crystallization, the morphology and the transport properties. From their works, it mainly appeared that PEDOT crystallites are made of a stack of 3 to 6 chains whose length has no tremendous impact neither on the morphology nor on the mobility. This latter one is rather enhanced by the percolation paths made from effectively connected π-π stacked chains that link the crystallites embedded in an amorphous matrix.[173] Tos counter-anions are located either on the top of the chains or on the sides of the crystallites with no apparent periodic arrangement.[173,174] Moreover the nature of the substrate has a strong effect on the molecular packing and molecular mobility. Face-on arrangement of the chains is mainly observed on ordered substrates such as graphite whereas amorphous substrates such as SiO_2 promote edge-on arrangement. A highly ordered structure and a high degree of edge-on are however not sufficient for a high mobility. Indeed, a high mobility is mainly function of an efficient network of π-π stacked chains.[157,175] This is consistent with experiment works from Ugur *et al*. and Wang *et al*. on o-CVD PEDOT oxidized with $FeCl_3$[25,99] The counter-anion also plays an important role in the structure of the films and the transport properties. Both its nature (small) and its concentration (doping level higher than 50 %) can lead to a semi-metallic transition.

6-4. PEDOT:OTf and PEDOT:Sulf

6-4-1. Electrical conductivity vs structure

Researches have put tremendous efforts on increasing, if not optimizing and even maximizing, the electrical conductivity of PEDOT as illustrated in Table 1. PEDOT:PSS, although commercially available and easily solution-processable, retains however an excess insulating polystyrene sulfonic acid (PSSH) which hinders its conductivity. PEDOT with small counter-anions, such as tosylate, genuinely show better electrical properties due to the absence of the sterically hindering polymeric counter-anion, which allows the formation of a more crystalline structure.[162] PEDOT:Tos is mainly deposited through VPP. However, due to the processing technique itself (growth of the PEDOT film from the top surface of the EDOT-copolymer layer down to the substrate), the glycol copolymer can remain in the film, leading to the same problem encountered for PEDOT:PSS, in other words, the undesirable presence of an insulating phase might be found within the film. This is yet not the case for solution cast process in which the bottom-up polymerization process allows an easy rinsing of the copolymer.[160] In that context Simonato's group developed solution-cast PEDOT:OTf using the oxidant iron (III) trifluoromethane sulfonate (iron(III) triflate or $Fe(OTf)_3$).[47] The obtained films exhibit conductivities up to 1218 S cm^{-1}. Later on, given that aprotic polar solvents may easily coordinate with Fe(III), addition of NMP, DMSO and DMF in the procedure allowed to raise up conductivities up to 3600 S cm^{-1}.[23] The PEDOT:OTf films were further treated with diluted sulfuric acid. Such treatment was shown not only to enhance the oxidation level but also to replace most triflate counter-anions by hydrogeno-sulfate ones. Conductivities up to 5400 S cm^{-1} were measured for these optimized materials. [23,47]

More recently, Farka *et al*. demonstrated both PEDOT:OTf and PEDOT:Sulf synthesized through other means. PEDOT:OTf was obtained by treating commercial PEDOT:PSS films deposited by spin-coating with an aqueous triflic solution. Conductivities of to 2100 S cm^{-1} were obtained.[48,176] They also considered that the synthesis of the polymer itself hinders the engineering of an ordered system. Despite having a van-der-Waals crystal, the oxidation with metallic ions disturbs the structure and the introduction of counter-anions

leads to the formation of a disordered salt. They used therefore o-CVD whereby they introduced both the EDOT monomer and the sulfuric acid oxidant. The authors achieved highly conductive PEDOT:Sulf films reaching 4050 S cm^{-1}.[48,108]

6-4-2. Structure

The structure of PEDOT:OTf was thoroughly studied as shown in Figure 33. GIWAXS with synchrotron radiation, SAXS and WAXS measurements revealed a highly oriented structure for PEDOT:OTf compared to pristine PEDOT:PSS. Crystalline domains are present in the films, whose average characteristic size (around 5 nm wide and 7 to 9 nm high) is confirmed both by GIWAXS and HR-TEM. Chains in those crystalline domains are found to be oriented edge-on while both edge-on and face-on could be observed for PEDOT:PSS. The structure of PEDOT becomes better packed after the addition of aprotic polar solvent and the crystalline domains broader.[23,47]

After treatment of PEDOT:OTf with sulfuric acid or direct growth of PEDOT:Sulf using o-CVD, the obtained PEDOT:Sulf films are also very well ordered, surpassing the orders in structures observed for PEDOT:OTf and commercial PEDOT:PSS.[23,47,48,176,177]

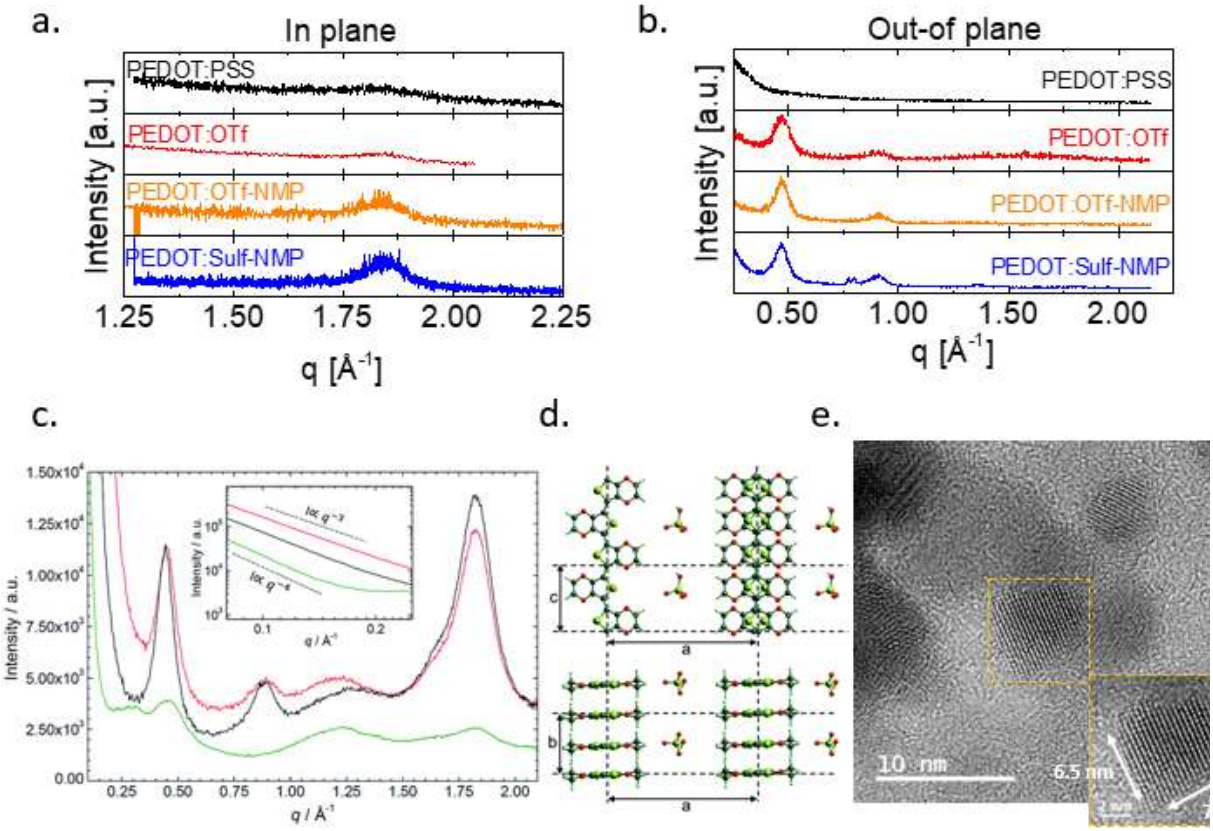

Figure 33. Structural characteristics of the PEDOT materials. (a) In-plane and (b) out-of plane synchrotron GIWAXS diffractograms of PEDOT:PSS, PEDOT:OTf, PEDOT:OTf-NMP, and PEDOT:Sulf-NMP.

(c) SAXS/WAXS intensity profile of PEDOT:PSS (green line), PEDOT:OTf in the pristine state (red line), and PEDOT:Sulf (black line). Top inset shows the intensity in the small angles domain.[47] (d) Scheme of stacking in the crystallites. (e) HRTEM image of PEDOT:OTf-NMP. Inset image is a magnification of the outlined square.[23] Copyright 2015, Royal Society of Chemistry (copyright review from Elsevier requested). Copyright 2016, American Chemical Society.

6-4-3. Transport

The transport mechanisms of PEDOT:OTf and PEDOT:Sulf were thoroughly studied along the characterization of the materials. Apart from the PEDOT:PSS-derived PEDOT:OTf, all materials depicted a very weak temperature dependence of their resistivity with a resistivity ratio ρ_r found to be smaller than 1.5.[23,48,177] This was attributed to a highly ordered structure and materials in the metallic side of the metal insulator transition. Thanks to their structure observed both with GIWAXS and TEM and their metallic features suggested by temperature dependence of conductivity measurements down to 3 K, Gueye *et al.* derived a heterogeneous conduction model that explains the transport mechanisms in these highly conductive films. In such model (see Figure 34) a quasi 1D-metallic conduction takes part in the crystalline domains (Equation 5), a disordered metallic one in the disordered regions (1st order of Equation 4) while a tunneling like conduction is allowed to take part between two crystalline regions close enough for that conduction model to take place (Equation 3).[23]

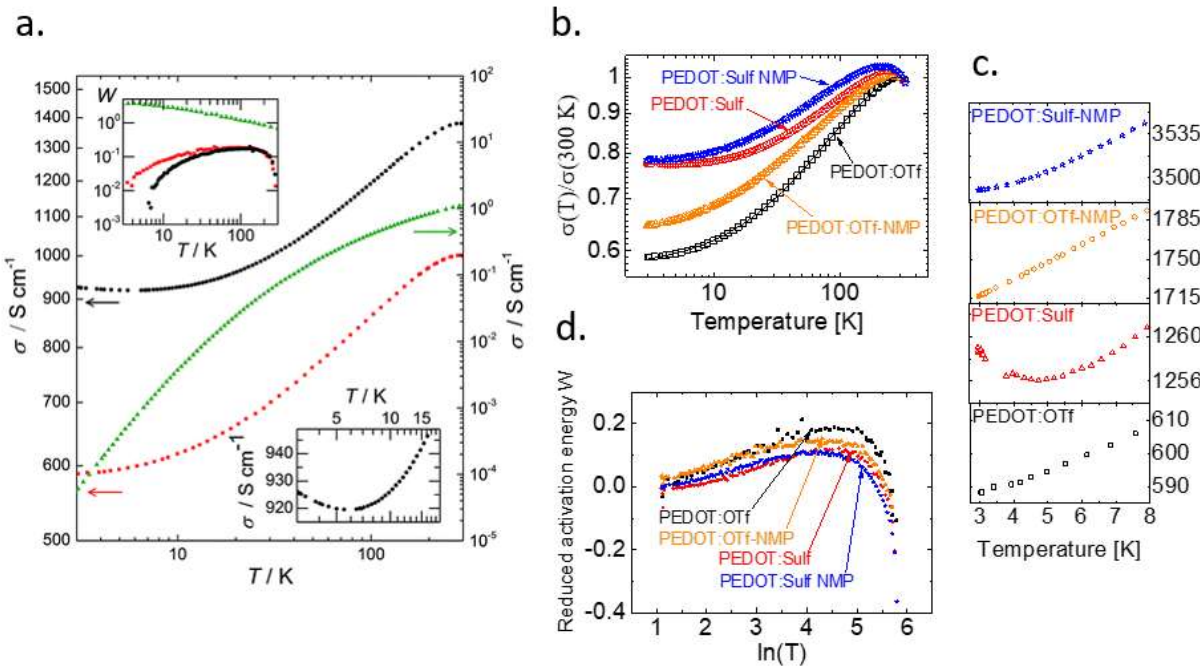

Figure 34. Transport properties of PEDOT based materials. (a) Log–log plot of the temperature dependence of conductivity of: (left Y axis) PEDOT:OTf (red squares) and PEDOT:Sulf (black circles); (right Y axis) PEDOT:PSS (green triangles). The top inset represents the corresponding reduced activation energy W as in Equation 6. W is found negative in the [3 K; 5.5 K] range for PEDOT:Sulf, demonstrating metallic behavior. The bottom inset represents the magnified electrical conductivity of PEDOT:Sulf in the [3 K; 20 K] range. [47]. (b) Temperature dependence of electrical conductivity (symbols) and calculated heterogeneous model of conduction (solid lines), (c) Low temperature dependence of electrical conductivity and (d) Reduced activation energy (W) of PEDOT materials vs ln(T). [23] Copyright 2015, Royal Society of Chemistry (copyright review from Elsevier requested). Copyright 2016, American Chemical Society.

With both temperature dependence of resistivity down to 1.8 K and magneto-conductance measurements, Farka *et al*. described PEDOT:Sulf as standing at the metallic side of the metal-insulator transition and as a glassy metal approaching the Mott-Ioffe-Regel limit as explained in Figure 6 and evidenced in Figure 35, limit by which the material can be considered as a metal.[48] They also demonstrated a minimum conductivity at

4 K, which could be shifted upwards to 10 K by increasing the pressure, hence allowing a metallic behavior on a longer temperature range.[177]

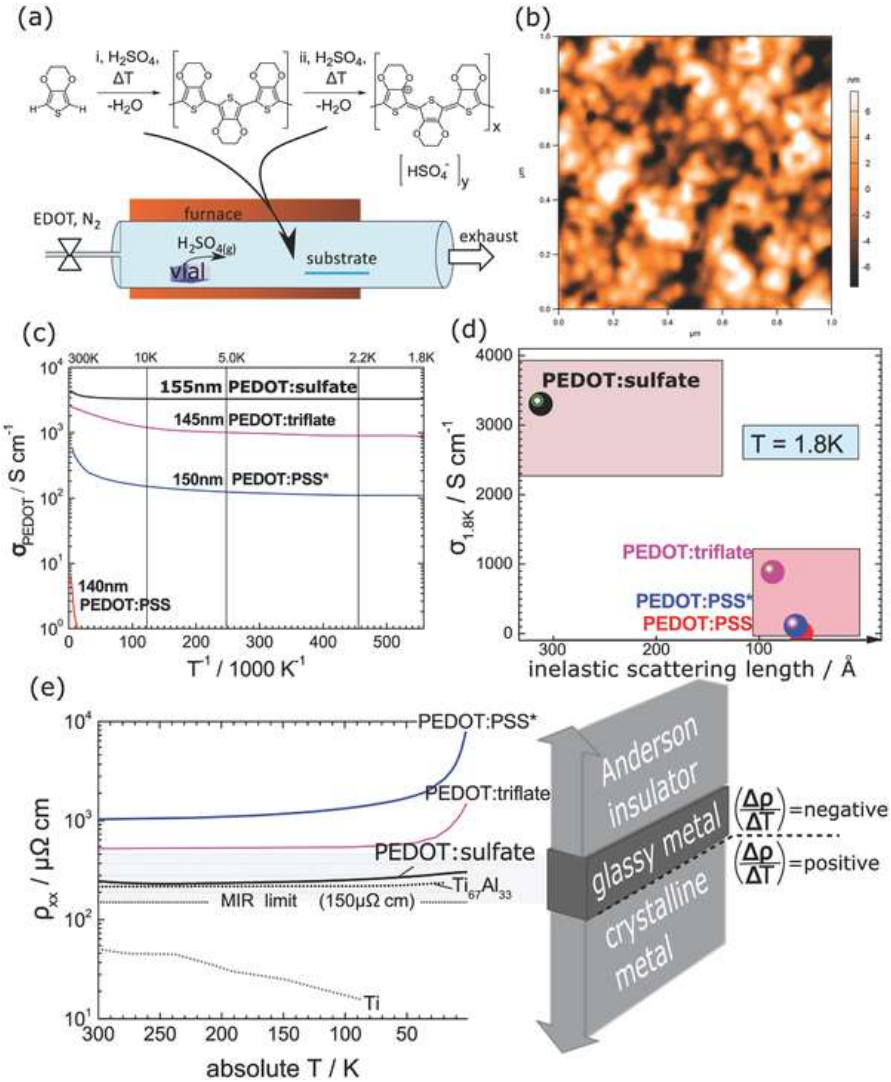

Figure 35. (a) Scheme of the o-CVD technique accompanied with a proposed reaction mechanism of the synthesis. (b) AFM topography of o-CVD grown PEDOT:sulfate thin film with an RMS roughness of 4.5 nm. (c) ρT-plot highlighting the flat *T*-profile of PEDOT:sulfate in particular at low temperatures. (d) Comparison between O-CVD PEDOT:sulfate compared and the solution processed PEDOT:PSS, PEDOT:PSS* (treated with DMSO), and PEDOT:triflate which exhibit lower performances. The role of disorder on σT→0 is schematized. (e) The Mott-Ioffe-Regel limit, as described in Figure 6, describes a critical resistivity (typically 150 μΩ cm), at which the sign of the temperature coefficient of resistivity $\frac{\Delta\rho}{\Delta T}$ in a metal changes (glassy to crystalline). In this article, the authors showed that PEDOT:sulfate behaves like glassy metal alloys such as $Al_{33}Ti_{67}$.[48]

Copyright 2017, John Wiley and Sons.

6-4-4. Conclusion

PEDOT:OTf and PEDOT:Sulf are recently developed materials. As a result of progress done on PEDOT:PSS and PEDOT:Tos, these materials are far more ordered with conductivities at the state of the art. Similarly to PEDOT:Tos and PEDOT:Br strong metallic features are observed and contrarily to PEDOT:Tos and PEDOT:PSS, transport properties were systematically studied down to liquid helium temperature or even lower. Particularly they are shown to stand near the limit of pure metallic conduction, limit that seems not to have been crossed mainly due to the inherently remaining disorder in PEDOT materials.

7. Rising importance of PEDOT in applications

The importance of PEDOT can truly be appreciated while acknowledging the numerous applications that are being commercialized or investigated.[6,178,179] We do not aim here to give an exhaustive overview of the applications for PEDOT materials, which would require a whole new report, but rather to give a quick grasp on the importance this material has gained across the years and in the different applications it is used for. The interested reader can refer to more exhaustive reviews dealing with PEDOT related applications. [6,7,9,14,18,20,180–183]

Early electro-polymerized PEDOT was readily described as counter-electrode for capacitors.[21] As a matter of fact, the counter-electrode used at that time, namely manganese dioxide, was less conductive than PEDOT and in addition, reduced the safety of the device during operation due to its strong redox couple with the metal electrode.[14] The use of a conducting polymer as counter-electrode settled both issues. Later on, PEDOT:PSS was developed as an antistatic coating for photographic films and was first introduced as an industrial product.[4,70] Soon after, PEDOT:PSS was proposed as an antistatic coater for cathode ray tubes

and up to now, this product is found in several antistatic applications where moderate conductivities from 10^{-9} to 10^{-5} S per square are generally required.

The high electrical conductivity of PEDOT materials combined to a great optical transparency in visible light range, a good film forming ability, a compatibility with various deposition techniques and a relatively good stability make them valuable materials for the development of low-cost, flexible, high performance electronic devices with applications in various domains. The development of various grades of PEDOT:PSS and PEDOT based formulations over the last two decades opened the doors for applications in a wide range of fields spanning from antistatic coatings to energy conversion and energy storage devices.[20,184–186] Nowadays PEDOT-based materials are still studied and developed with potential applications in new domains such as thin film transparent heaters, thermoelectricity or bioelectronics to name a few.[107,187–189]

One of the first application of PEDOT in optoelectronic was related to the fabrication of transparent and conductive electrode for organic solar cells or light emitting diodes.[190] The main motivation behind the use of PEDOT was to get rid of Indium tin oxide (ITO) which is too expensive and rigid despite showing a good combination of transparency and conductivity. PEDOT:PSS owing to its easy processability and physical properties appears quickly as a good material for use as transparent electrode.[191]

As the reported conductivities exceeded 1000 S cm^{-1}, the conductivity of PEDOT became comparable to that of ITO and applications such as transparent electrodes for organic photovoltaics and organic light emitting diodes and organic transistors for sensors have been widely developed. [7,10,16,20,115,192–197]

The replacement of ITO by PEDOT:PSS opens up the door for the fabrication of flexible solar cells and the use of printing techniques such as slot die coating, gravure printing and flexography were employed to manufacture PEDOT-based electrodes with a roll-to-roll process.[198,199]

Dye-sensitized solar cells also benefit from the unique properties of PEDOT:PSS. Indeed, PEDOT has been investigated as a low cost alternative of Pt that is commonly employed as the counter electrode material in

DSSCs. Interestingly PEDOT demonstrates a higher conductivity and a good electro-catalytic activity with respect to Pt counter electrodes. Consequently, comparable efficiencies can be achieved using PEDOT-based materials instead of Pt.[200]

Apart from solar cells applications, PEDOT appears useful in the development of electrochemical energy storage devices such as supercapacitors or batteries.[201,202] PEDOT possesses a low oxidation potential and a high charge mobility that permit fast electrochemical kinetics particularly interesting for this application. In addition PEDOT has a relatively wide electrochemical window of 1.2–1.5 V. However, its poor stability caused by over-oxidation process is often a limitation. Its low mechanical stability upon cycling is certainly another drawback but the development of PEDOT based composites is expected to circumvent this problem.[203]

More recently, organic materials have emerged in the field of thermoelectricity and PEDOT-based materials are certainly going to play a main role in the development of future thermoelectric generators for low temperature energy conversion. Organic thermoelectric generators (OTEGs) exploit the Seebeck effect for heat-to-electricity production. Thermoelectric materials can convert heat to electricity when they are placed in between hot and cold sources. When a temperature gradient is applied to these materials, more energetic electrons flow from the hot side to the cold side. At steady-state, the electron concentration gradient is balanced by the resulting internal electric field. Organic materials are nowadays attracting a huge interest for such applications not only because they exhibit low thermal conductivity, but also because they reveal intrinsic advantages such as low toxicity, light-weight, good mechanical properties, and they can be processed from solutions which is a tremendous advantage compared to expensive, and often toxic, inorganic metallic alloys.

In that field, PEDOT-based materials and composites quickly showed encouraging ZT values.[204] More interestingly, some outstanding ZT figures of 1.02 and 2.0 were reported at room temperature, which are competing with the best inorganic semiconductor (*i.e.* $Bi_{0,5}Sb_{1,5}Te_3$, ZT = 1.86 at 47°C).[205–207]

These recent developments render organic thermoelectrics the next-generation wearable and flexible energy harvesting system and active cooling system.[208]

PEDOT materials are however not only characterized by their electrical conductivity, but also their electroactive, electrochromic, thermoelectric properties and thermal stability.[209,210] In that respect, PEDOT was demonstrated as an actuator that contracts or expands when subjected to a bias and in a relatively humid atmosphere, or as the active material of thermochromic and electrochromic devices. [106] They were also showed to depict power factors and figures of merit barely one order of magnitude lower than their inorganic counterparts for thermoelectricity. [9,31,105,205,211] Thanks to the conductivity improvement of PEDOT materials, new applications are now possible. For instance, it was recently demonstrated for the first time that 100 % polymeric thin films proved very efficient for the fabrication or transparent flexible film heaters.[107]

Another great feature of PEDOT is its compatibility with biologic systems and flexible devices combined with its electronic properties. These properties have allowed the emergence of organic bioelectronics as a major and fast developing application field.[10] Since a biochemical reaction may change the doping state of PEDOT materials and that an electronic signal from a device may simulate a biological event, applications such as biosensors, drug delivery systems or health monitoring devices are also taking advantage of the unique properties of PEDOT-based materials.[181] While it is commonly used in flexible devices, PEDOT in general, and PEDOT:PSS in particular is recently highly studied as a stretchable conductive material for applications in wearable and implantable electronics. [212,213] Stretchable conductive materials require to be stretched past some defined engineering strain, typically 10%. PEDOT being not intrinsically stretchable to that extent, strategies to increase the stretchability include the addition of plasticizers, the blending with soft materials, ionic liquids or polymers, the deposition on elastomers or the engineering of 1D structures of PEDOT:PSS. Interesting applications such as soft robotics, human machine interfaces and electronic skins with organic materials are hence emerging and new challenges including the mechanical, thermal and

chemical stability for compatibility with the targeted electronic device, mainly biologic systems, are to overcome.

As shown hereinbefore, the progress achieved through all these years has rendered all these applications possible and is still opening new possibilities. Even though an exhaustive description of past and current applications was not given in this review, this short overview points out the great potential behind PEDOT based materials as well as the perspectives they are opening.

8. Conclusions

Tremendous efforts have been devoted to the development of conductive polymers during the last decades. In particular, PEDOT based materials have been intensively studied and developed, due to their outstanding properties. The electrical conductivity value which was only few S cm^{-1} at the beginning has been raised to more than 6200 S cm^{-1}, which is only one order of magnitude below the bulk conductivity of the most conductive metals, namely silver and copper. As pointed out in this review, the evolution of the electrical conductivity is closely related to several parameters such as the fabrication process, the crystallinity of the material and the choice of the counter-anions. An increased understanding and control of key parameters concerning transport mechanisms have also been unveiled, leading to an improved comprehension of the strong relationship existing between structural features and electronic transport properties. Understanding the electronic transport could allow not only to better comprehend the dispersion of the data in the literature, but also to design materials with better performances. Thanks to the enhanced properties of up to date PEDOT materials, new functionalities appear feasible and extend their already large applicative potential. The recent developments on the enhancement and comprehension of the electrical properties of PEDOT, its stability, film forming properties, bio compatibility, optical and thermoelectric properties open a wide panel of possibilities for its engineering and integration in organic devices. There is no doubt that further improvements are still to be achieved and that PEDOT conductive polymers will be increasingly used in commercial high performance products.

Acknowledgements

The authors acknowledge the LABEX Laboratoire d'Alliances Nanosciences-Energies du Futur (LANEF, ANR-10-LABX-51-01) and the ANR project Harvesters (ANR-16-CE05-0029-01) for funding this work.

Appendix

AFM	Atomic force microscopy
CSA	Camphorsulfonic acid
DEG	Diethylene glycol
DMF	Dimethyl formamide
DMSO	Dimethylsulfoxide
EDOT	3,4-ethylene dioxythiophene
EMIM-TCB	1-ethyl-3-methylimidazolium tetracyanoborate
EG	Ethylene glycol
EPR	Electron paramagnetic resistance
HAADF-STEM	High-angle annular dark field scanning transmission electron microscopy
LPDP	Liquid phase deposition polymerization
MDOT	Methylene dioxythiophene
NMP	N-methyl-2-pyrrolidone
o-CVD	Oxidative chemical vapor deposition

PANI	Polyaniline
PEDOT	Poly(3,4-ethylene dioxythiophene)
PSS	Polystyrene sulfonate
SCP	Solution cast polymerization
STM	Scanning tunneling microscopy
TEM	Transmission electron microscopy
UV-Vis-NIR	Ultraviolet – Visible – Near infrared
VPP	Vapor phase polymerization
VRH	Variable range hopping
XPS	X-ray photoelectron spectroscopy
XRD	X-ray diffraction

References

[1] Park YW, Heeger AJ, Druy MA, MacDiarmid AG. Electrical transport in doped polyacetylene. J Chem Phys 1980;73:946–57. doi:10.1063/1.440214.

[2] Park YW, Park C, Lee YS, Yoon CO, Shirakawa H, Suezaki Y, et al. Electrical conductivity of highly-oriented-polyacetylene. Solid State Commun 1988;65:147–50. doi:10.1016/0038-1098(88)90675-8.

[3] Heeger AJ. Semiconducting and Metallic Polymers: The Fourth Generation of Polymeric Materials (Nobel Lecture). Angew Chemie Int Ed 2001;40:2591–611. doi:10.1002/1521-3773(20010716)40:14<2591::AID-ANIE2591>3.0.CO;2-0.

[4] Jonas F, Morrison JT. 3,4-polyethylenedioxythiophene (PEDT): Conductive coatings technical applications and properties. Synth Met 1997;85:1397–8. doi:10.1016/S0379-6779(97)80290-1.

[5] Groenendaal L, Jonas F, Freitag D, Pielartzik H, Reynolds JR. Poly(3,4-ethylenedioxythiophene) and Its Derivatives: Past, Present, and Future. Adv Mater 2000;12:481–94. doi:10.1002/(SICI)1521-4095(200004)12:7<481::AID-ADMA481>3.0.CO;2-C.

[6] Wen Y, Xu J. Scientific Importance of Water-Processable PEDOT–PSS and Preparation, Challenge and New Application in Sensors of Its Film Electrode: A Review. J Polym Sci Part A Polym Chem 2017;55:1121–50. doi:10.1002/pola.28482.

[7] Wei W, Wang H, Hu YH. A review on PEDOT-based counter electrodes for dye-sensitized solar cells. Int J Energy Res 2014;38:1099–111. doi:10.1002/er.

[8] Ouyang J. “Secondary doping” methods to significantly enhance the conductivity of PEDOT:PSS for its application as transparent electrode of optoelectronic devices. Displays 2013;34:423–36. doi:10.1016/j.displa.2013.08.007.

[9] Li Y, Du Y, Dou Y, Cai K, Xu J. PEDOT-based thermoelectric nanocomposites – A mini-review. Synth Met 2017;226:119–28. doi:10.1016/j.synthmet.2017.02.007.

[10] Nikolou M, Malliaras GG. Applications of poly (3,4-ethylenedioxythiophene) doped with poly(styrene sulfonic acid) transistors in chemical and biological sensors. Chem Rec 2008;8:13–22. doi:10.1002/tcr.20133.

[11] Hui Y, Bian C, Xia S, Tong J, Wang J. Synthesis and electrochemical sensing application of poly(3,4-ethylenedioxythiophene)-based materials: A review. Anal Chim Acta 2018;1022:1–19. doi:10.1016/j.aca.2018.02.080.

[12] Ouyang J. Recent advances of intrinsically conductive polymers. Wuli Huaxue Xuebao/ Acta Phys - Chim Sin 2018;34:1211–20. doi:10.3866/PKU.WHXB201804095.

[13] Greczynski G, Kugler T, Keil M, Osikowicz W, Fahlman M, Salaneck WR. Photoelectron spectroscopy of thin films of PEDOT – PSS conjugated polymer blend : a mini-review and some new results. J Electron Spectros Relat Phenomena 2001;121:1–17. doi:10.1016/S0368-2048(01)00323-1.

[14] Kirchmeyer S, Reuter K. Scientific importance, properties and growing applications of poly(3,4-ethylenedioxythiophene). J Mater Chem 2005;15:2077. doi:10.1039/b417803n.

[15] Andreas Elschner; Stephan Kirchmeyer; Wilfried Lövenich; Udo Merker; Knud Reuter. PEDOT Principples and applications of an Intrinsically Conductive Polymer. 2011.

[16] Rozlosnik N. New directions in medical biosensors employing poly(3,4-ethylenedioxy thiophene) derivative-based electrodes. Anal Bioanal Chem 2009;395:637–45. doi:10.1007/s00216-009-2981-8.

[17] Martin DC, Wu J, Shaw CM, King Z, Spanninga SA, Richardson-Burns S, et al. The Morphology of Poly(3,4-Ethylenedioxythiophene). Polym Rev 2010;50:340–84. doi:10.1080/15583724.2010.495440.

[18] Yue R, Xu J. Poly(3,4-ethylenedioxythiophene) as promising organic thermoelectric materials: A mini-review. Synth Met 2012;162:912–7. doi:10.1016/j.synthmet.2012.04.005.

[19] Shi H, Liu C, Jiang Q, Xu J. Effective Approaches to Improve the Electrical Conductivity of PEDOT:PSS: A Review. Adv Electron Mater 2015;1:1500017. doi:10.1002/aelm.201500017.

[20] Sun K, Zhang S, Li P, Xia Y, Zhang X, Du D, et al. Review on application of PEDOTs and PEDOT:PSS in energy conversion and storage devices. J Mater Sci Mater Electron 2015;26:4438–62. doi:10.1007/s10854-015-2895-5.

[21] Jonas F, Heywang G, Schmidtberg W. Feststoff-elektrolyte und diese enthaltende elektrolyt-kondensatoren. DE 3814730 A1, 1988.

[22] Heywang G, Jonas F, Heinze J, Dietrich M. Neue polythiophene, verfahren zu ihrer herstellung und ihre verwendung. DE 3843412 A1, 1988.

[23] Gueye MN, Carella A, Massonnet N, Yvenou E, Brenet S, Faure-Vincent J, et al. Structure and Dopant Engineering in PEDOT Thin Films: Practical Tools for a Dramatic Conductivity Enhancement. Chem Mater 2016;28:3462–8. doi:10.1021/acs.chemmater.6b01035.

[24] Cho B, Park KS, Baek J, Oh HS, Koo Lee Y-E, Sung MM. Single-Crystal Poly(3,4-ethylenedioxythiophene) Nanowires with Ultrahigh Conductivity. Nano Lett 2014;14:3321–7. doi:10.1021/nl500748y.

[25] Wang X, Zhang X, Sun L, Lee D, Lee S, Wang M, et al. High electrical conductivity and carrier mobility in oCVD PEDOT thin films by engineered crystallization and acid treatment. Sci Adv 2018;4:eaat5780. doi:10.1126/sciadv.aat5780.

[26] Zhou J, Liao B, Chen G. First-principles calculations of thermal, electrical, and thermoelectric transport properties of semiconductors. Semicond Sci Technol 2016;31:043001. doi:10.1088/0268-1242/31/4/043001.

[27] Tessler N, Preezant Y, Rappaport N, Roichman Y. Charge transport in disordered organic materials and its relevance to thin-film devices: A tutorial review. Adv Mater 2009;21:2741–61. doi:10.1002/adma.200803541.

[28] Noriega R, Rivnay J, Vandewal K, Koch FP V, Stingelin N, Smith P, et al. A general relationship between disorder, aggregation and charge transport in conjugated polymers. Nat Mater 2013;12:1038–44. doi:10.1038/nmat3722.

[29] Yao Y, Dong H, Hu W. Charge transport in organic and polymeric semiconductors for flexible and stretchable devices. Adv Mater 2015;28:4513–23. doi:10.1002/adma.201503007.

[30] Wei Q, Mukaida M, Kirihara K, Ishida T. Experimental Studies on the Anisotropic Thermoelectric Properties of Conducting Polymer Films. ACS Macro Lett 2014;3:948–52. doi:10.1021/mz500446z.

[31] Patel SN, Chabinyc ML. Anisotropies and the thermoelectric properties of semiconducting polymers.

J Appl Polym Sci 2017;134:44403. doi:10.1002/app.44456.

[32] Coropceanu V, Cornil J, da Silva Filho DA, Olivier Y, Silbey R, Brédas JL. Charge transport in organic semiconductors. Chem Rev 2007;107:926–52. doi:10.1021/cr050140x.

[33] Anderson P. Absence of Diffusion in Certain Random Lattices. Phys Rev 1958;109:1492–505.

[34] Böhm W, Fritz T, Leo K. Charge Transport in Thin Organic Semiconducting Films: Seebeck and Field Effect Studies. Phys Status Solidi 1997;160:81–7. doi:10.1002/1521-396X(199703)160:1<81::AID-PSSA81>3.0.CO;2-S.

[35] Aleshin a. N. Charge carrier transport in conducting polymers on the metal side of the metal-insulator transition: A review. Phys Solid State 2010;52:2307–32. doi:10.1134/S106378341011017X.

[36] Kaiser AB. Electronic transport properties of conducting polymers and carbon nanotubes. Reports Prog Phys 2001;64:1–49.

[37] Mott NF. Conduction in non-crystalline materials. Philos Mag 1969;19:835–52. doi:10.1080/14786436908216338.

[38] Ihnatsenka S, Crispin X, Zozoulenko I V. Understanding hopping transport and thermoelectric properties of conducting polymers. Phys Rev B 2015;92:035201. doi:10.1103/PhysRevB.92.035201.

[39] Efros AL, Shklovskii BI. Coulomb gap and low temperature conductivity of disordered systems. J Phys C Solid State Phys 1975;8. doi:10.1088/0022-3719/8/4/003.

[40] Efros AL, Shklovskii BI. Influence of electron-electron interaction on hopping conduction of disordered systems. J Non Cryst Solids 1987;97–98:31–8. doi:10.1016/0022-3093(87)90010-X.

[41] Sheng P, Abeles B, Arie Y. Hopping Conductivity in Granular Metals. Phys Rev Lett 1973;31:44–7.

[42] Sheng P. Fluctuation-induced tunneling conduction in disordered materials. Phys Rev B 1980;21:2180–95. doi:10.1103/PhysRevB.21.2180.

[43] Zuppiroli L, Bussac MN, Paschen S, Chauvet O, Forro L. Hopping in disordered conducting polymers. Phys Rev B 1994;50:5196–203. doi:10.1103/PhysRevB.50.5196.

[44] Menon R, Yoon CO, Moses D, Heeger AJ, Cao Y. Transport in polyaniline near the critical regime of the metal-insulator transition. Phys Rev B 1993;48:17685–94. doi:10.1103/PhysRevB.48.17685.

[45] Ishiguro T, Kaneko H, Nogami Y, Ishimoto H, Nishiyama H, Tsukamoto J, et al. Logarithmic temperature dependence of resistivity in heavily doped conducting polymers at low temperature. Phys Rev Lett 1992;69:660–3. doi:10.1103/PhysRevLett.69.660.

[46] Lee K, Cho S, Park SH, Heeger a J, Lee C-W, Lee S-H. Metallic transport in polyaniline. Nature 2006;441:65–8. doi:10.1038/nature04705.

[47] Massonnet N, Carella A, de Geyer A, Faure-Vincent J, Simonato J-P. Metallic behaviour of acid doped highly conductive polymers. Chem Sci 2015;6:412–7. doi:10.1039/C4SC02463J.

[48] Farka D, Coskun H, Gasiorowski J, Cobet C, Hingerl K, Uiberlacker LM, et al. Anderson-Localization and the Mott-Ioffe-Regel Limit in Glassy-Metallic PEDOT. Adv Electron Mater 2017;3:1700050. doi:10.1002/aelm.201700050.

[49] Kaiser AB. Metallic behaviour in highly conducting polymers. Synth Met 1991;45:183–96. doi:10.1016/0379-6779(91)91802-H.

[50] Kaiser AB, Graham SC. Temperature dependence of conductivity in 'metallic' polyacetylene. Synth Met 1990;36:367–80. doi:10.1016/0379-6779(90)90260-R.

[51] Ahlskog M, Reghu M, Heeger a J. The temperature dependence of the conductivity in the critical regime of the metal - insulator transition in conducting polymers. J Phys Condens Matter 1999;9:4145–56. doi:10.1088/0953-8984/9/20/014.

[52] Kivelson S, Heeger A. Intrinsic conductivity of conducting polymers. Synth Met 1988;22:371–84. doi:10.1016/0379-6779(88)90108-7.

[53] Kaiser AB. Electronic properties of conducting polymers. Berlin: Springer; 1987.

[54] Mott NF. Metal-insulator Transtion. 2nd editio. London: 1979.

[55] Dufour B, Rannou P, Fedorko P, Djurado D, Travers J-P, Pron A. Effect of Plasticizing Dopants on Spectroscopic Properties, Supramolecular Structure, and Electrical Transport in Metallic Polyaniline. Chem Mater 2001;13:4032–40. doi:10.1021/cm001224j.

[56] Dufour B, Rannou P, Djurado D, Janeczek H, Zagorska M, de Geyer A, et al. Low T g , Stretchable Polyaniline of Metallic-Type Conductivity: Role of Dopant Engineering in the Control of Polymer Supramolecular Organization and in the Tuning of Its Properties. Chem Mater 2003;15:1587–92. doi:10.1021/cm021354n.

[57] Ahlskog M, Menon R, Heeger A, Noguchi T, Ohnishi T. Electronic transport in the metallic state of oriented poly(p-phenylenevinylene). Phys Rev B 1996;53:15529–37. doi:10.1103/PhysRevB.53.15529.

[58] Zabrodskii AG, Zinov'eva KN. Low-temperature conductivity and metal-insulator transition in compensate n-Ge. Sov Phys JETP 1984;59:425–33.

[59] Kang SD, Snyder GJ. Charge-transport model for conducting polymers. Nat Mater 2017;16:252–7. doi:10.1038/nmat4784.

[60] Naarmann H, Theophilou N. New process for the production of metal-like, stable polyacetylene. Synth Met 1987;22:1–8. doi:10.1016/0379-6779(87)90564-9.

[61] Münstedt H. Ageing of electrically conducting organic materials. Polymer (Guildf) 1988;29:296–302. doi:10.1016/0032-3861(88)90337-0.

[62] Roth S, Filzmoser M. Conducting polymers?thirteen years of Polyacetylene Doping. Adv Mater 1990;2:356–60. doi:10.1002/adma.19900020804.

[63] Jonas F, Schrader L. Conductive modifications of polymers with polypyrroles and polythiophenes. Synth Met 1991;41:831–6. doi:10.1016/0379-6779(91)91506-6.

[64] McNeill R, Siudak R, Wardlaw J, Weiss D. Electronic Conduction in Polymers. I. The Chemical Structure of Polypyrrole. Aust J Chem 1963;16:1056–75. doi:10.1071/CH9631056.

[65] Bolto B, Weiss D. Electronic Conduction in Polymers. II. The Electrochemical Reduction of Polypyrrole at Controlled Potential. Aust J Chem 1963;16:1076–89. doi:10.1071/CH9631076.

[66] Bolto BA, McNeill R, Weiss DE. Electronic conduction in polymers III. The electronic properties of polypyrrole. Aust J Chem 1963;16:1090–103.

[67] Fichou D. Handbook of oligo- and polythiophenes. Weinheim. 1999.

[68] Heywang G, Jonas F. Poly(alkylenedioxythiophene)s—new, very stable conducting polymers. Adv Mater 1992;4:116–8. doi:10.1002/adma.19920040213.

[69] Jonas F, Heywang G, Schmidtberg W, Heinze J, Dietrich M. Procédé pour la préparation de Polythiophènes. EP0339340, 1988.

[70] Jonas F, Krafft W. Dispersions de polythiophènes nouvelles, leur préparation et leur utilisation. EP0440957, 1990.

[71] MacDiarmid AG, Epstein AJ. The concept of secondary doping as applied to polyaniline. Synth Met 1994;65:103–16. doi:10.1016/0379-6779(94)90171-6.

[72] Roncali J, Blanchard P, Frère P. 3,4-Ethylenedioxythiophene (EDOT) as a versatile building block for advanced functional pi-conjugated systems. J Mater Chem 2005;15:1589–610. doi:10.1039/b415481a.

[73] Yamamoto T, Abla M. Synthesis of non-doped poly(3,4-ethylenedioxythiophene) and its spectroscopic data. Synth Met 1999;100:237–9. doi:10.1016/S0379-6779(99)00005-3.

[74] Pei Q, Zuccarello G, Ahlskog M, Inganäs O. Electrochromic and highly stable poly(3,4-ethylenedioxythiophene) switches between opaque blue-black and transparent sky blue. Polymer (Guildf) 1994;35:1347–51. doi:10.1016/0032-3861(94)90332-8.

[75] Aleshin A, Kiebooms R, Menon R, Heeger AJ. Electronic transport in doped poly (3,4-ethylenedioxythiophene) near the metal-insulator transition. Synth Met 1997;90:61–8. doi:10.1016/S0379-6779(97)81227-1.

[76] Granström M, Inganäs O. Electrically conductive polymer fibres with mesoscopic diameters: 1. Studies of structure and electrical properties. Polymer (Guildf) 1995;36:2867–72. doi:10.1016/0032-3861(95)94335-Q.

[77] Zotti G, Zecchin S, Schiavon G, Louwet F, Groenendaal L, Crispin X, et al. Electrochemical and XPS studies toward the role of monomeric and polymeric sulfonate counterions in the synthesis, composition, and properties of poly(3,4-ethylenedioxythiophene). Macromolecules 2003;36:3337–44. doi:10.1021/ma021715k.

[78] Culebras M, Gómez CM, Cantarero A. Enhanced thermoelectric performance of PEDOT with different counter-ions optimized by chemical reduction. J Mater Chem A 2014;2:10109–15. doi:10.1039/C4TA01012D.

[79] Mueller M, Fabretto M, Evans D, Hojati-Talemi P, Gruber C, Murphy P. Vacuum vapour phase polymerization of high conductivity PEDOT: Role of PEG-PPG-PEG, the origin of water, and choice of oxidant. Polymer (Guildf) 2012;53:2146–51. doi:10.1016/j.polymer.2012.03.028.

[80] Brooke R, Cottis P, Talemi P, Fabretto M, Murphy P, Evans D. Recent advances in the synthesis of conducting polymers from the vapour phase. Prog Mater Sci 2017;86:127–46. doi:10.1016/j.pmatsci.2017.01.004.

[81] Massonnet N. Développement et optimisation de matériaux à base de poly (3,4-

éthylènedioxythiphène) pour des applications thermoélectriques. Université Grenoble Alpes, 2014.

[82] Jin Bae E, Hun Kang Y, Jang K-S, Yun Cho S. Enhancement of thermoelectric properties of PEDOT:PSS and tellurium-PEDOT:PSS hybrid composites by simple chemical treatment. Sci Rep 2016;6:DOI: 10.1038/srep18805. doi:10.1038/srep18805.

[83] Hofmann AI, Katsigiannopoulos D, Mumtaz M, Petsagkourakis I, Pecastaings G, Fleury G, et al. How To Choose Polyelectrolytes for Aqueous Dispersions of Conducting PEDOT Complexes. Macromolecules 2017;50:1959–69. doi:10.1021/acs.macromol.6b02504.

[84] de Leeuw DM, Kraakman PA, Bongaerts PFG, Mutsaers CMJ, Klaassen DBM. Electroplating of conductive polymers for the metallization of insulators. Synth Met 1994;66:263–73. doi:10.1016/0379-6779(94)90076-0.

[85] Pettersson LAA, Carlsson F, Inganäs O, Arwin H. Spectroscopic ellipsometry studies of the optical properties of doped poly(3,4-ethylenedioxythiophene): an anisotropic metal. Thin Solid Films 1998;313–314:356–61. doi:10.1016/S0040-6090(97)00846-8.

[86] Hohnholz D, MacDiarmid AG, Sarno DM, E. Johnes Jr. W. Uniform thin films of poly-3,4-ethylenedioxythiophene (PEDOT) prepared by in-situ deposition. Chem Commun 2001;0:2444–5. doi:10.1039/b107130k.

[87] Winther-Jensen B, West K. Vapor-phase polymerization of 3,4-ethylenedioxythiophene: A route to highly conducting polymer surface layers. Macromolecules 2004;37:4538–43. doi:10.1021/ma049864l.

[88] Lock JP, Im SG, Gleason KK. Oxidative Chemical Vapor Deposition of Electrically Conducting Poly(3,4-ethylenedioxythiophene) Films. Macromolecules 2006;39:5326–9. doi:10.1021/ma060113o.

[89] Kim J, Kwon M, Min Y, Kwon S, Ihm D. Self-Assembly and Crystalline Growth of Poly (3 , 4-ethylenedioxythiophene) Nanofilms. Adv Mater 2007;19:3501–6. doi:10.1002/adma.200602163.

[90] Fabretto M, Müller M, Hall C, Murphy P, Short RD, Griesser HJ. In-situ QCM-D analysis reveals four distinct stages during vapour phase polymerisation of PEDOT thin films. Polymer (Guildf) 2010;51:1737–43. doi:10.1016/j.polymer.2010.02.019.

[91] Winther-Jensen B, Breiby DW, West K. Base inhibited oxidative polymerization of 3,4-ethylenedioxythiophene with iron(III)tosylate. Synth Met 2005;152:1–4. doi:10.1016/j.synthmet.2005.07.085.

[92] Howden RM, McVay ED, Gleason KK. oCVD poly(3,4-ethylenedioxythiophene) conductivity and lifetime enhancement via acid rinse dopant exchange. J Mater Chem A 2013;1:1334–40. doi:10.1039/C2TA00321J.

[93] Li J, Zhang M, Liu J, Ma Y. Effect of attached peroxyacid on liquid phase depositional polymerization of EDOT over PI film with adsorbed ferric chloride. Synth Met 2014;198:161–6. doi:10.1016/j.synthmet.2014.10.008.

[94] Li J, Ma Y. In-situ synthesis of transparent conductive PEDOT coating on PET foil by liquid phase depositional polymerization of EDOT. Synth Met 2016;217:185–8. doi:10.1016/j.synthmet.2016.03.007.

[95] Metsik J, Timusk M, Šutka A, Mooste M, Tammeveski K, Mäeorg U. In situ investigation of poly(3,4-ethylenedioxythiophene) film growth during liquid phase deposition polymerization. Thin Solid Films 2018;653:274–83. doi:10.1016/j.tsf.2018.02.019.

[96] Greczynski G, Kugler T, Salaneck W. Characterization of the PEDOT-PSS system by means of X-ray and ultraviolet photoelectron spectroscopy. Thin Solid Films 1999;354:129–35. doi:10.1016/S0040-6090(99)00422-8.

[97] Jönsson SKM, Birgerson J, Crispin X, Greczynski G, Osikowicz W, Denier van der Gon a. W, et al. The effects of solvents on the morphology and sheet resistance in poly(3,4-ethylenedioxythiophene)-

polystyrenesulfonic acid (PEDOT-PSS) films. Synth Met 2003;139:1–10. doi:10.1016/S0379-6779(02)01259-6.

[98] Lapitan LDS, Tongol BJ V, Yau SL. In situ scanning tunneling microscopy imaging of electropolymerized poly(3,4-ethylenedioxythiophene) on an iodine-modified Au(1 1 1) single crystal electrode. Electrochim Acta 2012;62:433–40. doi:10.1016/j.electacta.2011.12.053.

[99] Ugur A, Katmis F, Li M, Wu L, Zhu Y, Varanasi KK, et al. Low-Dimensional Conduction Mechanisms in Highly Conductive and Transparent Conjugated Polymers. Adv Mater 2015;27:4604–10. doi:10.1002/adma.201502340.

[100] Kirchmeyer S, Reuter K. Scientific importance , properties and growing applications of poly(3,4-ethylenedioxythiophene). J Mater Chem 2005;15:2077–88. doi:10.1039/b417803n.

[101] Attias A-J. Polymères conjugués et électronique organique. Tech l'ingénieur 2017:E1862 V2.

[102] Patil AO, Heeger AJ, Wudl F. Optical Properties of Conducting Polymers. Chem Rev 1988;88:183–200. doi:10.1021/cr00083a009.

[103] Gustafsson J, Liedberg B, Inganas O. In situ spectroscopic investigations of electrochromism and ion transport in a poly (3,4-ethylenedioxythiophene) electrode in a solid state electrochemical cell. Solid State Ionics 1994;69:145–52. doi:10.1016/0167-2738(94)90403-0.

[104] Bubnova O, Crispin X. Towards polymer-based organic thermoelectric generators. Energy Environ Sci 2012;5:9345–62. doi:10.1039/c2ee22777k.

[105] Massonnet N, Carella A, Jaudouin O, Rannou P, Laval G, Celle C, et al. Improvement of the Seebeck coefficient of PEDOT:PSS by chemical reduction combined with a novel method for its transfer using free-standing thin films. J Mater Chem C Chem C 2014;2:1278–83. doi:10.1039/C3TC31674B.

[106] Karabay B, Pekel LC, Cihaner A. A Pure Blue to Highly Transmissive Electrochromic Polymer Based on Poly(3,4-propylenedioxyselenophene) with a High Optical Contrast Ratio. Macromolecules

2015;48:1352–7. doi:10.1021/acs.macromol.5b00022.

[107] Gueye MN, Carella A, Demadrille R, Simonato J-P. All-Polymeric Flexible Transparent Heaters. ACS Appl Mater Interfaces 2017;9. doi:10.1021/acsami.7b08578.

[108] Brooke R, Franco-Gonzalez JF, Wijeratne K, Pavlopoulou E, Galliani D, Liu X, et al. Vapor phase synthesized poly(3,4-ethylenedioxythiophene)-trifluoromethanesulfonate as a transparent conductor material. J Mater Chem A 2018. doi:10.1039/C8TA04744H.

[109] Crispin X, Marciniak S. Conductivity, morphology, interfacial chemistry, and stability of poly (3, 4-ethylene dioxythiophene)–poly (styrene sulfonate): A photoelectron spectroscopy study. J Polym Sci Part B Polym Phys 2003;41:2561–83. doi:10.1002/polb.10659.

[110] Kim JY, Jung JH, Lee DE, Joo J. Enhancement of electrical conductivity of poly(3,4-ethylenedioxythiophene)/poly(4-styrenesulfonate) by a change of solvents. Synth Met 2002;126:311–6. doi:10.1016/S0379-6779(01)00576-8.

[111] Crispin X, Jakobsson FLE, Crispin A, Grim PCM, Andersson P, Volodin A, et al. The origin of the high conductivity of poly(3,4-ethylenedioxythiophene)-poly(styrenesulfonate) (PEDOT- PSS) plastic electrodes. Chem Mater 2006;18:4354–60. doi:10.1021/cm061032+.

[112] Ouyang J, Xu Q, Chu C, Yang Y, Li G, Shinar J. On the mechanism of conductivity enhancement in poly(3,4-ethylenedioxythiophene):poly(styrene sulfonate) film through solvent treatment. Polymer (Guildf) 2004;45:8443–50. doi:10.1016/j.polymer.2004.10.001.

[113] Nardes AM, Kemerink M, Kok MM De, Vinken E, Maturova K, Janssen RAJ. Conductivity , work function , and environmental stability of PEDOT : PSS thin films treated with sorbitol. Org Electron 2008;9:727–34. doi:10.1016/j.orgel.2008.05.006.

[114] Nardes AM, Janssen R a J, Kemerink M. A Morphological Model for the Solvent-Enhanced Conductivity of PEDOT:PSS Thin Films. Adv Funct Mater 2008;18:865–71.

doi:10.1002/adfm.200700796.

[115] Kim YH, Sachse C, Machala ML, May C, Müller-Meskamp L, Leo K. Highly conductive PEDOT:PSS electrode with optimized solvent and thermal post-treatment for ITO-free organic solar cells. Adv Funct Mater 2011;21:1076–81. doi:10.1002/adfm.201002290.

[116] Worfolk BJ, Andrews SC, Park S, Reinspach J, Liu N, Toney MF, et al. Ultrahigh electrical conductivity in solution-sheared polymeric transparent films. Proc Natl Acad Sci 2015;12:14138–43. doi:10.1073/pnas.1509958112.

[117] Lee SH, Park H, Kim S, Son W, Cheong IW, Kim JH. Transparent and flexible organic semiconductor nanofilms with enhanced thermoelectric efficiency. J Mater Chem A 2014;2:7288–94. doi:10.1039/C4TA00700J.

[118] Kroon R, Mengistie DA, Kiefer D, Hynynen J, Ryan JD, Yu L, et al. Thermoelectric plastics: from design to synthesis, processing and structure–property relationships. Chem Soc Rev 2016;45:6147–64. doi:10.1039/C6CS00149A.

[119] Niu Q, Huang W, Tong J, Lv H, Deng Y, Ma Y, et al. Understanding the mechanism of PEDOT: PSS modification via solvent on the morphology of perovskite films for efficient solar cells. Synth Met 2018;243:17–24. doi:10.1016/j.synthmet.2018.05.012.

[120] Ouyang L, Musumeci C, Jafari MJ, Ederth T, Inganäs O. Imaging the Phase Separation Between PEDOT and Polyelectrolytes During Processing of Highly Conductive PEDOT:PSS Films. ACS Appl Mater Interfaces 2015;7:19764–73. doi:10.1021/acsami.5b05439.

[121] Döbbelin M, Marcilla R, Salsamendi M, Pozo-Gonzalo C, Carrasco PM, Pomposo JA, et al. Influence of Ionic Liquids on the Electrical Conductivity and Morphology of PEDOT:PSS Films. Chem Mater 2007;19:2147–9. doi:10.1021/cm070398z.

[122] Badre C, Marquant L, Alsayed AM, Hough LA. Highly conductive poly(3,4-

ethylenedioxythiophene):Poly (styrenesulfonate) films using 1-ethyl-3-methylimidazolium tetracyanoborate ionic liquid. Adv Funct Mater 2012;22:2723–7. doi:10.1002/adfm.201200225.

[123] Fan B, Mei X, Ouyang J. Significant Conductivity Enhancement of Conductive Poly(3,4-ethylenedioxythiophene):Poly(styrenesulfonate) Films by Adding Anionic Surfactants into Polymer Solution. Macromolecules 2008;41:5971–3. doi:10.1021/ma8012459.

[124] Xia Y, Ouyang J. Salt-Induced Charge Screening and Significant Conductivity Enhancement of Conducting Poly(3,4-ethylenedioxythiophene):Poly(styrenesulfonate). Macromolecules 2009;42:4141–7. doi:10.1021/ma900327d.

[125] De Izarra A, Park S, Lee J, Lansac Y, Jang YH. Ionic Liquid Designed for PEDOT:PSS Conductivity Enhancement. J Am Chem Soc 2018;140:5375–84. doi:10.1021/jacs.7b10306.

[126] Mazaheripour A, Majumdar S, Hanemann-Rawlings D, Thomas EM, McGuiness C, D'Alencon L, et al. Tailoring the Seebeck Coefficient of PEDOT:PSS by Controlling Ion Stoichiometry in Ionic Liquid Additives. Chem Mater 2018;30:4816–22. doi:10.1021/acs.chemmater.8b02114.

[127] Wang Y, Zhu C, Pfattner R, Yan H, Jin L, Chen S, et al. A highly stretchable, transparent, and conductive polymer. Sci Adv 2017;3:e1602076. doi:10.1126/sciadv.1602076.

[128] Jiang F, Xu J, Lu B, Xie Y, Huang R, Li L. Thermoelectric Performance of Poly(3,4-ethylenedioxythiophene): Poly(styrenesulfonate). Chinese Phys Lett 2008;25:2202.

[129] Xia Y, Ouyang J. Significant Conductivity Enhancement of Conductive Poly(3,4-ethylenedioxythiophene): Poly(styrenesulfonate) Films through a Treatment with Organic Carboxylic Acids and Inorganic Acids. ACS Appl Mater Interfaces 2010;2:474–83. doi:10.1021/am900708x.

[130] Xia Y, Sun K, Ouyang J. Solution-processed metallic conducting polymer films as transparent electrode of optoelectronic devices. Adv Mater 2012;24:2436–40. doi:10.1002/adma.201104795.

[131] Mukherjee S, Singh R, Gopinathan S, Murugan S, Gawali S, Saha B, et al. Solution-Processed Poly(3,4-

ethylenedioxythiophene) Thin Films as Transparent Conductors: Effect of p -Toluenesulfonic Acid in Dimethyl Sulfoxide. ACS Appl Mater Interfaces 2014;6:17792–803. doi:10.1021/am504150n.

[132] Kim N, Kee S, Lee SH, Lee BH, Kahng YH, Jo Y-R, et al. Highly Conductive PEDOT:PSS Nanofibrils Induced by Solution-Processed Crystallization. Adv Mater 2014;26:2268–72. doi:10.1002/adma.201304611.

[133] Kim N, Kang H, Lee J-H, Kee S, Lee SH, Lee K. Highly conductive all-plastic electrodes fabricated using a novel chemically controlled transfer-printing method. Adv Mater 2015;27:2317–23. doi:10.1002/adma.201500078.

[134] Meng W, Ge R, Li Z, Tong J, Liu T, Zhao Q, et al. Conductivity enhancement of PEDOT:PSS films via phosphoric acid treatment for flexible all-plastic solar cells. ACS Appl Mater Interfaces 2015;7:14089–94. doi:10.1021/acsami.5b03309.

[135] Kumar SRS, Kurra N, Alshareef HN. Enhanced high temperature thermoelectric response of sulphuric acid treated conducting polymer thin films. J Mater Chem C 2016;4:215–21. doi:10.1039/C5TC03145A.

[136] Naujoks N, Dual J, Lang BU, Mu E. Microscopical Investigations of PEDOT : PSS Thin Films. Adv Funct Mater 2009;19:1215–20. doi:10.1002/adfm.200801258.

[137] Zhou J, Anjum DH, Lubineau G, Li EQ, Thoroddsen ST. Unraveling the order and disorder in poly(3,4-ethylenedioxythiophene)/poly(styrenesulfonate) nanofilms. Macromolecules 2015;48:5688–96. doi:10.1021/acs.macromol.5b00851.

[138] Wei Q, Mukaida M, Naitoh Y, Ishida T. Morphological change and mobility enhancement in PEDOT:PSS by adding co-solvents. Adv Mater 2013;25:2831–6. doi:10.1002/adma.201205158.

[139] Takano T, Masunaga H, Fujiwara A, Okuzaki H, Sasaki T. PEDOT Nanocrystal in Highly Conductive PEDOT:PSS Polymer Films. Macromolecules 2012;45:3859–65. doi:10.1021/ma300120g.

[140] Horii T, Hikawa H, Katsunuma M, Okuzaki H. Synthesis of highly conductive PEDOT:PSS and correlation with hierarchical structure. Polymer (Guildf) 2018;140:33–8. doi:10.1016/j.polymer.2018.02.034.

[141] Shi K, Wu Y, Lu Z, Liu H, Wang J, Pei J. Enhanced Molecular Packing of a Conjugated Polymer with High Organic Thermoelectric Power Factor. ACS Appl Mater Interfaces 2016;8:24737–43. doi:10.1021/acsami.6b06899.

[142] Wei Q, Mukaida M, Kirihara K, Naitoh Y, Ishida T. Recent Progress on PEDOT-Based Thermoelectric Materials. Materials (Basel) 2015;8:732–50. doi:10.3390/ma8020732.

[143] Palumbiny CM, Liu F, Russell TP, Hexemer A, Wang C, Müller-Buschbaum P. The Crystallization of PEDOT:PSS Polymeric Electrodes Probed In Situ during Printing. Adv Mater 2015;27:3391–7. doi:10.1002/adma.201500315.

[144] Skotheim TA, Reynolds J. Handbook of Conducting Polymers. Third Edit. CRC Press; 2007.

[145] Aleshin AN, Williams SR, Heeger AJ. Transport properties of poly(3,4-ethylenedioxythiophene)/poly(styrenesulfonate). Synth Met 1998;94:173–7. doi:10.1016/S0379-6779(97)04167-2.

[146] Ashizawa S, Horikawa R, Okuzaki H. Effects of solvent on carrier transport in poly(3,4-ethylenedioxythiophene)/poly(4-styrenesulfonate). Synth Met 2005;153:5–8. doi:10.1016/j.synthmet.2005.07.214.

[147] Xiong J, Jiang F, Zhou W, Liu C, Xu J. Highly electrical and thermoelectric properties of a PEDOT:PSS thin-film via direct dilution–filtration. RSC Adv 2015;5:60708–12. doi:10.1039/C5RA07820B.

[148] Yildrim E, Wu G, Xue Y, Tan TL, Qiang Z, Xu J, et al. A Theoretical Mechanistic Study on Electrical Conductivity Enhancement of DMSO Treated PEDOT:PSS. J Mater Chem C 2018:DOI: 10.1039/c8tc00917a. doi:10.1039/C8TC00917A.

[149] Aleshin AN, Kiebooms R, Heeger AJ. Metallic conductivity of highly doped poly(3,4-ethylenedioxythiophene). Synth Met 1999;101:369–70. doi:10.1016/S0379-6779(98)00758-9.

[150] Aleshin AN, Kiebooms R, Yu H, Levin M, Shlimak I. Conductivity and magnetoconductivity below 1 K in films of poly(3,4-ethylenedioxythiophene) doped with CF3SO3. Synth Met 1998;94:157–9. doi:10.1016/S0379-6779(98)00021-6.

[151] Kiebooms R, Aleshin A, Hutchison K, Wudl F, Heeger A. Doped poly(3,4-ethylenedioxythiophene) films: Thermal, electromagnetical and morphological analysis. Synth Met 1999;101:436–7. doi:10.1016/S0379-6779(98)01121-7.

[152] Chang Y, Lee K, Kiebooms R, Aleshin A, Heeger A. Reflectance of conducting poly(3,4-ethylenedioxythiophene). Synth Met 1999;105:203–6. doi:10.1016/S0379-6779(99)00095-8.

[153] Ali MA, Wu KH, McEwan J, Lee J. Translated structural morphology of conductive polymer nanofilms synthesized by vapor phase polymerization. Synth Met 2018;48:113–9. doi:10.1016/j.synthmet.2018.07.007.

[154] Coclite AM, Howden RM, Borrelli DC, Petruczok CD, Yang R, Yagüe JL, et al. 25th Anniversary Article: CVD polymers: A new paradigm for surface modification and device fabrication. Adv Mater 2013;25:5392–423. doi:10.1002/adma.201301878.

[155] Poverenov E, Li M, Bitler A, Bendikov M. Major effect of electropolymerization solvent on morphology and electrochromic properties of PEDOT films. Chem Mater 2010;22:4019–25. doi:10.1021/cm100561d.

[156] Im SG, Yoo PJ, Hammond PT, Gleason KK. Grafted conducting polymer films for nano-patterning onto various organic and inorganic substrates by oxidative chemical vapor deposition. Adv Mater 2007;19:2863–7. doi:10.1002/adma.200701170.

[157] Franco-Gonzalez JF, Rolland N, Zozoulenko I V. Substrate-Dependent Morphology and Its Effect on

Electrical Mobility of Doped Poly(3,4-ethylenedioxythiophene) (PEDOT) Thin Films. ACS Appl Mater Interfaces 2018;10:29115–26. doi:10.1021/acsami.8b08774.

[158] Lindell L, Burquel A, Jakobsson FLE, Lemaur V, Berggren M, Lazzaroni R, et al. Transparent, plastic, low-work-function poly(3,4-ethylenedioxythiophene) electrodes. Chem Mater 2006;18:4246–52. doi:10.1021/cm061081m.

[159] Zuber K, Fabretto M, Hall C, Murphy P. Improved PEDOT Conductivity via Suppression of Crystallite Formation in Fe(III) Tosylate During Vapor Phase Polymerization. Macromol Rapid Commun 2008;29:1503–8. doi:10.1002/marc.200800325.

[160] Fabretto M, Müller M, Zuber K, Murphy P. Influence of peg-ran-ppg surfactant on vapour phase polymerised PEDOT thin films. Macromol Rapid Commun 2009;30:1846–51. doi:10.1002/marc.200900371.

[161] Fabretto M, Jariego-Moncunill C, Autere JP, Michelmore A, Short RD, Murphy P. High conductivity PEDOT resulting from glycol/oxidant complex and glycol/polymer intercalation during vacuum vapour phase polymerisation. Polymer (Guildf) 2011;52:1725–30. doi:10.1016/j.polymer.2011.02.028.

[162] Fabretto M V., Evans DR, Mueller M, Zuber K, Hojati-Talemi P, Short RD, et al. Polymeric material with metal-like conductivity for next generation organic electronic devices. Chem Mater 2012;24:3998–4003. doi:10.1021/cm302899v.

[163] Bubnova O, Khan ZU, Wang H, Braun S, Evans DR, Fabretto M, et al. Semi-metallic polymers. Nat Mater 2014;13:190–4. doi:10.1038/nmat3824.

[164] Khan ZU, Bubnova O, Jafari MJ, Brooke R, Liu X, Gabrielsson R, et al. Acido-basic control of the thermoelectric properties of poly(3,4-ethylenedioxythiophene)tosylate (PEDOT-Tos) thin films. J Mater Chem C 2015;3:10616–23. doi:10.1039/C5TC01952D.

[165] Lee YH, Oh J, Lee S, Kim H, Son JG. Highly Ordered Nanoconfinement Effect from Evaporation-Induced Self-Assembly of Block Copolymers on In Situ Polymerized PEDOT:Tos. ACS Macro Lett 2017;6:386–92. doi:10.1021/acsmacrolett.7b00137.

[166] Wang J, Cai K, Shen SZ. Enhanced Thermoelectric Properties of Poly (3 , 4-ethylenedioxythiophene) Thin Films Treated with H2SO4. Org Electron 2014;15:3087–95. doi:10.1016/j.orgel.2014.09.012.

[167] Aasmundtveit KE, Samuelsen EJ, Pettersson LAA, Inganäs O, Johansson T, Feidenhans'l R. Structure of thin films of poly(3,4-ethylenedioxythiophene). Synth Met 1999;101:561–4. doi:10.1016/S0379-6779(98)00315-4.

[168] Yu SH, Lee JH, Choi MS, Park JH, Yoo PJ, Lee JY. Improvement of Electrical Conductivity of Poly(3,4-ethylenedioxythiophene) (PEDOT) Thin Film. Mol Cryst Liq Cryst 2013;580:76–82. doi:10.1080/15421406.2013.804761.

[169] Madl CM, Kariuki PN, Gendron J, Piper LFJ, Jones WE. Vapor phase polymerization of poly (3,4-ethylenedioxythiophene) on flexible substrates for enhanced transparent electrodes. Synth Met 2011;161:1159–65. doi:10.1016/j.synthmet.2011.03.024.

[170] Suchand Sangeeth CS, Jaiswal M, Menon R. Correlation of morphology and charge transport in poly(3,4-ethylenedioxythiophene)-polystyrenesulfonic acid (PEDOT-PSS) films. J Phys Condens Matter 2009;21:072101. doi:10.1088/0953-8984/21/7/072101.

[171] Petsagkourakis I, Pavlopoulou E, Cloutet E, Chen YF, Liu X, Fahlman M, et al. Correlating the Seebeck coefficient of thermoelectric polymer thin films to their charge transport mechanism. Org Electron 2018;52:335–41. doi:10.1016/j.orgel.2017.11.018.

[172] Muñoz WA, Singh SK, Franco-Gonzalez JF, Linares M, Crispin X, Zozoulenko I V. Insulator to semimetallic transition in conducting polymers. Phys Rev B 2016;94:205202. doi:10.1103/PhysRevB.94.205202.

[173] Franco-Gonzalez JF, Zozoulenko I V. Molecular Dynamics Study of Morphology of Doped PEDOT: From Solution to Dry Phase. J Phys Chem B 2017;121:4299–307. doi:10.1021/acs.jpcb.7b01510.

[174] Rudd S, Franco-Gonzalez JF, Kumar Singh S, Ullah Khan Z, Crispin X, Andreasen JW, et al. Charge transport and structure in semimetallic polymers. J Polym Sci Part B Polym Phys 2018;56:97–104. doi:10.1002/polb.24530.

[175] Rolland N, Franco-Gonzalez JF, Volpi R, Linares M, Zozoulenko I V. Understanding morphology-mobility dependence in PEDOT:Tos. Phys Rev Mater 2018;2:045605. doi:10.1103/PhysRevMaterials.2.045605.

[176] Farka D, Coskun H, Bauer P, Roth D, Bruckner B, Klapetek P, et al. Increase in electron scattering length in PEDOT:PSS by a triflic acid post-processing. Monatshefte Fur Chemie 2017;148:871–7. doi:10.1007/s00706-017-1973-1.

[177] Dominik F, Jones AOF, Menon R, Sariciftci NS, Stadler P. Metallic conductivity beyond the Mott minimum in PEDOT: Sulphate at low temperatures. Synth Met 2018;240:59–66. doi:10.1016/j.synthmet.2018.03.015.

[178] Skotheim TA, Elsenbaumer RL, Reynolds JR. Handbook of conducting polymers. 2nd editio. 1998.

[179] Grancarić AM, Jerković I, Koncar V, Cochrane C, Kelly FM, Soulat D, et al. Conductive polymers for smart textile applications. vol. 48. 2018. doi:10.1177/1528083717699368.

[180] Bharti M, Singh A, Samanta S, Aswal DK. Conductive polymers for thermoelectric power generation. Prog Mater Sci 2018;93:270–310. doi:10.1016/j.pmatsci.2017.09.004.

[181] Inal S, Rivnay J, Suiu A-O, Malliaras GG, McCulloch I. Conjugated Polymers in Bioelectronics. Acc Chem Res 2018;51:1368–76. doi:10.1021/acs.accounts.7b00624.

[182] Evans D. A bird's eye view of the synthesis and practical application of conducting polymers. Polym Int 2018;67:351–5. doi:10.1002/pi.5531.

[183] Tee BCK, Ouyang J. Soft Electronically Functional Polymeric Composite Materials for a Flexible and Stretchable Digital Future. Adv Mater 2018:1802560. doi:10.1002/adma.201802560.

[184] Elschner A, Kirchmeyer S, Lovenich W, Merker U, Reuter K. PEDOT. 1st editio. CRC Press; 2010. doi:10.1201/b10318.

[185] Huang F, Wu H, Cao Y. Water/alcohol soluble conjugated polymers as highly efficient electron transporting/injection layer in optoelectronic devices. Chem Soc Rev 2010;39:2500. doi:10.1039/b907991m.

[186] Liu Y, Weng B, Razal JM, Xu Q, Zhao C, Hou Y, et al. High-Performance Flexible All-Solid-State Supercapacitor from Large Free-Standing Graphene-PEDOT/PSS Films. Sci Rep 2015;5:17045. doi:10.1038/srep17045.

[187] Ludwig KA, Uram JD, Yang J, Martin DC, Kipke DR. Chronic neural recordings using silicon microelectrode arrays electrochemically deposited with a poly(3,4-ethylenedioxythiophene) (PEDOT) film. J Neural Eng 2006;3:59–70. doi:10.1088/1741-2560/3/1/007.

[188] Paulsen BD, Tybrandt K, Stavrinidou E, Rivnay J. Organic mixed ionic–electronic conductors. Nat Mater 2019. doi:10.1038/s41563-019-0435-z.

[189] Solazzo M, Krukiewicz K, Zhussupbekova A, Fleischer K, Biggs MJ, Monaghan MG. PEDOT:PSS interfaces stabilised using a PEGylated crosslinker yield improved conductivity and biocompatibility. J Mater Chem B 2019;7:4811–20. doi:10.1039/C9TB01028A.

[190] Arias AC, Granström M, Petritsch K, Friend RH. Organic Photodiodes using Polymeric Anodes. Synth Met 1999;102:953–4. doi:10.1016/S0379-6779(98)00976-X.

[191] Aernouts T, Vanlaeke P, Geens W, Poortmans J, Heremans P, Borghs S, et al. Printable anodes for flexible organic solar cell modules. Thin Solid Films 2004;451–452:22–5. doi:10.1016/j.tsf.2003.11.038.

[192] Kwon SJ, Seok WC, Leem JT, Kang JH, Koh WG, Song HJ, et al. Enhancement of conductivity and transparency for of poly(3,4-ethylenedioxythiophene) films using photo-acid generator as dopant. Polym (United Kingdom) 2018;147:30–7. doi:10.1016/j.polymer.2018.05.067.

[193] Zhou Y, Cheun H, Choi S, Potscavage WJ, Fuentes-Hernandez C, Kippelen B. Indium tin oxide-free and metal-free semitransparent organic solar cells. Appl Phys Lett 2010;97:153304. doi:10.1063/1.3499299.

[194] Angmo D, Krebs FC. Flexible ITO-free polymer solar cells. J Appl Polym Sci 2013;129:1–14. doi:10.1002/app.38854.

[195] Po R, Carbonera C, Bernardi A, Tinti F, Camaioni N. Polymer- and carbon-based electrodes for polymer solar cells: Toward low-cost, continuous fabrication over large area. Sol Energy Mater Sol Cells 2012;100:97–114. doi:10.1016/j.solmat.2011.12.022.

[196] Fallahzadeh A, Saghaei J, Saghaei T. Ultra-smooth poly(3,4-ethylene dioxythiophene):poly(styrene sulfonate) films for flexible indium tin oxide-free organic light-emitting diodes. J Lumin 2016;169:251–5. doi:10.1016/j.jlumin.2015.09.021.

[197] Zhang Y, Chen L, Hu X, Zhang L, Chen Y. Low Work-function Poly(3,4-ethylenedioxylenethiophene): Poly(styrene sulfonate) as Electron-transport Layer for High-efficient and Stable Polymer Solar Cells. Sci Rep 2015;5:12839. doi:10.1038/srep12839.

[198] Hübler A, Trnovec B, Zillger T, Ali M, Wetzold N, Mingebach M, et al. Printed Paper Photovoltaic Cells. Adv Energy Mater 2011;1:1018–22. doi:10.1002/aenm.201100394.

[199] Cho C-K, Hwang W-J, Eun K, Choa S-H, Na S-I, Kim H-K. Mechanical flexibility of transparent PEDOT:PSS electrodes prepared by gravure printing for flexible organic solar cells. Sol Energy Mater Sol Cells 2011;95:3269–75. doi:10.1016/j.solmat.2011.07.009.

[200] Liu WC, Liu Y, Jennings JR, Huang H, Wang Q. Low-cost and flexible poly(3,4-

ethylenedioxythiophene) based counter electrodes for efficient energy conversion in dye-sensitized solar cells. J Mater Chem A 2014;2:10938. doi:10.1039/c4ta00563e.

[201] Villers D, Jobin D, Soucy C, Cossement D, Chahine R, Breau L, et al. The Influence of the Range of Electroactivity and Capacitance of Conducting Polymers on the Performance of Carbon Conducting Polymer Hybrid Supercapacitor. J Electrochem Soc 2003;150:A747. doi:10.1149/1.1571530.

[202] Yan L, Gao X, Thomas JP, Ngai J, Altounian H, Leung KT, et al. Ionically cross-linked PEDOT:PSS as a multi-functional conductive binder for high-performance lithium–sulfur batteries. Sustain Energy Fuels 2018;2:1574–81. doi:10.1039/C8SE00167G.

[203] Xia X, Chao D, Fan Z, Guan C, Cao X, Zhang H, et al. A New Type of Porous Graphite Foams and Their Integrated Composites with Oxide/Polymer Core/Shell Nanowires for Supercapacitors: Structural Design, Fabrication, and Full Supercapacitor Demonstrations. Nano Lett 2014;14:1651–8. doi:10.1021/nl5001778.

[204] Bubnova O, Khan ZU, Malti A, Braun S, Fahlman M, Berggren M, et al. Optimization of the thermoelectric figure of merit in the conducting polymer poly(3,4-ethylenedioxythiophene). Nat Mater 2011;10:429–33. doi:10.1038/nmat3012.

[205] Park BT, Park C, Kim B, Shin H, Kim E, Park T. Flexible PEDOT electrodes with large thermoelectric power factors to generate electricity by the touch of fingertips. Energy Environ Sci 2013;6:788–92. doi:10.1039/c3ee23729j.

[206] Cho C, Wallace KL, Tzeng P, Hsu J-H, Yu C, Grunlan JC. Outstanding Low Temperature Thermoelectric Power Factor from Completely Organic Thin Films Enabled by Multidimensional Conjugated Nanomaterials. Adv Energy Mater 2016;6:1502168. doi:10.1002/aenm.201502168.

[207] Kim S Il, Lee KH, Mun HA, Kim HS, Hwang SW, Roh JW, et al. Dense dislocation arrays embedded in grain boundaries for high-performance bulk thermoelectrics. Science (80-) 2015;348:109–14.

doi:10.1126/science.aaa4166.

[208] Xu S, Hong M, Shi X-L, Wang Y, Ge L, Bai Y, et al. High-Performance PEDOT:PSS Flexible Thermoelectric Materials and Their Devices by Triple Post-Treatments. Chem Mater 2019;31:5238–44. doi:10.1021/acs.chemmater.9b01500.

[209] Gao C, Chen G. Conducting polymer/carbon particle thermoelectric composites: Emerging green energy materials. Compos Sci Technol 2016;124:52–70. doi:10.1016/j.compscitech.2016.01.014.

[210] McGrail BT, Sehirlioglu A, Pentzer E. Polymer Composites for Thermoelectric Applications. Angew Chemie Int Ed 2015;54:1710–23. doi:10.1002/anie.201408431.

[211] Shi W, Zhao T, Xi J, Wang D, Shuai Z. Unravelling doping effects on PEDOT at the molecular level: from geometry to thermoelectric transport properties. J Am Chem Soc 2015;137:12929–38. doi:10.1021/jacs.5b06584.

[212] Kayser L V, Lipomi DJ. Stretchable Conductive Polymers and Composites Based on PEDOT and PEDOT : PSS. Adv Mater 2018;1806133:1–13. doi:10.1002/adma.201806133.

[213] Fan X, Nie W, Tsai H, Wang N, Huang H, Cheng Y. PEDOT : PSS for Flexible and Stretchable Electronics : Modifications , Strategies , and Applications. Adv Sci 2019;1900813. doi:10.1002/advs.201900813.

[214] Aleshin AN, Kiebooms R, Menon R, Heeger AJ. Electronic transport in doped poly (3 , 4-ethylenedioxythiophene) near the metal- insulator transition. Synth Met 1997;90:61–8. doi:10.1016/S0379-6779(97)81227-1.

[215] Pyshkina O. Poly(3,4-ethylenedioxythiophene):Synthesis and Properties. Sci J Riga Tech Univ Mater Sci Appl Chem 2010;21:51–4. doi:10.1039/c2jm32457a.

[216] Kim G-H, Shao L, Zhang K, Pipe KP. Engineered doping of organic semiconductors for enhanced thermoelectric efficiency. Nat Mater 2013;12:719–23. doi:10.1038/nmat3635.

[217] Hojati-Talemi P, Bächler C, Fabretto M, Murphy P, Evans D. Ultrathin Polymer Films for Transparent Electrode Applications Prepared by Controlled Nucleation. ACS Appl Mater Interfaces 2013;5:11654–60. doi:10.1021/am403135p.

[218] Tsai TC, Chang HC, Chen CH, Huang YC, Whang WT. A facile dedoping approach for effectively tuning thermoelectricity and acidity of PEDOT:PSS films. Org Electron Physics, Mater Appl 2014;15:641–5. doi:10.1016/j.orgel.2013.12.023.

[219] Yang E, Kim J, Jung BJ, Kwak J. Enhanced thermoelectric properties of sorbitol-mixed PEDOT:PSS thin films by chemical reduction. J Mater Sci Mater Electron 2015;26:2838–43. doi:10.1007/s10854-015-2766-0.

[220] Liu S, Deng H, Zhao Y, Ren S, Fu Q. The optimization of thermoelectric properties in a PEDOT:PSS thin film through post-treatment. RSC Adv 2015;5:1910–7. doi:10.1039/C4RA09147G.

[221] Anno H, Nishinaka T, Hokazono M, Oshima N, Toshima N. Thermoelectric power-generation characteristics of PEDOT:PSS thin-film devices with different thicknesses on polyimide substrates. J Electron Mater 2015;44:2105–12. doi:10.1007/s11664-015-3668-x.

[222] Mengistie DA, Chen C, Boopathi KM, Pranoto FW, Li L, Chu C. Enhanced Thermoelectric Performance of PEDOT:PSS Flexible Bulky Papers by Treatment with Secondary Dopants. ACS Appl Mater Interfaces 2015;7:94–100. doi:10.1021/am507032e.

[223] Petsagkourakis I, Pavlopoulou E, Portale G, Kuropatwa BA, Dilhaire S, Fleury G, et al. Structurally-driven Enhancement of Thermoelectric Properties within Poly(3,4-ethylenedioxythiophene) thin Films. Sci Rep 2016;6:30501. doi:10.1038/srep30501.

[224] Yamaguchi H, Aizawa K, Chonan Y, Komiyama T, Aoyama T, Sakai E, et al. Highly Flexible and Conductive Glycerol-Doped PEDOT:PSS Films Prepared Under an Electric Field. J Electron Mater 2018;47:3370–5. doi:10.1007/s11664-018-6292-8.

[225] Lee JH, Jeong YR, Lee G, Jin SW, Lee YH, Hong SY, et al. Highly Conductive, Stretchable, and Transparent PEDOT:PSS Electrodes Fabricated with Triblock Copolymer Additives and Acid Treatment. ACS Appl Mater Interfaces 2018;10:28027–35. doi:10.1021/acsami.8b07287.

[226] Zhang S, Fan Z, Wang X, Zhang Z, Ouyang J. Enhancement of the thermoelectric properties of PEDOT:PSS: Via one-step treatment with cosolvents or their solutions of organic salts. J Mater Chem A 2018;6:7080–7. doi:10.1039/c7ta11148g.

[227] Wang X, Kyaw AKK, Yin C, Wang F, Zhu Q, Tang T, et al. Enhancement of thermoelectric performance of PEDOT:PSS films by post-treatment with a superacid. RSC Adv 2018;8:18334–40. doi:10.1039/c8ra02058b.

[228] Rudd S, Murphy PJ, Evans DR. Diffusion controlled vapour deposition of mixed doped PEDOT. Synth Met 2018;242:61–6. doi:10.1016/j.synthmet.2018.04.010.

Vitae

Magatte Niang Gueye is currently a Postdoc fellow at the Institute for Electronics, Microelectronics and Nanotechnology (IEMN) in France, where her research focuses on the nanoscale electrical and thermal properties of conducting polymers. In 2014, she received a French engineering degree in Materials Science and Mechanics from Ecole des Mines de Saint-Etienne and a MSc degree in Materials Science and Engineering from the Seoul National University in South Korea. She then received her PhD from University Grenoble Alpes in 2017, for her work conducted in CEA Grenoble and dealing with the electrical, optoelectronic and thermoelectric properties of PEDOT materials.

Alexandre Carella is a researcher and project leader at the Alternative Energies and Atomic Energy Commission (CEA) in Grenoble, France since 2006. He received a Ph.D. in Chemistry from University of Toulouse, France in 2004 and spent 2 years as postdoctoral fellow in the Prof. Julius Rebek, Jr. laboratory at

The Scripps Research Institute, La Jolla, CA from 2004 to 2006. In 2017, he received his habilitation. He has been involved as coordinator or partner in many industrial, national or European projects.

His research interests are in the field of gas sensors and conductive polymers for thermoelectric applications and thin film heaters. He has authored or co-authored 35 publications and 23 patent applications.

Jérôme Faure Vincent is a researcher at the Alternative Energies and Atomic Energy Commission in Grenoble, France since 2007. He received his Ph. D. degree in Physics from National Polytechnic Institute of Lorraine (Nancy, France) in 2004. Then he spent 2 years as a post-doctoral fellow in the Spintec laboratory (Dr. Bernard Dieny's group, France) working on the performances and reliability of spin valves for Magnetic Random-Access Memory applications. His actual research focuses on electronic transport properties of conducting polymers, carbon-based materials and 2D or 3D networks of nanowires for organic electronics, photovoltaic, thermoelectric or energy storage applications. He has authored or co-authored 40 publications in peer-reviewed journals.

Renaud Demadrille received his PhD in organic chemistry in 2000 from the University of Aix-Marseille II in France. He was a fellowship of PPG Industries and Essilor International and his PhD project was dealing with the study of photo-degradation mechanisms of photochromic dyes in polymer matrixes. After his PhD, he spent one year in the R&D center of an international chemical company to develop high performances silicone elastomers. Then he joined in 2002 the Atomic Energy Commission (CEA) as a postdoctoral fellow under the supervision of Prof. Adam Pron, to synthesize semiconducting polymers for organic photovoltaics before being appointed in 2005 as a permanent researcher at CEA-Grenoble in the Fundamental Research Division.

His research focuses on the synthesis and the characterization of new pi-conjugated molecules and macromolecules for organic and hybrid photovoltaics and thermoelectricity. He is also interested in the development of functional materials and nanomaterials for organic electronics. He has co-authored 69 articles and holds 8 patents.

Jean-Pierre Simonato received his PhD in 1999. He worked for seven years in industry at Rhône-Poulenc and Rhodia as Senior Scientist and Technical Service & Development Manager before joining CEA in 2005. He passed his habilitation in 2006, became CEA Senior Expert in 2009 and Director of Research in 2015. He was the Head of the Laboratory of Synthesis and Integration of Nanomaterials for four years (2014-2017). He is lecturer at the University Grenoble Alpes, and author or co-author of more than 70 patent applications and 75 publications in peer-reviewed journals. He has been involved as coordinator or partner in many industrial, national or European projects. Dr Simonato is also Expert Evaluator at the European Commission. His research interests are mainly in chemistry, in particular nanomaterials synthesis and conducting polymers, and their applications up to the industrial stage.

Figure captions

Figure 1. Schematic structure of polymers with different disorder levels. (a) Very ordered, (b) disordered aggregates and (c) completely disordered. Depending on the density of the polymer, long chains (highlighted in red) can connect ordered regions (darker orange ones) without significant loss of the conjugation length. [28]. Copyright 2013, Springer Nature.

Figure 2. Fast, moderate and slow transport along the chain backbone, the π-π stacking and the lamellar stacking respectively in conducting polymers.[28]. Copyright 2013, Springer Nature.

Figure 3. Temperature dependence of conductivity from a semiconductor to a metal: (a) semiconductor, (b) & (c) semiconductor or disordered metal with metallic behavior, (d) metal.

Figure 4. Schematic representation of (a) the variable range hopping model *vs* (b) the tunneling model. Due to the disorder, Anderson localization predicts the localization of the charges carriers' wavefunctions. While charges are strongly delocalized in the first place, inducing VRH, a less pronounced disorder in the second

case results in charges that are close enough to induce a local delocalization, the formation of more densely charges zones (polaronic and bipolaronic clusters) and therefore another transport mechanism.

Figure 5. (a) Typical metallic thermopower in Zr-Ni alloy. (b) Approximately linear thermopower in doped polyacetylene. (c) Temperature dependence of conductivity in doped polyacetylene. [49]. Copyright 1991 by Elsevier B.V. (copyright review from Elsevier requested).

Figure 6. Scheme representing the place of conjugated polymers between metals, semiconductors and insulators. Examples of materials are given as function of their electrical conductivity. The inset corresponds to conducting polymers and schematizes the different transport regimes that can be found around the critical regime of the insulator to metal transition.

Figure 7. (a) Methylene dioxythiophene (MDOT), (b) 3,4-ethylene dioxythiophene (EDOT) and (c) poly(3,4-ethylene dioxythiophene) (PEDOT).

Figure 8. Nickel based polycondensation for neutral PEDOT synthesis. [73]

Figure 9. Proposed mechanism for the synthesis of PEDOT:Tos as reproduced from Mueller and coworkers' work.[79] Copyright 2012, Elsevier Ltd. (copyright review from Elsevier requested).

Figure 10. Chemical structure of PEDOT:PSS.

Figure 11. (a) Vapor phase polymerization principle (VPP). (b) VPP chamber, as reproduced from Murphy and coworkers' work.[90] (c) Another quite similar principle (chemical vapor deposition, CVD) principle as reproduced from Gleason and coworker's work.[88] It is slightly different from VPP. In here, no solvents are used and the oxidant is heated in the crucible that faces the substrate on which EDOT is adsorbed. Copyright 2010, Elsevier Ltd. (copyright review from Elsevier requested) Copyright 2006, American Chemical Society.

Figure 12. PEDOT in different states: (a) neutral, (b) polaron, (c) bipolaron.

Figure 13. Band structure building in conjugated polymers. Reproduced after[101].

Figure 14. Evolution of the electronic characteristic of PEDOT at different doping levels.

(A) Upper image: from left to right: a neutral chain ('**a**' no charges are present in the chain and the corresponding transition in UV-Vis-NIR in the lower image is a band in the visible range), a chain with a polaron ('**b** & **c**' in UV-Vis-NIR, the energy transitions that are detected correspond to the transition from the VB to the polaronic band and the transition from the occupied state to the non-occupied state of the polaronic band. Those transitions appear at the end of the visible range), a chain with a bipolaron ('**e**' the transition in the bipolaronic band occurs in the NIR region), an intrachain or interchain polaron network inducing a polaronic band and an intrachain or interchain bipolaron network inducing a bipolaronic band ('**e**' in these last two cases, all transitions that can occur and which are due to the neutral chains, the polarons and the bipolarons are represented, hence giving such so know UV-Vis-NIR spectrum of PEDOT).[104]

(B) PEDOT chains with different doping states (upper image) and their corresponding UV-Vis-NIR spectra (lower image), from the most oxidized (i) to the less oxidized state (v).[105] Copyright 2012, Royal Society of Chemistry (copyright review from Elsevier requested). Copyright 2014, Royal Society of Chemistry (copyright review from Elsevier requested).

Figure 15. (a) Dependence of the specular transmittance at 550 nm as function of the sheet resistance of PEDOT:PSS and PEDOT:OTf. (b) Optical properties of PEDOT:Sulf in the visible range.[107]

Figure 16. Typical sulfur doublet response of PEDOT:PSS polymer blends probed using XPS. The shift of S2p doublet between thiophene and PSS is clearly represented. The two figures represent PEDOT:PSS with more (left) or less (right) excess PSS.[13] Copyright 2001, Elsevier Science B.V. (copyright review from Elsevier requested).

Figure 17. AFM topography images (A, C) and phase images (B, D) of PEDOT: PSS without solvent addition. In the phase images, darker areas correspond to softer zones. The sharp contrast suggests two phases, one PEDOT-rich (the brighter zones) and one PSS-rich (the darker zones). Therefore, PEDOT:PSS particles are surrounded by excess PSS.[111]

AFM topography images (E, G) and phase images (F, H) of PEDOT: PSS after DEG addition. PSS rich regions are swollen after the solvent addition so that PEDOT-rich regions are more interconnected.[111] Copyright 2006, American Chemical Society.

Figure 18. Upper scheme: illustration of the phase separation when a high boiling point solvent is added in the PEDOT dispersion. That illustration is accompanied with an optical proof of such phase segregation (lower figure).[120] Copyright 2015, American Chemical Society.

Figure 19. (A) Schematic structure of a PEDOT segment and a PSS segment in water (a) without and (b) with the addition of anionic surfactant.[123] (B) Schematic structures of PEDOT:PSS before and after $CuCl_2$ treatment.[124] Copyrights 2008 and 2009, American Chemical Society.

Figure 20. (a) Conductivity enhancement after post-treatment with various acids. (b) SEM images of PEDOT:PSS films treated with 8 M propionic acid (upper) and 6 M butyric acid (lower). The particles are PSSH particles which segregate after acid treatment and can easily be washed off.[129] Copyright 2010, American Chemical Society.

Figure 21. (a) Timeline of conductivity values for PEDOT:PSS.[19] Copyright 2015, John Wiley and Sons. (b) Conductivity enhancement of PEDOT:PSS through years. References are given in Table 1.

Figure 22. Schematic model of the kinetic processes during film formation of (a) pure, (b) EG-doped, and (c) EG-post-treated PEDOT:PSS.[143] Copyright 2015, John Wiley and Sons.

Figure 23. (a) HAAD-STEM images of PEDOT:PSS treated with different sulfuric acid concentrations. (b) A mechanism is proposed for the structural rearrangement of PEDOT:PSS after acid treatment. Sulfuric acid undergoes auto-pyrolysis leading to HSO_4^- and $H_3SO_4^+$, helping segregation of the negatively charged PSS and the positively charged PEDOT. Thanks to strong π-π interactions between PEDOT chains, the amorphous PEDOT:PSS grains (left) are reformed into crystalline PEDOT:PSS nanofibrils (right).[132] Copyright 2013, John Wiley and Sons.

Figure 24. Temperature dependence of the conductivity for (a) pristine PEDOT:PSS sample and (b) PEDOT:PSS samples treated with (Δ) 2.5 wt%, (○) 5 wt% and (□) 10 wt% of sorbitol concentration added to the aqueous dispersion used for spin-coating of the films. Straight lines are fits to Equation (2) to the data in the main panel plotted versus α=1/n+1. The vertical dashed line represents α = ¼ in (a) and ½ in (b). Lower left inset of (b): evolution of T_0 and σ at 300 K as a function of sorbitol concentration, the dashed lines serve to guide the eye.[114] Copyright 2008, John Wiley and Sons.

Figure 25. PEDOT conformation in the presence of different counter-anions.[78] Copyright 2014, Royal Society of Chemistry (copyright review from Elsevier requested).

Figure 26. The HAADF STEM image of cross sections of the interfaces of grafted PEDOT films grown at (a) 100 °C and (b) 200 °C. The top halves of both images are color-enhanced to clearly elucidate the crystalline domains surrounded by an amorphous matrix. High-resolution images for the film synthesized at 200 °C are shown in (c) and enlarged in (d), providing a direct evidence on the well-organized large crystallites. (e) Histogram of statistical domain size distribution obtained from images (a) and (b), showing the broader distribution and larger crystallite size for the film grown at high temperature (200 °C).[99] Copyright 2015, John Wiley and Sons.

Figure 27. Crystallization of the oxidant. PEDOT:Tos film post-polymerization (VPP) and prior to ethanol wash. (a) No PEG-ran—PPG, (b) 5wt. % PEG-ran-PPG, (c) 10 wt. % PEG-ran-PPG, (d) 15 wt. % PEG-ran-PPG. Image reproduced from Murphy and coworkers' article.[159] Copyright 2008, John Wiley and Sons.

Figure 28. Conductivity enhancement through years. PEDOT:Tos materials are represented with spheres, PEDOT stabilized with other counter-anions with stars. The corresponding counter-anions are displayed accordingly. References are given in Table 1.

Figure 29. Structure model of PEDOT:Tos. The substrate is normal to the a-axis.[167] Copyright 1999, Elsevier B.V. (copyright review from Elsevier requested).

Figure 30. Single crystal PEDOT nanowires as synthesized by Cho *et al*.[24] (a) TEM images of a PEDOT nanowire and the corresponding SAED patterns taken at three different areas. (b) XRD pattern of a PEDOT nanowire. (c) Illustration of the crystal structure of the single-crystal PEDOT nanowire along the nanowire direction. Copyright 2014, American Chemical Society.

Figure 31. Temperature dependence of the electrical conductivity (normalized to 300K) for various PEDOT:Tos and PEDOT:PSS samples.[163] Copyright 2013, Springer Nature.

Figure 32. Representation of the electronic structure in PEDOT materials and in conducting polymers in general. a–c, If the majority charge carriers are polarons: (a) a polymer chain with one polaron, (b) the logarithm of the density of states (DOS) lnN(E) disordered material (c) as well as for a more ordered (metallic) system. In the latter case, the Fermi level lies in a delocalized polaron band while it was surrounded with localized states in the former case. d–f, If the majority charge carriers are bipolarons: (d) a polymer chain with one bipolaron, (e) lnN(E) for an disordered bipolaronic polymer solid, (f) as well as for a more ordered (semi-metallic) solid. The Fermi level lies between the valence band and the empty bipolaron band in the latter case.[163] Copyright 2013, Springer Nature.

Figure 33. Structural characteristics of the PEDOT materials. (a) In-plane and (b) out-of plane synchrotron GIWAXS diffractograms of PEDOT:PSS, PEDOT:OTf, PEDOT:OTf-NMP, and PEDOT:Sulf-NMP. (c) SAXS/WAXS intensity profile of PEDOT:PSS (green line), PEDOT:OTf in the pristine state (red line), and PEDOT:Sulf (black line). Top inset shows the intensity in the small angles domain.[47] (d) Scheme of stacking in the crystallites. (e) HRTEM image of PEDOT:OTf-NMP. Inset image is a magnification of the outlined square.[23] Copyright 2015, Royal Society of Chemistry (copyright review from Elsevier requested). Copyright 2016, American Chemical Society.

Figure 34. Transport properties of PEDOT based materials. (a) Log–log plot of the temperature dependence of conductivity of: (left Y axis) PEDOT:OTf (red squares) and PEDOT:Sulf (black circles); (right Y axis) PEDOT:PSS (green triangles). The top inset represents the corresponding reduced activation energy W as in

Equation 6. W is found negative in the [3 K; 5.5 K] range for PEDOT:Sulf, demonstrating metallic behavior. The bottom inset represents the magnified electrical conductivity of PEDOT:Sulf in the [3 K; 20 K] range. [47]. (b) Temperature dependence of electrical conductivity (symbols) and calculated heterogeneous model of conduction (solid lines), (c) Low temperature dependence of electrical conductivity and (d) Reduced activation energy (W) of PEDOT materials vs ln(T). [23] Copyright 2015, Royal Society of Chemistry (copyright review from Elsevier requested). Copyright 2016, American Chemical Society.

Figure 35. (a) Scheme of the o-CVD technique accompanied with a proposed reaction mechanism of the synthesis. (b) AFM topography of o-CVD grown PEDOT:sulfate thin film with an RMS roughness of 4.5 nm. (c) ρT-plot highlighting the flat *T*-profile of PEDOT:sulfate in particular at low temperatures. (d) Comparison between O-CVD PEDOT:sulfate compared and the solution processed PEDOT:PSS, PEDOT:PSS* (treated with DMSO), and PEDOT:triflate which exhibit lower performances. The role of disorder on σT→0 is schematized. (e) The Mott-Ioffe-Regel limit, as described in Figure 6, describes a critical resistivity (typically 150 μΩ cm), at which the sign of the temperature coefficient of resistivity $\frac{\Delta\rho}{\Delta T}$ in a metal changes (glassy to crystalline). In this article, the authors showed that PEDOT:sulfate behaves like glassy metal alloys such as $Al_{33}Ti_{67}$.[48] Copyright 2017, John Wiley and Sons.

Tables

Table 1. Literature review on electrical conductivity in PEDOT materials. This list is not exhaustive. It gives an overview of the progression of the research on electrical conductivity enhancement.

Year	Counter-anion + grade	Processing	Conductivity [S cm^{-1}]	Thickness [nm]	Carrier concentration [cm^{-3}]	Mobility [$cm^2V^{-1}s^{-1}$]	References
1992	($FeCl_3$)	electrochemical polymerization	200	n/a, bulk	n/a	n/a	Heywang *et al.*[68]
1994	Tos	SCP	300	150	n/a	n/a	De Leeuw

							et al.[84]
1995	ClO_4^-	electrochemical polymerization	780	n/a	n/a	n/a	Granström et al.[76]
1997	PF6	Electrochemical polymerization	300	n/a	n/a	n/a	Aleshin *et al.*[214]
2002	PSS, Baytron P	Organic solvent addition	80	n/a	n/a	n/a	Kim *et al.*[110]
2003	Tos	Electrochemical polymerization	450	n/a	n/a	n/a	Zotti *et al.*[77]
2003	ClO_4^-	Electrochemical polymerization	650	n/a	n/a	n/a	Zotti *et al.*[77]
2004	PSS, Baytron P V4071	Organic solvent addition	200	n/a	n/a	n/a	Ouyang *et al.*[112]
2004	Tos	VPP	1025	250	n/a	n/a	Winther-Jensen *et al.*[87]
2005	Tos	SCP	1000	~260	n/a	n/a	Winther-Jensen *et al.*[91]
2006	Tos	VPP	1000	n/a	n/a	n/a	Lindel *et al.*[158]
2006	Tos	o-CVD	105	86	n/a	n/a	Lock *et al.*[88]
2007	Tos	VPP	4500	n/a	n/a	n/a	Kim *et al.*[89]
2007	PSS, Baytron P-V4, HC Starck	Ionic liquid	136	n/a	n/a	n/a	Döbbelin *et al.*[121]
2008	PSS, Baytron P, Item No. 1802705, Lot No. HCE07P107	Anionic surfactants	80	n/a	n/a	n/a	Fan *et al.*[123]
2008	Tos	VPP	761	n/a	n/a	n/a	Zuber *et*

							al.[159]
2009	PSS, Baytron P, Item No. 1802705, Lot No. HCE07P107	Salt	140	130	n/a	n/a	Xia *et al.*[124]
2010	2-naphthalenesulfonic acid	Thermal treatment	2000	n/a	n/a	n/a	Pyshkina *et al.*[215]
2010	PSS, Baytron P, renamed as Clevios P, Item No. 1802705, Lot No. HCE07P107	Acid	200	130	n/a	n/a	Xia *et al.*[129]
2010	Tos	VPP	1078	n/a	n/a	n/a	Fabretto *et al.*[90]
2011	PSS, PH 1000 from H. C. Starck	Organic pre- and post-treatment	1418	15	n/a	n/a	Kim *et al.*[115]
2011	Tos	VPP	575	24	n/a	n/a	Madl *et al.*[169]
2011	Tos	VPP	1487	66	n/a	n/a	Fabretto *et al.*[161]
2011	Tos	VPP	300	3000	n/a	n/a	Bubnova *et al.*[204]
2012	PSS	Ionic liquid	2084	96	n/a	n/a	Badre *et al.*[122]
2012	Tos	VPP	3400	66	n/a	n/a	Fabretto *et al.*[162]
2012	PSS, Clevios PH1000	Acid	3065	24	n/a	n/a	Xia *et al.*[130]
2013	PSS, Clevios PH1000 from H. C. Starck	Organic solvent	~900	~135	n/a	n/a	Kim *et al.*[216]
2013	Tos	SCP	1500	n/a	n/a	n/a	Yu *et al.*[168]
2013	PSS, Clevios PH1000	Organic solvents	830	20-30	10^{21}	1.7	Wei *et al.*[138]
2013	Tos	SCP	1355	122	n/a	n/a	Park *et al.*[205]
2013	Tos	SCP	2120	120-140	n/a	n/a	Park *et al.*[205]
2013	Tos	VPP + organic solvent	3305	121	n/a	n/a	Hojati-Talemi *et al.*[217]

2014	PSS, Clevios PH 1000 from Heraeus	Organic solvent	1647	110	8×10^{22}	0.129	Lee *et al.*[117]
2014	PSS, Clevios PH1000, Heraeus	Acid	3500	38	n/a	n/a	Mukherjee *et al.*[131]
2014	PSS Clevios PH 1000, Heraeus		944	~7000	2.7×10^{20}	~20	Tsai *et al.*[218]
2014	Tos	Acid	1750	110		n/a	Wang *et al.*[166]
2014	($FeCl_3$)	VPP, Single crystal	8797	Nanocrystallite : 95 nm wide and 100 nm thick	6.23×10^{20}	88	Cho *et al.*[24]
2014	PSS, Clevios PH1000	Acid	4380	<100	$\sim 6 \times 10^{21}$	4	Kim *et al.*[132]
2014	ClO_4^-	Electrochemical polymerization	753	110-120	n/a	n/a	Culebras *et al.*[78]
2014	PF_6	Electrochemical polymerization	1000	110-120	n/a	n/a	Culebras *et al.*[78]
2014	BTFMSI	Electrochemical polymerization	2074	110-120	n/a	n/a	Culebras *et al.*[78]
2015	PSS, Clevios PH1000	Acid	1460	85	n/a	n/a	Meng *et al.*[134]
2015	OTf	SCP	1218	n/a	n/a	n/a	Massonnet *et al.*[47]
2015	Sulf	SCP + acid	2273	n/a	n/a	n/a	Massonnet *et al.*[47]
2015	PSS, Clevios PH1000	Shearing	4600	~130	n/a	n/a	Worfolk *et al.*[116]
2015	PSS, Clevios PH1000	Organic solvent	1470	230	5.73×10^{22}	0.15	Xiong *et al.*[147]
2015	PSS, Clevios PH1000 from H.C. Starck GmbH.	Sorbitol	722	60-65	n/a	n/a	Yang *et al.*[219]
2015	PSS, Clevios PH1000 from H.C.	Mixed organic solvent +	953	n/a	n/a	n/a	Liu *et al.*[220]

	Starck	thermal treatment					
2015	PSS, Clevios PH1000; Heraeus Precious Metals	Film thickness	1200	3000	8.9×10^{20}	8.4	Anno *et al.*[221]
2015	Br	o-CVD + acid treatment	2050	52	n/a	n/a	Ugur *et al.*[99]
2015	PSS, Clevios PH1000	Acid	1900	~200	n/a	n/a	Mengistie *et al.*[222]
2016	PSS, PH1000 Clevios	Acid	2600	n/a	n/a	n/a	Kumar *et al.*[135]
2016	Tos	Organic solvents + acid	640	n/a	1.7×10^{21}	2.3	Petsagkourakis *et al.*[223]
2016	PSS	Acid	4840	~100	n/a	n/a	Bae *et al.*[82]
2016	OTf	SCP	3600	~10	n/a	n/a	Gueye *et al.*[23]
2016	Sulf	SCP + H_2SO_4	5400	~10	n/a	n/a	Gueye *et al.*[23]
2017	Tos	SCP + organic solvent	2200	120	n/a	n/a	Lee *et al.*[165]
2017	Tos	SCP + organic solvent	1250	80	n/a	n/a	Lee *et al.*[165]
2017	OTf	Triflate treatment of PEDOT :PSS	2100	~150	n/a	n/a	Farka *et al.*[48]
2017	Sulf	o-CVD	4050	~150	$\sim 5 \times 10^{20}$ at T < 10 K	40 at T < 10 K	Farka *et al.*[48]
2017	PSS, PH1000 Clevios	Ionic liquid + stretching	4100	600 – 800	n/a	1 ± 10%	Wang *et al.*[127]
2018	PSS, Clevios PH1000, Heraeus	EG + electric field	1300	n/a	n/a	n/a	Yamaguchi *et al.*[224]
2018	PSS, Clevios PH1000, Heraeus	Organic solvent + acid	1700	n/a	n/a	n/a	Lee *et al.*[225]
2018	PSS, Clevios PH1000, Heraeus	Organic solvent + salt	1866	n/a	n/a	n/a	Zhang *et al.*[226]
2018	PSS, Clevios PH1000, Heraeus	Triflic acid	2980	25	1.45×10^{22}	0.73 $cm^2V^{-1}s^{-1}$	Wang *et al.*[227]

2018	Tos + ClO_4	VPP + electrochemical treatment	> 2750	n/a	4.5×10^{21}	3.2	Rudd *et al.*[174, 228]
2018	($FeCl_3$)	o-CVD + acid treatment	6259	10	2.12×10^{21}	18.45	Wang *et al.*[25]

Declarations of interest

None